

UNIVERSIDADE FEDERAL DE SÃO CARLOS
CENTRO DE CIÊNCIAS EXATAS E DE TECNOLOGIA
DEPARTAMENTO DE QUÍMICA
PROGRAMA DE PÓS-GRADUAÇÃO EM QUÍMICA

**“UVC-BASED ADVANCED OXIDATION PROCESSES FOR
WATER TREATMENT: LABORATORY AND PILOT PLANT
SCALE STUDIES”**

Isaac José Sánchez Montes*

Thesis presented as part of the requirements to obtain the title of DOCTOR IN SCIENCES, concentration area: PHYSICAL-CHEMISTRY

Advisor: Prof. Dr. José Mario de Aquino

***Scholarship holder of CNPq (sandwich doctorate at *Plataforma Solar de Almería*)**

São Carlos – SP

2020



Folha de Aprovação

Defesa de Tese de Doutorado do candidato Isaac Jose Sanchez Montes, realizada em 21/09/2020.

Comissão Julgadora:

Prof. Dr. José Mario de Aquino (UFSCar)

Prof. Dr. Marcos Roberto de Vasconcelos Lanza (IQSC/USP)

Prof. Dr. Pedro Sergio Fadini (UFSCar)

Prof. Dr. Ricardo Francisco Brocenschi (UFPR)

Prof. Dr. Adilson José da Silva (UFSCar)

O presente trabalho foi realizado com apoio da Coordenação de Aperfeiçoamento de Pessoal de Nível Superior - Brasil (CAPES) - Código de Financiamento 001.

O Relatório de Defesa assinado pelos membros da Comissão Julgadora encontra-se arquivado junto ao Programa de Pós-Graduação em Química.

A mi bella esposa Liany. Estoy muy agradecido de que Dios haya unido nuestros caminos y quiero que te quedes en mi vida hasta el final de mis días. Deseo ver nuestro amor corriendo en el jardín, jugando incansablemente y llenando nuestro hogar de eterna felicidad...

A mi familia con todas las fuerzas de mi ser y a mis angelitos en el cielo que ven cada uno de mis pasos...

ACKNOWLEDGMENTS

I would like to express my deepest and sincerest gratitude to all people who in one way or another have contributed in order to make this work possible.

First and foremost, I am indebted to my advisor Prof. Dr. José Mario de Aquino for the continuous support, dedication, and valuable guidance along these years. I will be always so grateful.

My sincere thanks to Drs. Isabel Oller and Sixto Malato from *Plataforma Solar de Almería* (Spain) for giving me the opportunity to work on diverse exciting projects during my sandwich doctorate period.

I would like to express my heartiest appreciation to *Laboratório de Pesquisas em Eletroquímica* (LaPE), especially to Drs. Romeu Cardozo Rocha Filho, Sonia Regina Biaggio, Nerilso Bocchi, and my fellow labmates André, Carlos, Diego, Jussara, Kallyni, Karina, Naihara, Rogério, and Yeison for the support and friendship. Thanks a lot LaPE!

My thanks to PPGQ secretary for the assistance in all bureaucratic services. It is sincerely appreciated.

Last but not least, I also thank the Brazilian funding agencies, CNPq (grants #142350/2016-8 and #205818/2018-8), CAPES (Finance Code 001), and FAPESP (#2019/07943-4) for the scholarships and financial support. I must be also grateful to European Union's Horizon 2020 research and innovation program (PANIWATER project, grant #820718) and Spanish Ministry of Science, Innovation, and Universities.

SCIENTIFIC PRODUCTION RELATED TO THIS THESIS

The results obtained in this doctoral research have been published or are in process of being published in international journals:

1. SÁNCHEZ-MONTES, ISAAC; SALMERÓN, IRENE; IBAÑEZ, GRACIA; AQUINO, JOSÉ M.; POLO-LÓPEZ, MARIA I.; OLLER, ISABEL; MALATO, SIXTO. UVC based advanced oxidation processes for simultaneous removal of microcontaminants and pathogens from simulated municipal wastewater at pilot plant scale. *Water Research & Technology*, v. 6, p. 2553, 2020.

2. SÁNCHEZ-MONTES, ISAAC; WACHTER, NAIHARA; SILVA, BIANCA F.; AQUINO, JOSÉ M. Comparison of UVC-based advanced oxidation processes in the mineralization of bisphenol A: identification of oxidation by products and toxicity evaluation. *Chemical Engineering Journal*, v. 386, p. 123986, 2020.

3. SÁNCHEZ-MONTES, ISAAC; PÉREZ, JOSÉ F.; SÁEZ, CRISTINA; RODRIGO, MANUEL A.; CAÑIZARES, PABLO; AQUINO, JOSÉ M. Assessing the performance of electrochemical oxidation using DSA[®] and BDD anodes in the presence of UVC light. *Chemosphere*, v. 238, p. 124575, 2020.

Under production:

4. SÁNCHEZ-MONTES, ISAAC; SALMERÓN, IRENE; AQUINO, JOSÉ M.; POLO-LÓPEZ, MARIA I.; OLLER, ISABEL; MALATO, SIXTO. Solar-driven free chlorine oxidation process for simultaneous removal of microcontaminants and microorganisms in natural water.

5. SÁNCHEZ-MONTES, ISAAC; SALMERÓN, IRENE; AQUINO, JOSÉ M.; POLO-LÓPEZ, MARIA I.; OLLER, ISABEL; MALATO, SIXTO. Free chlorine coupled with solar or UVC radiation for simultaneous removal of microcontaminants and pathogens from municipal wastewater at pilot plant scale.

In addition, the PhD candidate has collaborated with other researchers, from which is co-author of the following publications:

6. TRENCH, ALINE B.; MACHADO, THALES R.; GOUVEIA, AMANDA F.; FOGGI, CAMILA C.; TEODORO, VINÍCIUS; SÁNCHEZ-MONTES, ISAAC; TEIXEIRA, MAYARA M.; DA TRINDADE, LETÍCIA G.; JACOMACI, NATALIA; PERRIN, ANDRE; PERRIN, CHRISTIANE; AQUINO, JOSÉ M.; ANDRÉS, JUAN; LONGO, ELSON. Rational design of W-Doped Ag₃PO₄ as an efficient antibacterial agent and photocatalyst for organic pollutant degradation. *ACS Omega*, v. 5, p. 23808, 2020.

7. COLEDAM, DOUGLAS A. C.; SÁNCHEZ-MONTES, ISAAC; SILVA, BIANCA F.; AQUINO, JOSÉ M. On the performance of HOCl/Fe²⁺, HOCl/Fe²⁺/UVA, and HOCl/UVC

processes using in situ electrogenerated active chlorine to mineralize the herbicide picloram. *Applied Catalysis B: Environmental*, v. 227, p. 170, 2018.

8. SILVA, DIEGO D.; SÁNCHEZ-MONTES, ISAAC; HAMMER, PETER; AQUINO, JOSÉ M. On the supercapacitor performance of microwave heat treated self organized TiO₂ nanotubes: influence of the cathodic pre-treatment, water aging, and thermal oxide. *Electrochimica Acta*, v. 245, p. 165, 2017.

LIST OF ABBREVIATIONS

- ACT – acetaminophen
- AOPs – advanced oxidation processes
- A. salina* – *Artemia salina*
- BPA – bisphenol A
- CAF – caffeine
- CBZ – carbamazepine
- CEC – contaminants of emerging concern
- DCF – diclofenac
- DIC – dissolved inorganic carbon
- DL – detection limit
- DOC – dissolved organic carbon
- DOM – dissolved organic matter
- ECOSAR – ecological structure–activity relationship software
- E. coli* – *Escherichia coli* O157:H7
- E. faecalis* – *Enterococcus faecalis*
- GHS – globally harmonized system of classification and labelling of chemicals
- HPLC – high-performance liquid chromatography
- IPA – isopropyl alcohol
- LC–MS/MS – liquid chromatography tandem mass spectrometry
- MWWTPs – municipal wastewater treatment plants
- OMCs – organic microcontaminants
- Q_{UVC} – accumulative UVC energy expressed in kJ L^{-1}
- SMWW – simulated municipal wastewater
- SMX – sulfamethoxazole
- S. enteritidis* – *Salmonella enteritidis*
- TBA – tert-butyl alcohol
- TMP – trimethoprim
- TOC – total organic carbon
- UPLC – ultra-performance liquid chromatography
- USEPA – US Environmental Protection Agency
- UVC – ultra-violet radiation type C

UVC AOPs – ultraviolet-based advanced oxidation processes

$\sum C_t / \sum C_0$ – total degradation

φ – extent of total mineralization or conversion to CO_2

A_{254} – absorbance at 254 nm

ϵ_{254} ($\text{mg}^{-1} \text{ L cm}^{-1}$) – molar absorptivity coefficient at 254

Φ_{254} (mol E s^{-1}) – quantum yield at 254 nm

LIST OF TABLES

TABLE 2.1 – Pseudo-first order kinetic constants (<i>k</i>) for the removal of BPA and TOC using different UVC AOPs.	22
TABLE 2.2 – LC-MS/MS data of the main detected oxidation by-products during treatment of BPA solutions using different UVC AOPs.....	31
TABLE 2.3 – Estimated acute and chronic toxicity data for BPA and its initial oxidation by-products (with elucidated structure) predicted by the ECOSAR software.....	35
TABLE 2.4 – Economic comparison per order of BPA degradation using different UVC AOPs.	36
TABLE 3.1 – Physicochemical characterization of SMWW effluent.....	41
TABLE 3.2 – Photochemical properties of OMCs (at 254 nm) and experimental degradation percentages under UVC irradiation.	49
TABLE 3.3 – Pseudo-first order kinetic constants (<i>k</i>) for simultaneous inactivation of bacteria and OMCs degradation in a SMWW effluent by a UVC/H ₂ O ₂ process.	52
TABLE 3.4 – Pseudo-first order kinetic constants (<i>k</i>) for simultaneous inactivation of bacteria and OMC degradation in a SMWW effluent by the UVC/S ₂ O ₈ ²⁻ process.....	58

LIST OF FIGURES

FIGURE 1.1 – Severe water scarcity map in number of months per year.	1
FIGURE 1.2 – Global distribution of water contamination hazard.....	4
FIGURE 2.1 – Image of the experimental setup used during the degradation and mineralization of BPA solutions through different UVC AOPs: reservoir (1), quartz tube with the UVC lamp inside it (2), and peristaltic pump (3).	15
FIGURE 2.2 – Images of the experimental configuration used for breeding of <i>A. salina</i> : a) top and b) side views of the system composed by a fluorescent lamp (14 W), a plastic separator (5-mm holes), an air pump, and an aquarium (200×100×150 mm) containing the artificial seawater solution and <i>A. salina</i> cysts (opposite to the lighting side; darkest region).	18
FIGURE 2.3 – Remaining a) BPA and b) TOC fraction as a function of treatment time for the photochemical (●) and chemical ((H ₂ O ₂ (+), S ₂ O ₈ ²⁻ (+), and HClO (+)) processes. Conditions: 0.6 mol L ⁻¹ of oxidant (flow rate 0.1 mL min ⁻¹), pH 3, and 38 °C. Error bars refer to two and three repetitions for the BPA and TOC determinations, respectively.	20
FIGURE 2.4 – Remaining a) BPA and b) TOC fraction as a function of treatment time for the UVC/H ₂ O ₂ (◆), UVC/S ₂ O ₈ ²⁻ (▲), and UVC/HClO (■) processes. Conditions: 0.6 mol L ⁻¹ of oxidant (flow rate 0.1 mL min ⁻¹), pH 3, and 38 °C. Error bars refer to two and three repetitions for the BPA and TOC determinations, respectively.	21
FIGURE 2.5 – Extent of total mineralization (φ) as a function of time for the UVC/H ₂ O ₂ (◆), UVC/S ₂ O ₈ ²⁻ (▲), and UVC/HClO (■) processes. Conditions: 0.6 mol L ⁻¹ of oxidant (flow rate 0.1 mL min ⁻¹), pH 3, and 38 °C. Error bars refer to two and three repetitions for the BPA and TOC determinations.	23
FIGURE 2.6 – Remaining fraction of a) BPA and b) TOC as a function of treatment time for the photochemical method (●), chemical method (+), UVC/H ₂ O ₂ process (◆), and after summation of the experimental photochemical and chemical methods (---). Conditions: 0.6 mol L ⁻¹ of oxidant (flow rate 0.1 mL min ⁻¹), pH 3, and 38 °C. Error bars refer to two and three repetitions for the BPA and TOC determinations, respectively.	24
FIGURE 2.7 – Remaining fraction of a) BPA and b) TOC as a function of treatment time for the photochemical method (●), chemical method (+), UVC/S ₂ O ₈ ²⁻ (▲), and after summation of the experimental photochemical and chemical methods (---). Conditions: 0.6 mol L ⁻¹ of oxidant (flow rate 0.1 mL min ⁻¹), pH 3, and 38 °C. Error bars refer to two and three repetitions for the BPA and TOC determinations, respectively.	25

FIGURE 2.8 – Remaining fraction of a) BPA and b) TOC fraction as a function of treatment time for the photochemical method (●) chemical method (+), UVC/HClO process (■), and after summation of the experimental remaining fractions of the photochemical and chemical methods (---). Conditions: 0.6 mol L⁻¹ of oxidant (flow rate 0.1 mL min⁻¹), pH 3, and 38 °C. Error bars refer to two and three repetitions for the BPA and TOC determinations, respectively.

..... 25

FIGURE 2.9 – Concentration evolution of oxidant species as a function of time for the chemical (H₂O₂ (+), S₂O₈²⁻ (+), and HClO (+)) and UVC/Oxidant processes (UVC/H₂O₂ (◆), UVC/S₂O₈²⁻ (▲), and UVC/HClO (■)). Conditions: 0.6 mol L⁻¹ of oxidant (flow rate 0.1 mL min⁻¹), pH 3, and 38 °C. 26

FIGURE 2.10 – Chromatographic profiles of treated samples containing 100 mg L⁻¹ of benzoic acid at varying sampling times to show the evolution and formation of benzoic and salicylic acids peaks using the a) UVC/H₂O₂, b) UVC/S₂O₈²⁻, and c) UVC/HClO processes..... 27

FIGURE 2.11 – Remaining BPA fraction as a function of treatment time for the UVC/S₂O₈²⁻ process in the absence of scavenger (▲), in the presence of isopropanol (●), and in the presence of tert-butyl alcohol (▶). Conditions: 0.6 mol L⁻¹ of oxidant (flow rate 0.1 mL min⁻¹), pH 3, and 38 °C. 28

FIGURE 2.12 – Concentration evolution of the main detected carboxylic acids as a function of the treatment time for the a) UVC/H₂O₂, b) UVC/S₂O₈²⁻ and c) UVC/HClO processes: acetic (◇), butyric (○), dichloroacetic (×), formic (◻), glycolic (◁), glyoxylic (△), malic (◊), malonic (⊖), oxalic (▽), propionic (⊙), pyruvic (+), succinic (*), tartaric (▷) and tartronic (◻). Conditions: 0.6 mol L⁻¹ of oxidant (flow rate 0.1 mL min⁻¹), pH 3, and 38 °C. 32

FIGURE 2.13 – Concentration evolution of the main detected carboxylic acids as a function of the treatment time for the chemical process using HClO: acetic (◇), dichloroacetic (×), formic (◻), glyoxylic (△), malonic (⊖), oxalic (▽). Conditions: 0.6 mol L⁻¹ of oxidant (flow rate 0.1 mL min⁻¹), pH 3, and 38 °C. 33

FIGURE 2.14 – Evolution of mortality of *A. salina* (%) as a function of the treatment time for the UVC/H₂O₂ (◆), UVC/S₂O₈²⁻ (▲), and UVC/HClO (■) processes. The dashed line indicates the LC₅₀ value (28.9 mg L⁻¹) found for BPA. The error bars refer to the calculated errors for triplicate analyses. Conditions: 0.6 mol L⁻¹ of oxidant (flow rate 0.1 mL min⁻¹), pH 3, and 38°C. 34

FIGURE 2.15 – Energy consumption per unit mass of removed TOC (w) as a function of TOC removal for the UVC/H₂O₂ (◆), UVC/S₂O₈²⁻ (▲), and UVC/HClO (■) processes. Conditions:

0.6 mol L ⁻¹ of oxidant (flow rate 0.1 mL min ⁻¹), pH 3, and 38 °C. Error bars refer to three repetitions.	37
FIGURE 3.1 – UVC pilot plant: a) UVC photo-reactor scheme and main characteristics and b) real image of the experimental setup of the plant.....	45
FIGURE 3.2 – Simultaneous bacterial inactivation and total OMC degradation (inset) under UVC irradiation in SMWW effluent as a function of treatment time: <i>E. coli</i> (■), <i>E. faecalis</i> (●), <i>S. enteritidis</i> (▲), and $\sum C_t/\sum C_0$ (◆). Dashed lines (---) refer to detection limit of bacteria (DL = 1 CFU per 100 mL ⁻¹) and 80% removal of total OMCs.	47
FIGURE 3.3 – Effect of different H ₂ O ₂ concentration ([H ₂ O ₂]) on the a) <i>E. coli</i> , b) <i>E. faecalis</i> , and c) <i>S. enteritidis</i> inactivation by UVC/H ₂ O ₂ as a function of treatment time in SMWW effluent. [H ₂ O ₂] = 5 (■), 15 (●), 25 (▲), 35 (▼), and 50 mg L ⁻¹ (◄). Dashed lines (---) refer to detection limit (DL = 1 CFU per 100 mL ⁻¹).	51
FIGURE 3.4 – Effect of different H ₂ O ₂ concentration ([H ₂ O ₂]) on the total OMC degradation by UVC/H ₂ O ₂ as a function of treatment time in SMWW effluent. [H ₂ O ₂] = 5 (■), 15 (●), 25 (▲), 35 (▼), and 50 mg L ⁻¹ (◄). Dashed line (---) refers to 80% removal of total OMCs. ...	53
FIGURE 3.5 – Pseudo-first order kinetic constant (<i>k</i> ;■) as a function of H ₂ O ₂ concentration ([H ₂ O ₂]) for UVC/H ₂ O ₂ process. The obtained slope and R ² for the linear regression were 0.00196 L (mg min) ⁻¹ and 0.990, respectively.	54
FIGURE 3.6 – Effect of different S ₂ O ₈ ²⁻ concentration ([S ₂ O ₈ ²⁻]) on the a) <i>E. coli</i> , b) <i>E. faecalis</i> , and c) <i>S. enteritidis</i> inactivation by UVC/S ₂ O ₈ ²⁻ as a function of treatment time in SMWW effluent. [S ₂ O ₈ ²⁻] = 20 (◆) and 40 mg L ⁻¹ (◆). Dashed lines (---) refer to detection limit (DL = 1 CFU per 100 mL ⁻¹).	56
FIGURE 3.7 – Effect of different S ₂ O ₈ ²⁻ concentration ([S ₂ O ₈ ²⁻]) on the total OMC degradation by UVC/S ₂ O ₈ ²⁻ as a function of treatment time in SMWW effluent. [S ₂ O ₈ ²⁻] = 20 (◆), 40 (◆), and 100 mg L ⁻¹ (▶). Dashed line (---) refers to 80% removal of total OMCs.....	59
FIGURE 3.8 – Pseudo-first order kinetic constant (<i>k</i> ;■) as a function of S ₂ O ₈ ²⁻ concentration ([S ₂ O ₈ ²⁻]) for UVC/S ₂ O ₈ ²⁻ process. The obtained slope and R ² for the linear regression were 0.00125 L (mg min) ⁻¹ and 0.999, respectively	60
FIGURE 3.9 – Effect of high H ₂ O ₂ concentration ([H ₂ O ₂]) on the total OMC degradation under UVC irradiation as a function of treatment time in SMWW effluent: [H ₂ O ₂] = 150 (■), 300 (●), and 600 mg L ⁻¹ (▲). Dashed line (---) refers to 80% removal of total OMCs.	62
FIGURE 3.10 – Effect of high S ₂ O ₈ ²⁻ concentration ([S ₂ O ₈ ²⁻]) on the total OMC degradation under UVC irradiation as a function of treatment time in SMWW effluent. [S ₂ O ₈ ²⁻] = 200 (◆), 250 (◆), and 300 mg L ⁻¹ (▶). Dashed line (---) refers to 80% removal of total OMCs.....	62

RESUMO

PROCESSOS OXIDATIVOS AVANÇADOS BASEADOS EM UVC E APLICADOS NO TRATAMENTO DE ÁGUAS: ESTUDOS EM BANCADA E EM ESCALA PILOTO – O desafio de fornecer água livre de contaminantes orgânicos emergentes (incluindo microcontaminantes orgânicos; MCOs) e patógenos é um dos principais tópicos de estudo da atualidade. Neste sentido, a eficiência de diferentes processos oxidativos avançados baseados em UVC (POA UVC) para a remoção de poluentes orgânicos e/ou inativação de patógenos em distintas condições experimentais foi investigada. Na escala de bancada, o processo UVC/HClO apresentou a melhor performance para a degradação e mineralização de soluções contendo BPA, enquanto que o processo UVC/S₂O₈²⁻ teve uma melhor eficiência em comparação com o UVC/H₂O₂. Este comportamento deveu-se à geração de radicais de alto poder oxidante (*e.g.*, HO[•] e SO₄^{•-}) advindos da ativação do H₂O₂, S₂O₈²⁻ e HClO sob irradiação com luz UVC. Em relação aos intermediários de oxidação gerados, não foram detectados compostos organoclorados (após 6 h) utilizando o sistema UVC/HClO, o que contrasta com os resultados obtidos utilizando somente HClO (dois organoclorados foram detectados). Levando-se em consideração os parâmetros ambientais (testes de toxicidade experimentais e teóricos) e econômicos investigados, o método UVC/HClO apresentou os melhores resultados com baixo custo operacional. No entanto, em condições experimentais mais complexas, tecnologias em um estágio mais avançado de desenvolvimento, como UVC/H₂O₂ e UVC/S₂O₈²⁻ são mais recomendáveis. Nesse sentido, a eliminação simultânea de seis MCOs (ACT, CAF, CBZ, TMP, SMX e DCF) e três bactérias (*E. coli*, *E. faecalis* e *S. enteritidis*) de uma matriz residual simulada utilizando os processos UVC/H₂O₂ e UVC/S₂O₈²⁻ em escala piloto foi estudada. Os POA UVC foram comparados em termos da remoção de 80% do total dos MCOs, da inativação e o recrescimento bacteriano e do consumo de energia. O tratamento aplicando somente radiação UVC, embora eficiente para a inativação bacteriana, resultou inadequado para a remoção dos MCOs. Por outro lado, os processos UVC/H₂O₂ e UVC/S₂O₈²⁻ foram eficazes para eliminar simultaneamente MCOs e bactérias; contudo, somente o sistema UVC/H₂O₂ foi efetivo para evitar o recrescimento bacteriano em tempos posteriores ao tratamento. De acordo com isto e levando em consideração algumas regulações ambientais, águas tratadas pelo processo UVC/H₂O₂ representam uma alternativa real para serem reutilizadas em diversas atividades, como por exemplo, para fins agrícolas, visto que esta atividade é o setor de maior consumo/demanda de água doce em todo o mundo. Finalmente, um modelo simples baseado na lei de Beer-Lambert permitiu estimar razoavelmente a concentração necessária de oxidante para atingir a máxima taxa de oxidação (*i.e.*, um tempo de reação mais curto).

ABSTRACT

UVC-BASED ADVANCED OXIDATION PROCESSES FOR WATER TREATMENT: LABORATORY AND PILOT PLANT SCALE STUDIES – The challenge of providing good-quality water free from contaminants of emerging concern (including organic microcontaminants; OMCs) and pathogens is one of the main hot topics worldwide. Thus, the efficiency of different UVC-based advanced oxidation processes (UVC AOPs) to remove organic pollutants and/or inactivate pathogens under distinct experimental conditions was investigated. At laboratory scale, UVC/HClO process showed the best performance for the degradation and mineralization of BPA containing solutions, while the UVC/S₂O₈²⁻ process had a better efficiency in comparison to UVC/H₂O₂. This behavior is due to the generation of high oxidation power radicals (mainly HO[•] and SO₄^{•-}) by the activation of H₂O₂, S₂O₈²⁻, and HClO under UVC light. Considering the oxidation by-products generated, no organochlorine compounds were detected (after 6 h) using UVC/HClO contrasting to the results obtained using only HClO (two organochlorines were detected). In addition, taking into account the environmental (experimental and theoretical toxicity tests) and economical parameters investigated, the UVC/HClO method showed a higher efficiency under low operating costs. However, under complex experimental conditions, more mature technologies such as UVC/H₂O₂ and UVC/S₂O₈²⁻ are recommended. In this sense, simultaneous elimination of six OMCs (ACT, CAF, CBZ, TMP, SMX, and DCF) and three bacteria (*E. coli*, *E. faecalis*, and *S. enteritidis*) by UVC/H₂O₂ and UVC/S₂O₈²⁻ processes from a simulated municipal wastewater effluent were successfully investigated at pilot plant scale. UVC AOPs were compared in terms of the required treatment time to remove at least 80% of the sum of OMCs, bacterial inactivation and regrowth, and energy consumption. UVC treatment alone was not suitable mainly due to the very slow and incomplete removal of OMCs, while UVC/H₂O₂ and UVC/S₂O₈²⁻ were effective to simultaneously eliminate OMCs and bacteria; however, in comparison with the UVC/S₂O₈²⁻ system, the UVC/H₂O₂ process did not exhibit bacterial regrowth under dark conditions. According to these results and taking into account some environmental regulations, reclaimed water treated with the UVC/H₂O₂ process is a real alternative for water reuse purposes in many activities, for instance, in agriculture since this activity demands the highest freshwater consumption worldwide. Finally, a simple model based on the Beer–Lambert law enabled reasonable estimation of the oxidant concentration required to attain maximum oxidation rates (*i.e.*, shortest reactions time).

TABLE OF CONTENTS

1. OVERVIEW AND GOALS	1
2. CHAPTER 1: UVC-based removal of macrocontaminants at laboratory scale	12
2.1. ABSTRACT.....	12
2.2. SHORT INTRODUCTION	13
2.3. MATERIALS AND METHODS.....	14
2.3.1. Chemicals.....	14
2.3.2. Degradation and mineralization experiments.....	14
2.3.3. Analyses	15
2.4. RESULTS AND DISCUSSION	19
2.4.1. Degradation and mineralization of BPA using different UVC AOPs.....	19
2.4.2. Synergistic effect of UVC AOPs: the role of HO [•] , SO ₄ ^{•-} , and Cl [•] species	24
2.4.3. Identification of oxidation by-products.....	29
2.4.4. Toxicity: experimental and theoretical analyses	33
2.4.5. Economical comparison and energy consumption analysis	36
2.5. CONCLUSIONS.....	38
3. CHAPTER 2: UVC-based removal of microcontaminants and pathogens at pilot plant scale	39
3.1. ABSTRACT.....	39
3.2. SHORT INTRODUCTION	40
3.3. MATERIALS AND METHODS.....	41
3.3.1. Chemicals.....	41
3.3.2. Analyses	42
3.3.2.1. Analytical quantification of OMCs	42
3.3.2.2. Bacterial quantification analyses	43
3.3.3. UVC pilot plant description and experimental procedure.....	44
3.4. RESULTS AND DISCUSSION	46
3.4.1. UVC treatment	46
3.4.2. UVC/H ₂ O ₂ treatment for simultaneous bacterial inactivation and OMCs degradation	50
3.4.3. UVC/S ₂ O ₈ ²⁻ treatment for simultaneous bacterial inactivation and OMCs degradation.....	55
3.4.4. Preliminary model to determine the maximum yield of oxidant for UVC based system.....	61
3.5. CONCLUSIONS.....	63

4. GENERAL CONCLUSIONS AND PERSPECTIVES FOR FUTURE STUDIES 65

5. REFERENCES 69

APPENDIX A (CHAPTER 1)

APPENDIX B (CHAPTER 2)

1. OVERVIEW AND GOALS

The world is undergoing socio-economic changes that involve important environmental problems, and one of them is freshwater scarcity.¹ The accelerated growing of the global population (*e.g.*, urban areas) and anthropogenic activities (*e.g.*, change in consumption patterns, industrial development, and expansion of irrigated agriculture) are the main driving forces responsible for the rise in global demand for freshwater.^{2, 3} In addition, other factors, for instance, the global climate change, will lead to worsen the issue regarding freshwater scarcity.

Currently, it has been estimated that about half billion of people live under conditions of severe water scarcity throughout the year, while another four billion face severe water scarcity at least over a month per year (see FIGURE 1.1).^{4, 5} However, the impact of water scarcity is reasonably “low” in many regions around the world, including forested areas in South America (mostly Brazil), Central Africa, northern and subarctic regions of North America, and in wide regions of Europe and Asia. Nevertheless, from a general perspective, this parameter evaluates only the availability of freshwater resources in a specific geographical area and does not provide information on whether they are “safe” for the human health and biodiversity in general. In this sense, a global map on the availability of safe water is well-suited for the pressing need of information on safe water locations.

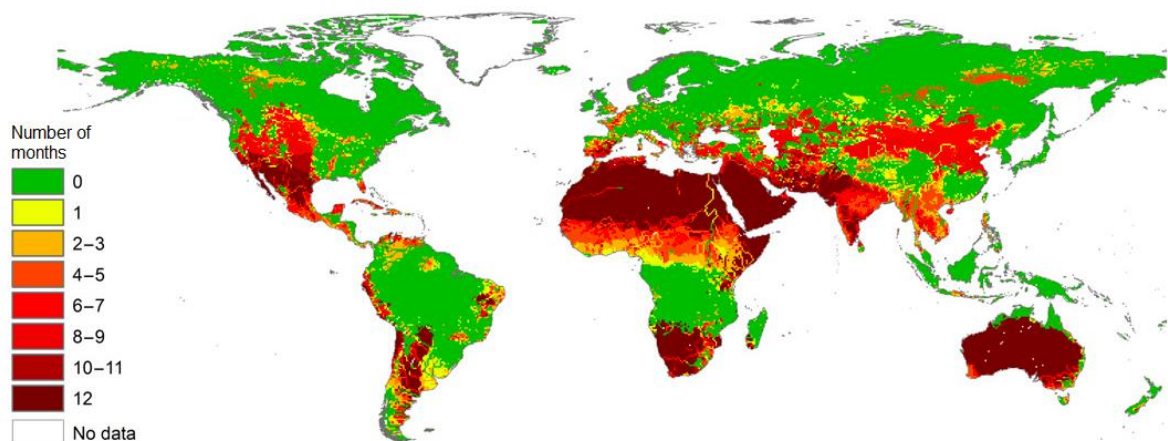


FIGURE 1.1 – Severe water scarcity map in number of months per year.

On the other hand, the main factors (*i.e.*, anthropogenic activities) that intensify the global freshwater scarcity can be briefly summarized as follows:

i) World water consumption rate: the demand for freshwater have increased by almost 1% per year since 1980 (when the world population was about 4.5 billion) and are still going up until the present day (world population estimated in 7.7 billion). In addition, a similar increase in the water consumption rate is expected until 2050 when the world population is projected to reach 9.7 billion.⁶ Even though this rate seems apparent stable, the average of freshwater consumed each year increases as a function of the population growth rate, which is mainly due to the high demand on food. In fact, agricultural and industrial activities are important factors that intensify the demand on freshwater. For instance, the water utilized to produce the daily food amount per person is around 2000-5000 L (*i.e.*, indirect water consumption), while the amount of daily drinking water required per person is about 2-4 L (*i.e.*, direct water consumption).⁷

ii) Global climate change: although the effect of these conditions on water resources is uncertain for many reasons, climate change represents an additional threat to water security due to current and future changes in precipitation patterns that might lead to significant changes in freshwater supply in many regions. Also, renewable water resources might be affected by changes in temperature, wind, ocean currents patterns, and other climate factors.⁸

iii) Water contamination: contamination of freshwater bodies, *e.g.*, surface and groundwater by a large number of contaminants generated from anthropogenic activities (including chemical and microbiological contaminants), represents one of the biggest challenges regarding water scarcity faced lately. These contaminants might decrease the availability of freshwater resources by transforming them into unsafe water and consequently are responsible for many waterborne diseases.

Concerning this last topic (*iii*), a wide variety of persistent chemical contaminants (*e.g.*, pharmaceuticals, hormones, personal care products, pesticides, microplastic, metal-based nanoparticles) – named contaminants of emerging concern (CEC) – have been detected in surface and groundwater, and even more serious, in drinking water after receiving treatment in conventional treatment plants.^{9, 10} When these CEC contaminants, in special organic pollutants, are detected in the environment at trace levels (*i.e.*, ng L⁻¹ to µg L⁻¹), they are called organic microcontaminants (OMCs). Indeed, as more sensitive analytical methods are developed, new compounds will be detected in the environment and they will significantly increase in number.

Pharmaceuticals and hormones contaminants may reach the sewers as a result of their ingestion and subsequent excretion by humans, while personal care products arise from

daily human hygiene practices.^{11, 12} Thus, the poor/inadequate management of these contaminants at the wastewater treatment plants (WWTPs) allow them to reach water bodies. In addition, agricultural and industrial activities are the main sources of pesticides and microplastic in the environment, respectively.^{13, 14} Furthermore, the physicochemical properties (*i.e.*, persistence and bioaccumulation) of CEC in the environment may affect the human health and aquatic ecosystems in the short and long terms, even when these contaminants are present at low concentrations.^{15, 16}

On the other hand, microbiological contaminants are classified as excreta-related pathogens (*i.e.*, bacteria, viruses, protozoa, helminths) and vector-borne pathogens (*e.g.*, *Plasmodium spp*, *Schistosoma spp*, and *Wuchereria bancrofti*), and they can be considered as another source of water contamination.¹⁷ These pathogens spend all or essential parts of their lives in water or depend on aquatic organisms to complete their life cycle. Large outbreaks caused by waterborne diseases (*e.g.*, amoebiasis, cholera, typhoid fever, shigellosis) have been mainly caused by: *Entamoeba spp*, *Campylobacter spp*, *Vibrio cholera*, *Escherichia coli*, *Salmonella spp*, *Shigella spp*, hepatitis A virus, norovirus, *Giardia duodenalis*, and *Cryptosporidium parvum* (a chlorine-resistant protozoan).¹⁸ The main origin of water contamination by pathogens are the cattle raising and municipal wastewater.¹⁹

Despite significant number of studies showing that the human health risks are associated with water contaminated by CEC and pathogens, waterborne diseases remain worldwide one of the main causes of human morbidity and mortality, especially in developing countries (*e.g.*, Brazil).²⁰ Indeed, it is estimated that one-tenth of the global load of diseases might be generated by consumption or/and exposition to polluted water. In this sense, many studies have been focused on estimating the global distribution of water contamination hazards.

Sadoff *et al.*²¹ based on many datasets (mainly on data from Vörösmarty *et al.*²²) classified the risk level of worldwide freshwater sources (water contamination index) according to the global distribution of harmful contaminants (FIGURE 1.2). This classification took into account only the effects of nutrient and pesticide load, mercury deposition, salinization, acidification, sediment, and organic load. Clearly, the addition of the effects of CEC and pathogens usually detected in freshwater bodies would improve by far the water contamination index in many regions, especially in areas with both high population density and intensely irrigated agriculture, or even highly industrialized zones. Furthermore, it is clear showed by contrasting FIGURES 1.1 and 1.2 that: even though several regions in the world have low levels

of water scarcity, *e.g.*, large parts of South America and Europe, these water sources might pose potential risks to biodiversity and human welfare.

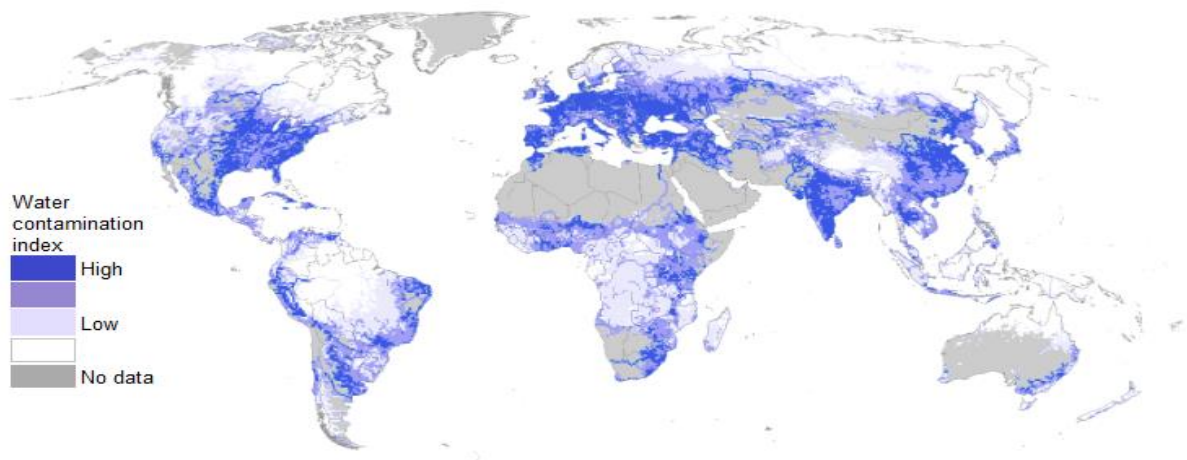


FIGURE 1.2 – Global distribution of water contamination hazard. Source: Sadoff *et al.*²¹ (2015) based on data from Vörösmarty *et al.*²² (2010).

Particularly, Brazil is a great paradox when it comes to having access to water. Despite having 12% of all freshwater reserves in the world, there are still profound inequalities among people (rural and urban communities) living in different geographical regions in Brazil and having access to water and sanitation.²³ In addition, most of the population in Brazil is concentrated in the southeast (*i.e.*, São Paulo and Rio de Janeiro) and in the northeast cities (*i.e.*, Fortaleza and Recife), where the water contamination index have showed increased rates (see FIGURE 1.2).

According to the Brazilian Sanitation Information System (*Sistema Nacional de Informações sobre Saneamento*), in 2018 about 35 million of Brazilians did not have access to drinking water and over 100 million (47% of the Brazilian population) lived without adequate sanitation or any kind of wastewater treatment (disposing of waste into a cesspool or by dumping sewage directly into the rivers).²⁴ Furthermore, Brazil is ranked as one of the topmost country in average infant death mortality and hospitalizations (adults and children), which is partly linked to severe lack of access to improved water and sanitation services.^{23, 25}

Moreover, in 2015 the severe water crisis in the metropolitan region of São Paulo kept over 20 million inhabitants of one of the largest cities in the world on edge. The Cantareira, Alto Tietê and Guarapiranga reservoirs, which are in charge of the water supply of São Paulo and other 62 metropolitan cities, reached historic low levels and, consequently, triggered the

worse crisis in water supply of the city since the past 84 years. In addition, an increasing number of studies have confirmed the presence of several CEC in different aquatic ecosystems across the state of São Paulo, for instance: paracetamol, caffeine, carbamazepine, diclofenac, naproxen, propranolol, triclosan, estrone, 17- β -estradiol, and 17- α -ethinylestradiol.²⁶⁻²⁹

Although the concentrations of pharmaceuticals found in natural waters apparently do not offer risks to human health, the continuous exposure of aquatic organisms to these compounds together with other contaminants is a serious concern to the aquatic biodiversity due to their known (and unknown) adverse effects. In addition, water supplies from non-traditional sources (including conventionally treated wastewater) have recently been proposed as an alternative to reduce the demand for freshwater (mainly for agricultural practices). However, it is believed that such practice could lead to worse problems in this environmental scenario.^{30, 31}

Consequently, the presence of these chemical and microbiological contaminants in the water have called the attention of the scientific community, regulatory agencies, environmental foundations, and governments leading to commitments to develop laws in an effort to answer issues related to the context of water quality, protection, and reclamation. However, only few countries in the world, especially European Union members and the United States, have environmental policies that include some types of CEC and their permissive levels in water, as well as regulation for water reclamation.

Therefore, The European Union Water Framework Directive established a watch list of eight substances and/or groups of substances usually detected in water that might represent environmental risks (Decision 2018/840/EU)³², among them are: pharmaceuticals (amoxicillin and ciprofloxacin), hormones (17- β -estradiol and estrone), and pesticides (imidacloprid and acetamiprid). Moreover, in 2020 The European Parliament and The Council of the European Union have approved a regulation stating the minimum requirements for wastewater reuse (Regulation 2020/741/EU)³³, which was based on the assessment and evaluation of health and environmental risks, as well as establishing minimum values of microbiological and physicochemical parameters in water.

Unfortunately, countries in developing stage such as Brazil, these contaminants are not yet regulated by any environmental law, and there is no regulation for wastewater reuse. Hence, it is extremely necessary to start debating this issue in order to get, in a near future, public policies on water quality in Brazil as well as study/develop technologies to adequately remove these contaminants. In this sense, the Brazilian Council of Water Resources (*Conselho*

Nacional dos Recursos Hídricos) by a notice of its motion nº 40 highlighted that any “research related to new contaminants in aquatic environments” and “advanced techniques to treat water for supply, with the aim to determine the new range of contaminants in the environment” should be prioritized for research and investment.³⁴

In the same way, in 2020 FAPESP (*Fundação de Amparo à Pesquisa do Estado de São Paulo*) announced a call for funding projects related to “Aquatic Pollutants: risks posed to human health and the environment by pollutants and pathogens present in water resources”.³⁵ This call was issued in collaboration with the European Union along with the JPI Oceans Initiative and the Brazilian National Council of State Funding Agencies to support the planning outlined by the Sustainable Development Goals of the United Nations in order to ensure safe water supply for all and safeguarding fresh and salt aquatic ecosystems by 2030.³⁶ More recently, FAPESP in partnership with SABESP (*Companhia de Saneamento Básico do Estado de São Paulo*) has also opened a call for funding projects related to technology and scientific innovation to improve the current limitations of the sanitation sector.³⁷

Thus, there is a pressing need to investigate and develop suitable alternatives to eliminate the contaminants and pathogens present in the water in order to reduce environmental impacts and other problems associated with the present-day water treatment technologies. The main methods utilized to remove CEC and pathogens from aqueous media (*i.e.*, water-based matrix) can be categorized into biological, chemical, and physical-chemical methods, electrochemical oxidation (mainly anodic oxidation), and Advanced Oxidation Processes (AOPs). Notably, technologies based on AOPs involve several methods, as well as a high number of mechanisms for organic contaminants removal.³⁸ However, in this thesis, only ultraviolet-based advanced oxidation processes (UVC AOPs) were considered.

Among all technologies, the biological method is one of the most low-budget alternatives for water treatment, even though it requires a large operational area and that the chemical contaminants to be treated are biodegradable. Besides, the biodegradation efficiency could be affected by the presence of some pesticides or antibiotics in the effluent, that will in turn lead to the death of microorganisms.³⁹ On the other hand, chemical methods require large amounts of reagents and generate significant amounts of sludge (*i.e.*, residue), which need to be burned or disposed of in special landfills. While consolidated tertiary treatments, *e.g.*, chlorination and ozonation, might inactivate pathogens and remove CEC, the generation of toxic disinfection by-products (*e.g.*, organochlorine, nitrosodimethylamine, and bromate) have major drawbacks.⁴⁰⁻⁴²

UVC irradiation (200–280 nm) has been extensively used for water disinfection; however this technology pose serious limitations, such as microbial regrowth and mechanisms of self-repairing DNA in microorganisms after treatment.⁴³ In addition, depending on the chemical structure of the target molecule, UVC irradiation is not appropriate for the elimination of CEC. Other potential methods of disinfection such as ultrasonication, hydrodynamic cavitation, and membrane filtration, have been effectively used to inactivate or remove microorganisms from water with low chemicals consumption. Nevertheless, these physical technologies have common shortcomings including high-energy consumption and high operating costs as well as the requirement of sophisticated reactors.⁴⁴⁻⁴⁶

Electrochemical oxidation has been extensively investigated for the removal of a wide variety of organic and inorganic contaminants (concentrations usually ranging from 50 to 100 mg L⁻¹), as well as for the inactivation of bacteria and viruses. However, this technology has some limitations, such as high-energy consumption, relatively high costs of the electrodes utilized (mainly boron-doped diamond electrode), and poor energy efficiency to remove contaminants at low concentrations (mass transport controlled reaction).^{47, 48} Nevertheless, many studies have being designed to solve these limitations. For instance, the use of alternative electrode materials (MMO-RuO₂-TiO₂, Ti/SnO₂-Sb, PTFE-β-PbO₂, etc.)⁴⁹⁻⁵¹, renewable sources for energy supply⁵², and the coupling of turbulence promoters⁵³ or radiation sources⁵⁴ (solution bulk) which minimize the limitations of mass transfer.

To overcome some of these limitations, UVC AOPs (mainly $\lambda = 254$ nm) represent a suitable alternative to over other water treatments. UVC AOPs have been investigated due to its production of a variety of highly reactive free radicals, *e.g.*, hydroxyl (HO[•]), chlorine (Cl[•]), sulfate (SO₄^{•-}), carbonate (CO₃^{•-}), etc., which might in turn lead to high rates of contaminants and microorganisms elimination.⁵⁴⁻⁵⁶ Also, UVC AOPs offer several other advantages over the methods mentioned above, for example, high mineralization rates (conversion to CO₂ and inorganic ions), low quantity or no sludge generation, and elimination of contaminants even at low concentrations (μg L⁻¹ and ng L⁻¹). Additionally, commercial UVC reactors have already been used in water and wastewater treatment plants, thus, they could be easily adapted for these processes of water decontamination.⁵⁷

Previous studies on CEC removal and pathogens inactivation by AOPs have been mainly focused on the generation of hydroxyl radical (HO[•]), a non-selective species with high oxidizing power ($E^{\circ}(\text{HO}^{\bullet}/\text{H}_2\text{O}) = 1.8\text{--}2.7$ V).⁵⁸ Among the processes used to generated HO[•] species, methods based on the activation of hydrogen peroxide (H₂O₂) are the most widely

studied, such as UVC/H₂O₂, Fenton (H₂O₂/Fe²⁺), photo-Fenton (UVA/H₂O₂/Fe²⁺ and solar/H₂O₂/Fe²⁺), and Fenton-like processes (H₂O₂/Mⁿ⁺, Mⁿ⁺ = metallic ion).⁵⁹⁻⁶¹ Contrary to Fenton based processes which use acidic solutions and require the recovery of Fe²⁺ or Mⁿ⁺ species, UVC-based systems (*e.g.*, UVC/H₂O₂) does not need previous acidification of the treated water neither an additional step to neutralize it or recover ions before its final disposal (in the environment or for reuse purposes).

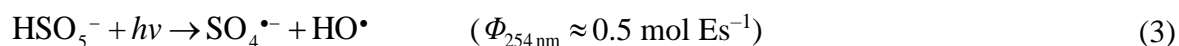
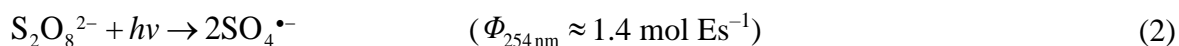
In this sense, UVC/H₂O₂ is one of the most disseminated AOPs used for organic compound degradation and water disinfection.^{61,62} In this process, HO[•] species can be produced from the homolytic cleavage of H₂O₂ by absorption of UVC radiation ($\lambda = 254$ nm), with a quantum yield of 0.5 mol Es⁻¹ (eq. 1).⁶³⁻⁶⁵



Due to its high oxidizing power, HO[•] can cause irreversible damage in microorganisms (*i.e.*, degradation of the cell membrane biomolecules) having the advantage of reacting non-selectively with organic compounds via electron transfer, hydrogen atom abstraction or electrophilic addition.⁶⁶

AOPs based on sulfate radicals (SO₄^{•-}) have been widely reported in the literature due to their property of removing recalcitrant organic compounds, and more recently, for inactivation of pathogens.⁶⁷⁻⁶⁹ This radical has an oxidation potential ($E^\circ(\text{SO}_4^{\bullet-}/\text{SO}_4^{2-}) = 2.5\text{--}3.1$ V)⁷⁰ comparable to the HO[•] species and can be generated by the activation of persulfate (S₂O₈²⁻) or peroxymonosulfate (HSO₅⁻) through heat, UVC irradiation, ultrasound, and transition-metal ions.⁷⁰⁻⁷²

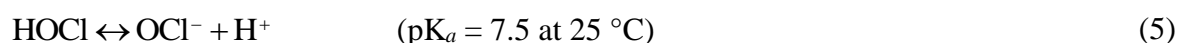
The activation (see eq. 2) of S₂O₈²⁻ by UVC light (at 254 nm) to produce SO₄^{•-} occurs through the homolytic cleavage of the “-O-O-” bond of this salt with a quantum yield 2.8 times higher than when using H₂O₂.⁷¹ Consequently, S₂O₈²⁻ absorbs photons more efficiently than H₂O₂ generating radicals with high oxidizing power. On the other hand, HSO₅⁻ photolysis occurs with a quantum yield similar to H₂O₂ but with a direct generation of SO₄^{•-} and HO[•] species (eq. 3). Another advantage is that the half-life of SO₄^{•-} is longer than the HO[•] species ($t_{1/2}$, SO₄^{•-} = 30-40 μ s *vs.* $t_{1/2}$, HO[•] = <1 μ s), which allows a greater availability and interaction with contaminants through the water matrix, possibly increasing the degradation/disinfection rate.⁷³ In addition, SO₄^{•-} species generated can react with H₂O molecules resulting in the production of HO[•] (see eq. 4).



Due to the electrophilic nature of $\text{SO}_4^{\bullet-}$ species, these radicals can react with aromatic compounds through three main mechanisms: *i*) radical adduct formation, *ii*) hydrogen atom abstraction, and *iii*) single electron transfer.⁷⁴⁻⁷⁶ In addition, depending on the properties of the electron-donating/withdrawing functional groups in the aromatic compound, the $\text{SO}_4^{\bullet-}$ can lead to high oxidation rates of specific contaminants.⁷⁴

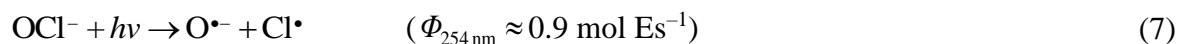
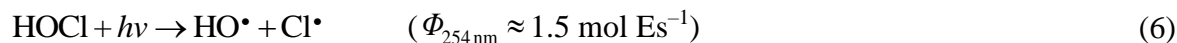
Regarding the disinfection process, fundamental investigations have been established on the inactivation of different microorganisms by $\text{SO}_4^{\bullet-}$, particularly the interaction of $\text{SO}_4^{\bullet-}$ with biomolecules of the cell wall. However, the molecular mechanisms of microorganisms inactivation are far to be fully understood.⁵⁶ Consequently, in recent years, this methodology has attracted growing attention due to its application in CEC degradation; however, there is still a huge gap to be filled when comparing to studies that have implemented this methodology for water disinfection purposes.

Free chlorine (*i.e.*, Cl_2 , HClO , and ClO^-) is one of the most recurrent oxidizing species in solutions used to deactivate dangerous pathogens due to their medium to high oxidation power, low cost, and high accessibility when compared to other reactive oxygen species used in AOPs.⁷⁷⁻⁷⁹ Hypochlorous acid (HClO) is a weak acid that can co-exist in aqueous solution with its conjugate base the hypochlorite ion (ClO^-), according to the equilibrium reaction shown in eq. (5). The relative concentration of each free chlorine species is strongly dependent on many variables, such as pH, temperature, and ionic strength. HClO is the main specie in acidic and neutral conditions ($\text{pH} = 3-7$).⁸⁰



Also, HClO can be also used to produce HO^\bullet through a homolysis reaction in combination with an UVC source, as showed in eq. (6).⁸⁰ However, the simultaneous formation of chlorine radical (Cl^\bullet), which might be as effective as HO^\bullet and $\text{SO}_4^{\bullet-}$ species to oxidation of pollutants ($E^\circ(\text{Cl}^\bullet/\text{Cl}^-) = 2.4 \text{ V}$)⁸¹, can produce chlorinated intermediate compounds as one of the main drawbacks. Cl^\bullet species can also degrade contaminants through hydrogen atom abstraction, single electron transfer or addition to unsaturated bonds.⁸² According to Chuang *et al.*⁸³ the UVC/ HClO method can achieve a higher HO^\bullet production than the UVC/ H_2O_2 process due to its

superior quantum yield.⁷¹ Consequently, the energy necessary to treat solutions containing organic pollutants using the UVC/HClO method can be significantly lower in comparison with conventional UVC AOPs.



In alkaline conditions, ClO^- is the predominant species, absorbing photons of energy and generating $\text{Cl}\cdot$ and the radical ion $\text{O}\cdot^-$ (eq. 7), which in turn will generate another $\text{HO}\cdot$ via hydrolysis (eq. 8). This latter system is less efficient in generating radicals when compared to the UVC/HClO system (acidic and neutral conditions) since the quantum yield for the ClO^- homolysis is lower than the HClO and remains constant regardless of its concentration in the system. As reported by Feng *et al.*,⁸⁰ the quantum yield for the HClO homolysis can increase until 4.5 ± 0.2 when the HClO concentration range from 71 to 1350 mg L^{-1} . However, it is speculated that the higher quantum yield at higher HClO concentrations might be due to parasitic propagation reactions as shown by eqs. (9–10).



Hypochlorite radicals ($\text{ClO}\cdot$) might also play an important role in the degradation of pollutants due to its medium-high oxidation potential ($E^\circ = 1.5\text{--}1.8 \text{ V}$); however, the reaction mechanism of this secondary radical with organic compounds is still unclear. Therefore, the UVC/HClO is one of the most efficient free chlorine-based systems for pollutant degradation and the most studied in the literature so far. Another advantage of this methodology is related to the residual amount of HClO after treatment using the UVC/HClO process, which is not considered a concern since the final post-chlorination step is usually required for water disinfection against regrowth of bacteria and external contamination.⁷⁸

As mentioned above, one of the main drawbacks of the UVC/HClO process is the possible generation of organochlorine by-products mainly related to the pollutant degradation process. However, in a previous study⁵⁴, this issue has demonstrated to be minimized by the optimization of important parameters of the system, such as the power of the UVC lamp and free chlorine concentration. Pertaining to the same study just mentioned above (tebuthiuron herbicide oxidation; 100 mg L^{-1}), no organochlorine compounds were detected

(after 6 h) and the total organic carbon was almost completely removed by the use of a low-pressure Hg lamp (UVC lamp; 9 W) with low energy consumption.

Within this framework, this thesis aimed to investigate and compare the efficiency of different UVC AOPs in the removal CEC and/or inactivate pathogens from distinct water matrices. The first study was focused on evaluating the degradation and mineralization rates of synthetic solutions containing bisphenol A (BPA) by the use of UVC/H₂O₂, UVC/S₂O₈²⁻, and UVC/HClO processes at a fundamental level (*i.e.*, at laboratory scale, using distilled water, and in the absence of any microorganisms). For the second study, UVC/H₂O₂ and UVC/S₂O₈²⁻ processes were investigated for the simultaneous removal of CEC and pathogens from a simulated wastewater effluent at pilot plant scale. Also, the influence of the oxidant residual concentration on the bacterial regrowth was analyzed to be considered in agricultural applications as a reusable source of water.

2. CHAPTER 1: UVC-based removal of macrocontaminants at laboratory scale

This chapter is an adaptation of the article “*Comparison of UVC-based advanced oxidation processes in the mineralization of bisphenol A: identification of oxidation by products and toxicity evaluation*” by Isaac Sánchez-Montes, Naihara Wachter, Bianca F. Silva, and José M. Aquino.

Chemical Engineering Journal, DOI: 10.1016/j.cej.2019.123986



Comparison of UVC-based advanced oxidation processes in the mineralization of bisphenol A: Identification of oxidation by products and toxicity evaluation

Isaac Sánchez-Montes^a, Naihara Wachter^a, Bianca F. Silva^b, José M. Aquino^{a,*}

^a Departamento de Química, Universidade Federal de São Carlos, C.P. 676, 13560-970 São Carlos SP, Brazil

^b Instituto de Química de Araraquara, Departamento de Química Analítica, Universidade Estadual Paulista, 14800-900 Araraquara SP, Brazil

2.1. ABSTRACT

The performance of three different UVC AOPs (UVC/H₂O₂, UVC/S₂O₈²⁻, and UVC/HClO) based on the homolysis of oxidants were investigated for the degradation and mineralization of BPA containing solutions as well as assessment of toxicity and identification of oxidation by-products. In all AOPs, UVC irradiation led to a significant improvement for the degradation and mineralization of BPA due to the production of HO[•]/SO₄^{•-} species. UVC/HClO method was able to achieve high rates of conversion of BPA and its oxidation by-products to CO₂. All detected oxidation by-products resulted from hydroxylation reactions. Considering the short chain carboxylic acids, mainly produced after opening the aromatic ring, high concentrations appeared mainly during the first two hours of treatment for the UVC/HClO method with a complete elimination within 6 h of treatment, including the dichloroacetic acid. Toxicity assays using *Artemia salina* crustacean showed that the mortality was ceased after 4 h of treatment using the UVC/HClO and UVC/S₂O₈²⁻ processes. In contrast, a low mortality decrease was observed when using the UVC/H₂O₂ process, probably due to the accumulation of toxic intermediates. In all scenarios, toxicity of the BPA compound and its oxidation by-products seem to be responsible for the distinct decays of mortality, as confirmed on the ECOSAR software. Finally, the UVC/HClO method is an interesting option considering the removal levels attained and operational costs.

2.2. SHORT INTRODUCTION

Many studies have reported the frequent toxic effect of some CEC, such as pharmaceuticals, hormones, pesticides, and microplastic, found in different sources of water.⁸⁴⁻⁸⁶ These findings emphasize the necessity to remove, inactivate, or transform CEC into less toxic by-products than the initial compound before their disposal into the environment.⁸⁷⁻⁸⁹

BPA is a controversial endocrine disruptor that may interfere with natural hormone activity in humans and aquatic organisms. This chemical may cause fish feminization and reproductive problems, which represents a risk to the ecological balance in the aquatic environment.⁹⁰ According to the US Environmental Protection Agency (USEPA), endocrine disruptors can be defined as exogenous agents, which even at low concentrations ($\mu\text{g L}^{-1}$), have the ability to interfere with the endocrine system. These effects can include: developmental malformations, interference with reproduction, increased cancer risk, and disturbances in the immune and nervous system function.⁹¹ On the other hand, BPA is one of the most common microcontaminants detected in freshwater bodies in Brazil.⁹²

Among the available methods to treat contaminated solutions, investigations have increasingly focused on the UVC AOPs for the production of a large variety of short-lived radicals, *e.g.*, hydroxyl (HO^{\bullet}), chlorine (Cl^{\bullet}), sulfate ($\text{SO}_4^{\bullet-}$), carbonate ($\text{CO}_3^{\bullet-}$), quite feasible leading to high elimination rates of organic pollutants at ambient temperature and pressure.^{62, 68, 88, 93} Even though previous studies had investigated the efficiency of different UVC AOPs using distinct oxidizing agents,^{55, 71, 94} such as H_2O_2 , $\text{S}_2\text{O}_8^{2-}$, HClO , and HSO_5^- , to the best of our knowledge none of those works compare the performances of UVC/ H_2O_2 , UVC/ $\text{S}_2\text{O}_8^{2-}$ and UVC/ HClO processes in terms of total organic carbon (TOC) removal, identification of oxidation by-products (long and short chain), and particularly toxicity evolution during treatment.

Thus, we aimed at investigating the degradation and mineralization (conversion to CO_2) levels and rates of synthetic solutions of BPA using the above-mentioned UVC AOPs, *i.e.*, UVC/ H_2O_2 , UVC/ $\text{S}_2\text{O}_8^{2-}$ and UVC/ HClO homogeneous processes. We will assess and compare the possible synergistic effects through experiments using only the UVC lamp (photochemical process) or addition of oxidants (chemical process). To investigate the main susceptible sites to the addition reactions generated from the electrophilic HO^{\bullet} species in the BPA molecule, high-performance liquid chromatography (HPLC) will be used to monitor the BPA concentration evolution, main generated short-chain carboxylic acids, and long chain oxidation by-products coupled to mass spectrometry. Finally, we will assess and compare the

toxicity evolution of the treated solutions towards *Artemia salina*, an aquatic crustacean, with the oxidation by-product compounds and TOC removal found.

2.3. MATERIALS AND METHODS

2.3.1. Chemicals

All chemicals including BPA (99%, Sigma-Aldrich), H₂O₂ (29–31%, Synth), Na₂S₂O₈ (a.r., Sigma-Aldrich), and NaClO (10–12%, Nalgon) were used without further purification. All carboxylic acid, benzoic acid, salicylic acid, and short-chain carboxylic acids were purchased from Sigma-Aldrich. For other analysis were used the following chemicals: H₂SO₄ (a.r., Mallinckrodt), NaOH (a.r., Synth), Na₂S₂O₃ (a.r., Qhemis), KI (a.r., Sigma-Aldrich), NH₄OH (28–30%, Macron), H₃PO₄ (85%, Mallinckrodt), ethanol (>99%, Synth), isopropanol (>99%, Qhemis), tert-butyl alcohol (99%, Exodo), acetonitrile (HPLC grade, JT Baker). The preparation of all solutions used deionized water (Millipore Milli-Q system, $\rho \geq 18.2 \text{ M}\Omega \text{ cm}$).

2.3.2. Degradation and mineralization experiments

UVC AOPs experiments for the oxidation of BPA (0.44 mmol L⁻¹) solutions were carried out using a glass vessel of 1.5 L equipped with a magnetic stirrer and a quartz tube. A 9 W UVC lamp (main emission line at 253.7 nm from Phillips) with a fluency rate of 20.2 mW cm⁻² was inserted inside the tube (see FIGURE 2.1). Details on the fluency rate calculation and other information is available in the APPENDIX A (TEXT A1 and FIGURE A1). Control experiments were carried out using only the oxidants (H₂O₂, Na₂S₂O₈, or HClO – chemical method) or UVC lamp (photochemical method) to better understand the synergistic effect resulting from coupling these methods.

As the literature reports⁹⁵⁻¹⁰², the use of high initial oxidant concentrations in UVC AOPs leads to recombination reactions of radicals, thus reducing their efficiency in the CEC degradation and mineralization (see rate constants for some self-scavenging reactions in the APPENDIX A (TABLE A1). To avoid these undesirable reactions, we continuously added freshly prepared solutions of the oxidants (0.6 mol L⁻¹) to the reaction vessel during the experiments at a flow rate of 0.1 mL min⁻¹ using a peristaltic pump (Gilson Miniplus 3).

The solution pH was maintained around 3.0 by adding concentrated H₂SO₄ or NaOH solutions. Other operational variables, such as treatment time, solution temperature, and solution volume, were maintained fixed at 360 min, 38 °C, and 1.0 L, respectively. Before

further analyses, a few drops of a concentrated reducing solution of $\text{Na}_2\text{S}_2\text{O}_3$ to BPA extracted samples in order to avoid oxidation generated from any residual oxidant.



FIGURE 2.1 – Image of the experimental setup used during the degradation and mineralization of BPA solutions through different UVC AOPs: reservoir (1), quartz tube with the UVC lamp inside it (2), and peristaltic pump (3).

2.3.3. Analyses

The concentration evolution of BPA (detected at 280 nm) was monitored through high-performance liquid chromatography (HPLC) using a core-shell C-18 reversed phase as the stationary phase (Phenomenex[®]: 150 mm×4.6 mm, 5 μm particle, 100 \AA) and a mixture (60:40 V/V) of aqueous 0.1% (V/V) formic acid and acetonitrile (ACN) as the mobile phase. An isocratic elution mode was used at 1.0 mL min^{-1} . The injection volume and temperature of the column were 25 μL and 23 $^{\circ}\text{C}$, respectively. For analysis purposes, the BPA removal during the UVC AOPs was expressed in its remaining fraction, *i.e.*, as $x_{\text{BPA}}^{\text{rem}} = [\text{BPA}]_t / [\text{BPA}]_0$, in which $[\text{BPA}]_t$ and $[\text{BPA}]_0$ are the values at time t and prior to the experiment, respectively.

Analyses of liquid chromatography coupled to a mass spectrometer (LC-MS/MS) were used to determine the intermediates produced during BPA degradation. For this purpose, samples (2 mL) were collected at predetermined times, filtered using a 0.22 μm polypropylene cartridge coupled to a glass syringe and injected without any further preparation. The analyses were performed in a 1200 Agilent Technologies HPLC coupled to a 3200 QTRAP mass spectrometer (QqLIT – Linear Ion Trap Quadrupole LC-MS/MS Mass Spectrometer),

AB SCIEX Instruments, operating in a negative mode, and TurboIonSpray ionization. The software Lightsight[®] 2.3 (Nominal Mass Metabolite ID Software, AB SCIEX) was used to investigate all possible by-products after optimizing the ionization and fragmentation parameters for the initial compound.

These parameters were obtained using a direct infusion of 10 $\mu\text{L min}^{-1}$ of a solution containing BPA (0.44 mmol L^{-1}) in ACN:H₂O (1:1 V/V) with 0.1% of ammonium hydroxide. The MS/MS conditions were: curtain gas at 20 psi, ion spray at -4500 V, gas 1 and gas 2 at 50 psi, temperature of 650 °C, interface heater on, declustering potential, entrance potential, and cell entrance potential were of -50, -9.5, and -21 V, respectively. Optimized selected multiple reaction monitoring (SRM) and fullscan experiments were performed automatically on the LightSight[®] software. Different types of reactions were investigated, such as oxidation, hydroxylation, reduction, C-C bond cleavage, chlorination, among others. During the MS/MS experiments, the HPLC analyses were performed as aforementioned, but with the addition of an injection volume of 20 μL and ammonium hydroxide into the H₂O component of the mobile phase to reach a final concentration of 0.1% (V/V).

The short chain carboxylic acids were also determined during the degradation experiments through HPLC using a Rezex[™] ROA-H column (Phenomenex[®]: 300 mm \times 7.8 mm, 8 μm particle) as the stationary phase and a 2.5 mmol L^{-1} H₂SO₄ solution as the mobile phase at 0.5 mL min^{-1} . Before these analyses, samples collected at predetermined times were filtered using a 0.22 μm polypropylene cartridge coupled to a glass syringe. The carboxylic acids (detected at 210 nm) were identified by comparison of their retention times with those of previously analyzed standards. The injection volume and column temperature were 25 μL and 23 °C, respectively.

The concentration evolution of oxidants was determined by two different methods using a UV-Vis spectrophotometer (Shimadzu UV-1800). The iodometric method used to determine S₂O₈²⁻ and HClO concentrations was adapted from Liang *et al.*¹⁰³ Briefly, 90 μL of a 0.093 mol L^{-1} ammonium molybdate solution and 140 μL of a 2.5 mol L^{-1} KI solution were added to 3.5 mL of sample previously acidified with glacial acetic acid; subsequently, the samples were analyzed at 351 nm. The spectrophotometric method used to measure the H₂O₂ concentration, in turn, was adapted from Chai *et al.*¹⁰⁴ following a similar procedure, but without KI addition. In this case, the peroxomolybdate complex formed was spectrophotometrically measured at 350 nm.

The extent of mineralization (*i.e.*, conversion to CO₂) was monitored through total organic carbon concentration ([TOC]) measurements using a GE Sievers Innovox analyzer. The [TOC] determination was carried out after mixing a diluted volume of the treated sample (collected every 1 h) with H₃PO₄ (6 mol L⁻¹) and Na₂S₂O₈ (30% *m/V*) solutions. The TOC content was determined by subtraction of the measured values of inorganic and total carbon, in terms of generated CO₂, and after comparison with a previously determined calibration curve, using a non-dispersive infrared detector. Once more, for analysis purposes, the removal of TOC during the treatment is expressed in its remaining fraction, *i.e.*, as $x_{\text{TOC}}^{\text{rem}} = [\text{TOC}]_t / [\text{TOC}]_0$, in which [TOC]_{*t*} and [TOC]₀ are the values at time *t* and prior to the experiment, respectively.

Acute toxicity assays were carried out using the crustacean *Artemia salina* (*A. salina*), whose main advantage is their tolerance to variable pH, temperature, and dissolved oxygen conditions in saline medium, despite being less sensitive than other testing organisms.^{105, 106} The tests were carried out according to the work of Vanhaecke *et al.*¹⁰⁷, with some modifications.¹¹¹ Initially, approximately 500 mg of *A. salina* cysts (from Maramar Brazil) was incubated in a rectangular aquarium containing 500 mL of freshly prepared artificial seawater (3.5% *m/m* synthetic sea salt from Blue Red Sea) at ambient temperature (23 °C). The experimental setup can be seen in FIGURE 2.2. After 24 h of incubation under constant illumination and aeration, *nauplii* that were in the illuminated side of the aquarium were sucked with a Pasteur pipette and transferred to a beaker containing freshly prepared artificial seawater. Then, the collected *nauplii* were incubated for another 24 h in the same conditions to molt to the instar II or III larval stages. At the end of this period, the crustaceans were poured into a Petri dish for counting.

The toxicity tests were carried out in triplicate using glass tubes containing 10 mL of initial and treated samples after adding a few drops of Na₂S₂O₃ solution. Negative and positive controls contained artificial seawater (3.5% *m/m*) with 20.0 mmol L⁻¹ Na₂S₂O₃ and artificial seawater with varying concentrations of sodium dodecyl sulfate (SDS; 10.0, 13.5, 18.0, 24.0, and 32.0 mg L⁻¹), respectively. SDS, which is known as a reference toxicant for *A. salina*, was used to ensure the quality of the cysts and conducted experiments to determine the median lethal concentration (LC₅₀) of BPA at specific values (3.12, 6.25, 12.5, 25.0 and 50.0 mg L⁻¹ in artificial seawater 3.5% *m/m*). The LC₅₀ values for the SDS positive control and BPA compound followed the Trimmed Spearman-Kärber

method.¹⁰⁸ The percentage of mortality was expressed by the ratio between the number of dead organisms and the total number of organisms.

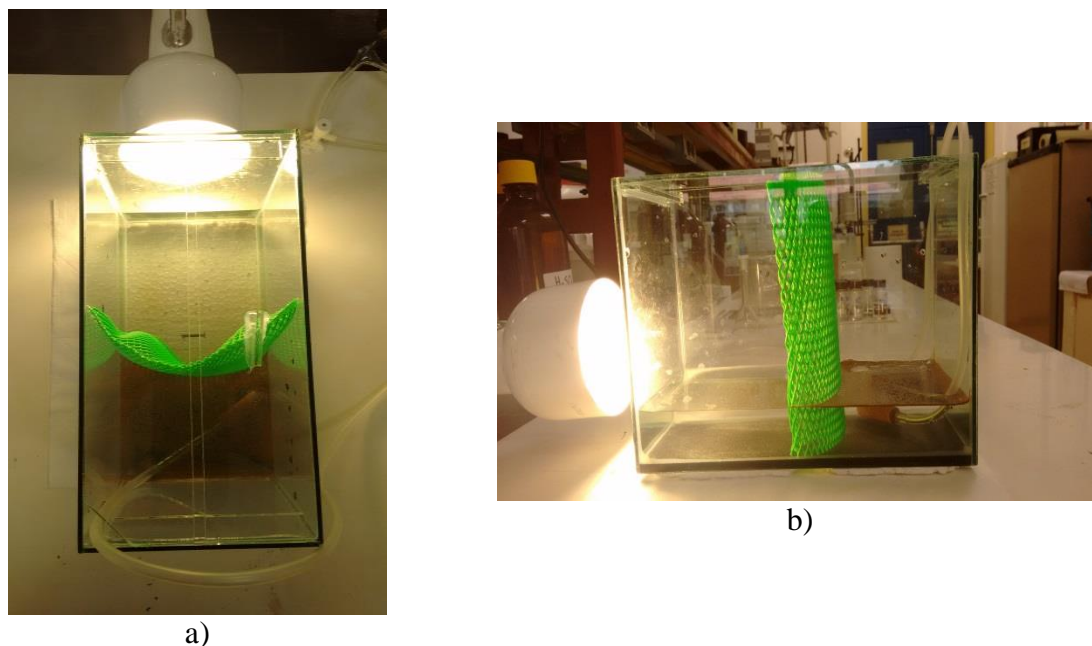


FIGURE 2.2 – Images of the experimental configuration used for breeding of *A. salina*: a) top and b) side views of the system composed by a fluorescent lamp (14 W), a plastic separator (5-mm holes), an air pump, and an aquarium (200×100×150 mm) containing the artificial seawater solution and *A. salina* cysts (opposite to the lighting side; darkest region).

It has been increasingly relevant to predict the toxicological effects of new chemical compounds and degradation by-products based on their chemical structure and physical properties since a trustworthy prediction can substitute experimental tests using animals. Thus, quantitative structure–activity relationships (QSARs) analysis through the ecological structure–activity relationship (ECOSAR) model was conducted to demonstrate the baseline acute and chronic toxicity at three different trophic levels (*i.e.*, *fish*, *daphnid*, and *green algae*) for the BPA molecule and by-products identified through LC–MS/MS analyses. The ECOSAR v1.11 program, developed by USEPA, can estimate toxicity of chemical compounds based on data from structurally similar chemical classes.¹⁰⁹⁻¹¹³

The extent of total mineralization (φ) was calculated through the ratio between the removal fractions of TOC and BPA after a given time of treatment and using eq. (11):¹¹⁴

$$\varphi = \frac{1 - x_{\text{TOC}}^{\text{rem}}}{1 - x_{\text{BPA}}^{\text{rem}}} \quad (11)$$

The φ value indicates the degree of BPA molecules conversion to CO₂ or other intermediate compounds, which can range from 0 to 1 – no mineralization or total mineralization of the oxidized BPA molecule, respectively.

Finally, an economic comparison between the investigated processes was performed based on the total cost per order of BPA or TOC removal, *i.e.*, Cost/O_{TOTAL} (\$ m⁻³ order⁻¹), encompassing costs of electric energy (Cost/O_{UVC}) added with 45% of maintenance costs¹¹⁵ and chemicals (Cost/O_{OX}), as shown in eq. (10). The Cost/O_{UVC} (\$ m⁻³ order⁻¹) is determined by the electric energy (EE in kW) required to oxidize or mineralize the target pollutant by one order of magnitude in 1.0 m³ of water per order (O_{UVC}), as shown in eqs. (12–14):¹¹⁶

$$\text{Cost/O}_{\text{TOTAL}} = \text{Cost/O}_{\text{UVC}} + \text{Cost/O}_{\text{OX}} \quad (12)$$

$$\text{Cost/O}_{\text{UVC}} = 1.45 \frac{\text{EE}}{\text{O}_{\text{UVC}}} \text{electricity cost} \quad (13)$$

$$\frac{\text{EE}}{\text{O}_{\text{UVC}}} = \frac{2.303P}{60Vk} \quad (14)$$

where P is the power output (*i.e.*, $P = \text{fluency rate} \times \text{illuminated area of the reservoir} = 20.2 \text{ mW cm}^{-2} \times 782 \text{ cm}^2 = 15.8 \text{ W}$), t the reaction time (h), V the solution volume (m³), k the rate constant (pseudo-first order in min⁻¹), 2.303 is a conversion factor for logarithm, and 60 is another conversion factor (min h⁻¹). On the other hand, for comparison purposes, P can be also used as the rated power of UVC lamp (9 W). The average electricity cost is 0.1 \$ kW⁻¹ h⁻¹ according to the Brazilian electricity regulatory agency in 2017.

2.4. RESULTS AND DISCUSSION

2.4.1. Degradation and mineralization of BPA using different UVC AOPs

Firstly, control experiments were carried out to explore the extent of BPA oxidation (0.44 mmol L⁻¹) in aqueous solution using only UVC irradiation (photochemical method) or distinct oxidants (H₂O₂, Na₂S₂O₈, or HClO – chemical method). FIGURE 2.3(a–b) shows the evolution of the remaining fraction of BPA ($x_{\text{BPA}}^{\text{rem}} = [\text{BPA}]_t/[\text{BPA}]_0$) and TOC ($x_{\text{TOC}}^{\text{rem}} = [\text{TOC}]_t/[\text{TOC}]_0$) as a function of treatment time for the photochemical and chemical methods at pH 3 and 38 °C.

As illustrated in FIGURE 2.3(a), a significant BPA removal (55%) was achieved after 360 min using exclusively the UVC lamp. The BPA degradation through the UVC

irradiation can be attributed to the absorption capacity of light by the BPA molecule, which is measured through the molar absorption coefficient ($\epsilon_{254 \text{ BPA}} = 912 \text{ M cm}^{-1}$) and quantum yield ($\Phi_{254 \text{ BPA}} = 0.0075 \text{ mol Es}^{-1}$). These two fundamental parameters drive the direct photolysis rate. Thus, under UVC irradiation, the BPA molecule absorbs emitted photons that are capable to induce electron state transitions resulting in the formation of excited BPA molecules (BPA*). These molecules may lose their excess energy after decomposition with the consequent generation of by-products.

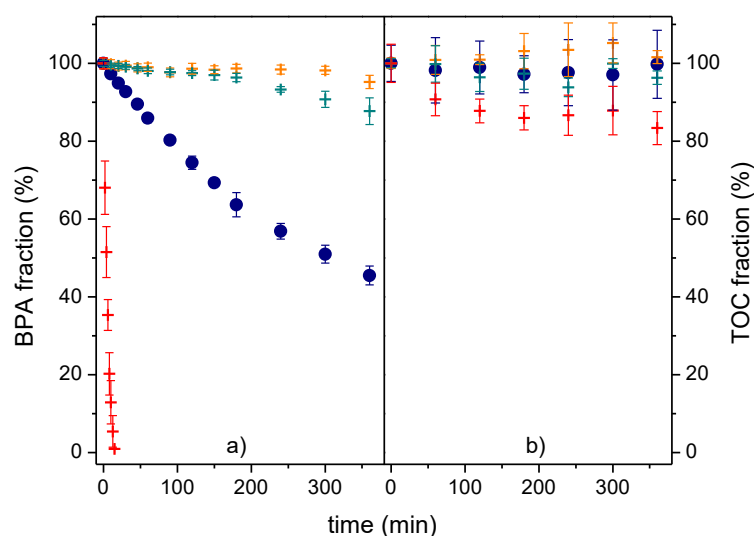


FIGURE 2.3 – Remaining a) BPA and b) TOC fraction as a function of treatment time for the photochemical (●) and chemical (H_2O_2 (+), $\text{S}_2\text{O}_8^{2-}$ (+), and HClO (+)) processes. Conditions: 0.6 mol L^{-1} of oxidant (flow rate 0.1 mL min^{-1}), pH 3, and $38 \text{ }^\circ\text{C}$. Error bars refer to two and three repetitions for the BPA and TOC determinations, respectively.

The chemical process using H_2O_2 and $\text{Na}_2\text{S}_2\text{O}_8$ as oxidant agent led to very low degradation rates even after 360 min, suggesting that the BPA molecule is recalcitrant towards oxidation using those chemicals. In contrast, the chemical method was able to quickly ($\sim 10 \text{ min}$) oxidize the BPA molecule in the presence of HClO ($3.2 \pm 0.5 \times 10^{-1} \text{ min}^{-1}$), probably due to the high rates of electrophilic substitution reactions in the aromatic rings of the BPA molecule. Yamamoto & Yasuhara¹¹⁷ and Lane *et al.*¹¹⁸ also found fast oxidation reaction of BPA when performing chlorination reaction in neutral to alkaline solutions. As expected for the photochemical and chemical processes, BPA oxidation did not result in significant levels of conversion to CO_2 , *i.e.*, mineralization, but only to accumulation of by-products in the reaction medium, as shown in FIGURE 2.3(b).

Subsequently, distinct UVC AOPs, *i.e.*, H_2O_2 , $\text{S}_2\text{O}_8^{2-}$, and HClO under UVC irradiation were carried out to assess their performance towards the degradation and mineralization of BPA, as shown in FIGURE 2.4(a–b). Clearly, oxidation of the BPA molecule improved significantly when using the UVC/ H_2O_2 or UVC/ $\text{S}_2\text{O}_8^{2-}$ methods in relation to their chemical processes, *i.e.*, complete removal was achieved after 300 and 120 min, respectively. This resulted from the activation of these oxidants by the UVC irradiation (particularly at 254 nm) to mainly produce the electrophilic HO^\bullet and $\text{SO}_4^{\bullet-}$ species (see eqs. 1–2), which react with the BPA molecule and its oxidation by-products through addition/abstraction reactions. In the case of the UVC/ HClO method, no significant improvements were observed in the degradation rate and level as the HClO species promptly react with the BPA molecule, as previously discussed.

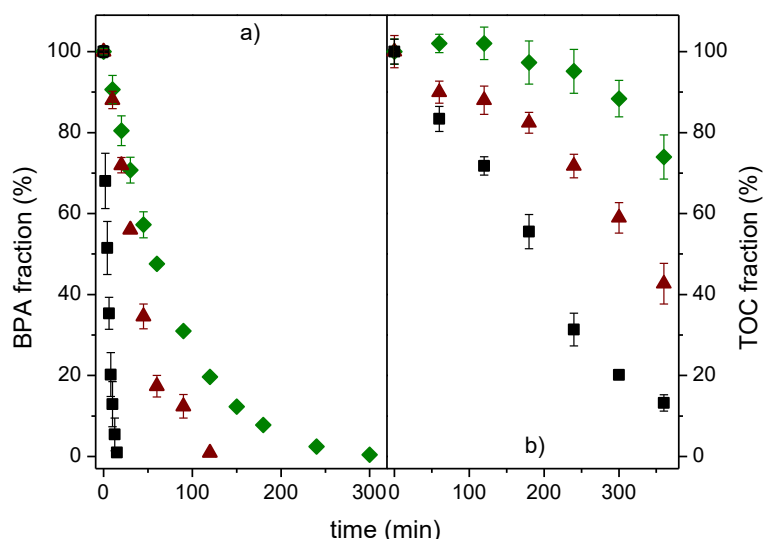


FIGURE 2.4 – Remaining a) BPA and b) TOC fraction as a function of treatment time for the UVC/ H_2O_2 (◆), UVC/ $\text{S}_2\text{O}_8^{2-}$ (▲), and UVC/ HClO (■) processes. Conditions: 0.6 mol L^{-1} of oxidant (flow rate 0.1 mL min^{-1}), pH 3, and $38 \text{ }^\circ\text{C}$. Error bars refer to two and three repetitions for the BPA and TOC determinations, respectively.

TABLE 2.1 presents the values obtained for the pseudo-first order kinetic constants (k) regarding the degradation and mineralization of BPA upon the use of distinct UVC AOPs. As expected, the UVC/ HClO process had higher degradation rate values ($270 \pm 6 \times 10^{-3} \text{ min}^{-1}$) than the UVC/ $\text{S}_2\text{O}_8^{2-}$ ($35 \pm 2 \times 10^{-3} \text{ min}^{-1}$) and UVC/ H_2O_2 ($15 \pm 0.3 \times 10^{-3} \text{ min}^{-1}$) processes. Therefore, for the last two methods, it is clear that the generation of HO^\bullet (and also $\text{SO}_4^{\bullet-}$ when using $\text{S}_2\text{O}_8^{2-}$) species might have improved the oxidation towards BPA. Furthermore, the rate constant in UVC/ $\text{S}_2\text{O}_8^{2-}$ is slightly higher than in UVC/ H_2O_2 due to the higher quantum yield

and the additional HO[•] species generated from the reaction of SO₄^{•-} species with H₂O (see eq. (4)).

TABLE 2.1 – Pseudo-first order kinetic constants (*k*) for the removal of BPA and TOC using different UVC AOPs.

Process	<i>k</i> (BPA [†]) / 10 ⁻³ min ⁻¹ *	<i>k</i> (TOC ^{††}) / 10 ⁻³ min ⁻¹ *
UVC/H ₂ O ₂	15.0±0.3 (0.994±0.004)	1.3±0.2 (0.889±0.06)
UVC/S ₂ O ₈ ²⁻	35±2 (0.950±0.001)	2.3±0.3 (0.870±0.02)
UVC/HClO	270±6 (0.921±0.05)	5.8±0.3 (0.938±0.04)

[†]mean values obtained after two repetitions.

^{††}mean values obtained after three repetitions.

*The value in parentheses refers to the mean coefficient of determination (R²) of the linear regression carried out to determine the respective value of *k*.

Similarly, Sharma *et al.*¹¹⁹ found that the UVC/S₂O₈²⁻ process ($k = 9.4 \times 10^{-3} \text{ min}^{-1}$) is more efficient for the BPA degradation (0.22 mmol L⁻¹) than the UVC/H₂O₂ process ($k = 5.4 \times 10^{-3} \text{ min}^{-1}$). The *k* values achieved ranged one order of magnitude below those found in this work, even when using a 40 W UVC lamp. Sanchez-Polo *et al.*¹²⁰ also obtained similar values for *k* (~10⁻³ min⁻¹) as well as 80% and 70% of BPA degradation (0.044 mmol L⁻¹) after 180 min for the UVC/S₂O₈²⁻ and UVC/H₂O₂ methods, respectively, despite using a high power (700 W) mercury medium pressure lamp. The low efficiency towards BPA oxidation reported in these works could be attributed to the self-scavenging reactions of radicals (SO₄^{•-}, HO[•], HO₂[•], O₂^{•-}, etc.) upon a high initial oxidant concentration in solution (TABLE A1). Clearly, this issue could be minimized by continuously adding oxidants, as carried out in this study.

On the other hand, for the UVC/HClO method, it is not clear whether the HO[•] and Cl[•] species (see eq. 6) mediated the BPA degradation process or if it was only the effect of direct chlorination reaction mediated by HClO oxidation. However, an analysis of the BPA mineralization, FIGURE 2.4(b), reveals a high conversion level to CO₂ (90% mineralization after 360 min), which is probably due to the action of radical species (mainly HO[•]). These results are more satisfactory than that achieved using the UVC/H₂O₂ (~30%) and UVC/S₂O₈²⁻ (60%) processes, which is also demonstrated in the calculated mineralization rate constants in TABLE 2.1. In addition, all coupled methods had improved their performance upon the use of UVC light due to the formation of HO[•] and SO₄^{•-} (when using S₂O₈²⁻) species, despite the distinct levels attained. Sharma *et al.*¹¹⁹ also reported similar mineralization levels for BPA when using UVC/H₂O₂ (38%) and UVC/S₂O₈²⁻ (55%) processes after 360 min of treatment.

More recently, researches have applied the UVC/HClO method to eliminate various CEC (herbicides, pharmaceuticals, insecticides, etc.)^{93, 121-123}; however, only few works have reported high TOC removal levels, which is an important parameter from the environmental point of view. Yin *et al.*¹²² investigated the oxidation of two neonicotinoid insecticides (imidacloprid and thiacloprid) using the UVC/HClO process (full HClO addition at the beginning of treatment) for both compounds and reached only ~30% of mineralization in relation to ~90% reported in this study, demonstrating the advantage of continuously adding the HClO oxidant.

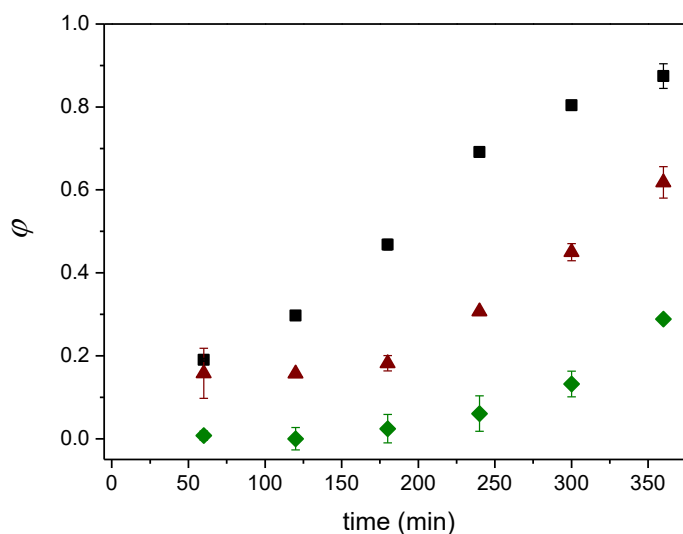


FIGURE 2.5 – Extent of total mineralization (ϕ) as a function of time for the UVC/H₂O₂ (◆), UVC/S₂O₈²⁻ (▲), and UVC/HClO (■) processes. Conditions: 0.6 mol L⁻¹ of oxidant (flow rate 0.1 mL min⁻¹), pH 3, and 38 °C. Error bars refer to two and three repetitions for the BPA and TOC determinations.

In contrast, degradation and mineralization rates obtained in this work corroborate to the theoretical kinetic model proposed by Li *et al.*⁷¹, which estimated the performance of these UV-based oxidation technologies. The model predicted that photolysis of the HClO, S₂O₈²⁻, and H₂O₂ oxidants mediated by UVC irradiation (*i.e.*, radical production) and their performance towards organics oxidation follows the order: UVC/HClO > UVC/S₂O₈²⁻ > UVC/H₂O₂. As expected for the superior degradation and mineralization of BPA using the HClO/UVC method, high values (close to 1.0) for the extent of total mineralization (ϕ) were achieved after 360 min, as shown in FIGURE 2.5. Low ϕ values for the UVC/S₂O₈²⁻ and UVC/H₂O₂ methods indicate an accumulation of oxidation by-products of BPA in the reaction medium.

2.4.2. Synergistic effect of UVC AOPs: the role of HO^\bullet , $\text{SO}_4^{\bullet-}$, and Cl^\bullet species

To better understand the synergistic effect associated with the coupled processes, the experimental curves for the remaining fractions of BPA and TOC as a function of treatment time using the different UVC AOPs were compared with the theoretical curves obtained from the summation of the experimental remaining fractions of the photochemical and chemical processes used separately.

The experimental and theoretical curves for the remaining fractions of BPA and TOC for the UVC/ H_2O_2 , UVC/ $\text{S}_2\text{O}_8^{2-}$, and UVC/ HClO processes can be seen in FIGURES 2.6–2.8. In the case of the UVC/ H_2O_2 and UVC/ $\text{S}_2\text{O}_8^{2-}$ processes, FIGURES 2.6 and 2.7, respectively, the slope of the experimental line of both methods for BPA degradation is higher than the summation line, confirming the synergistic effect of the combined processes. As above mentioned and due to the fast BPA degradation reaction in the presence of HClO , no synergistic effect resulting from the coupling with UVC irradiation is observed, *i.e.*, the experimental and summation/theoretical lines are coincident. Regarding TOC removal, once again by comparing the experimental and theoretical lines for its remaining fraction, all tested UVC AOPs exhibited mineralization removal levels above the results of a simple summation. It clearly suggests the production of HO^\bullet and $\text{SO}_4^{\bullet-}$ (from $\text{S}_2\text{O}_8^{2-}$ homolysis) species, which are the main species responsible for converting organic compounds into CO_2 .

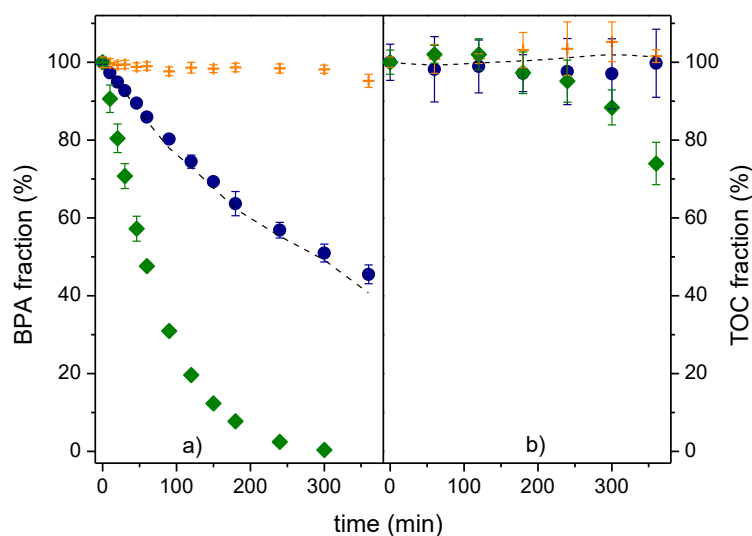


FIGURE 2.6 – Remaining fraction of a) BPA and b) TOC as a function of treatment time for the photochemical method (●), chemical method (+), UVC/ H_2O_2 process (◆), and after summation of the experimental photochemical and chemical methods (---). Conditions: 0.6 mol L^{-1} of oxidant (flow rate 0.1 mL min^{-1}), pH 3, and 38 °C. Error bars refer to two and three repetitions for the BPA and TOC determinations, respectively.

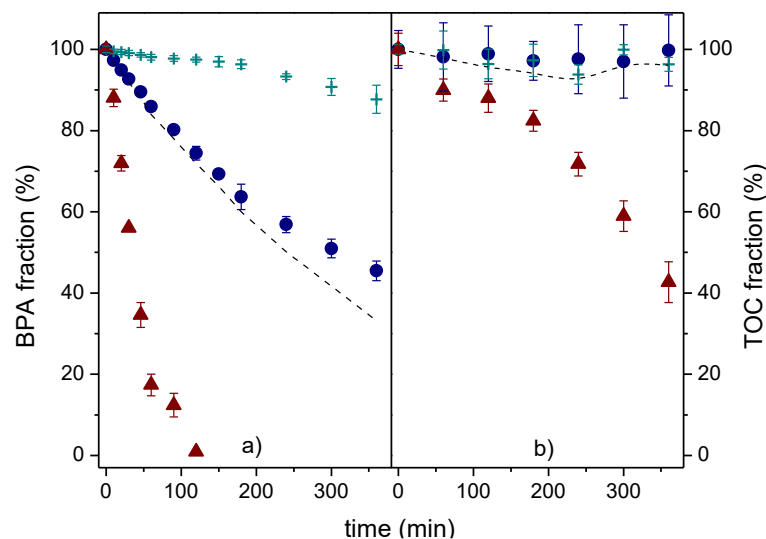


FIGURE 2.7 – Remaining fraction of a) BPA and b) TOC as a function of treatment time for the photochemical method (●), chemical method (+), UVC/S₂O₈²⁻ (▲), and after summation of the experimental photochemical and chemical methods (---). Conditions: 0.6 mol L⁻¹ of oxidant (flow rate 0.1 mL min⁻¹), pH 3, and 38 °C. Error bars refer to two and three repetitions for the BPA and TOC determinations, respectively.

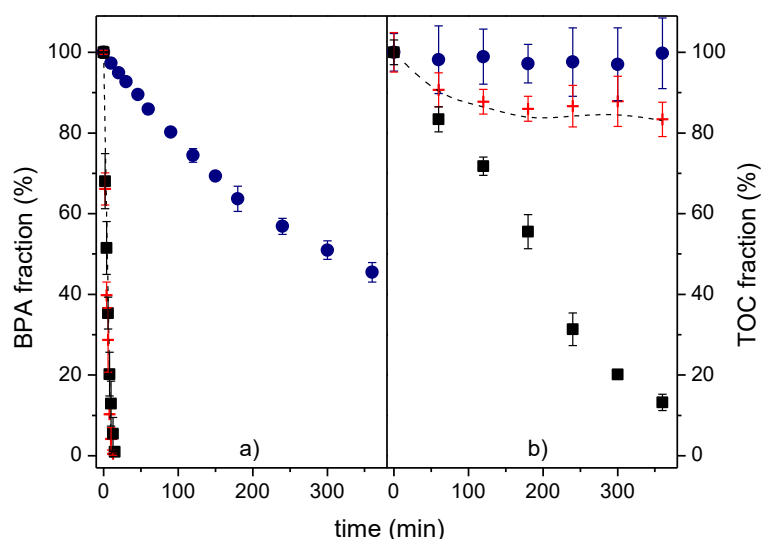


FIGURE 2.8 – Remaining fraction of a) BPA and b) TOC fraction as a function of treatment time for the photochemical method (●) chemical method (+), UVC/HClO process (■), and after summation of the experimental remaining fractions of the photochemical and chemical methods (---). Conditions: 0.6 mol L⁻¹ of oxidant (flow rate 0.1 mL min⁻¹), pH 3, and 38 °C. Error bars refer to two and three repetitions for the BPA and TOC determinations, respectively.

In order to understand the difference in the oxidation rates (degradation and mineralization) obtained between the chemical method (H₂O₂, S₂O₈²⁻ or HClO) and its corresponding UVC AOPs, photochemical experiments were carried out for each oxidant to

monitor its concentration in the absence of BPA. For such, concentration evolution of H_2O_2 , $\text{S}_2\text{O}_8^{2-}$ and HClO as a function of time were obtained for each experiment with and without UVC irradiation, as can be seen in FIGURE 2.9. As expected, a high concentration of the oxidants remains in solution in the absence of UVC irradiation, whereas low concentrations of these oxidants were measured in the experiments under UVC irradiation. Thus, these results suggest that oxidants are being consumed in the presence of UVC light to produce radical species, mainly HO^\bullet , $\text{SO}_4^{\bullet-}$, and Cl^\bullet .

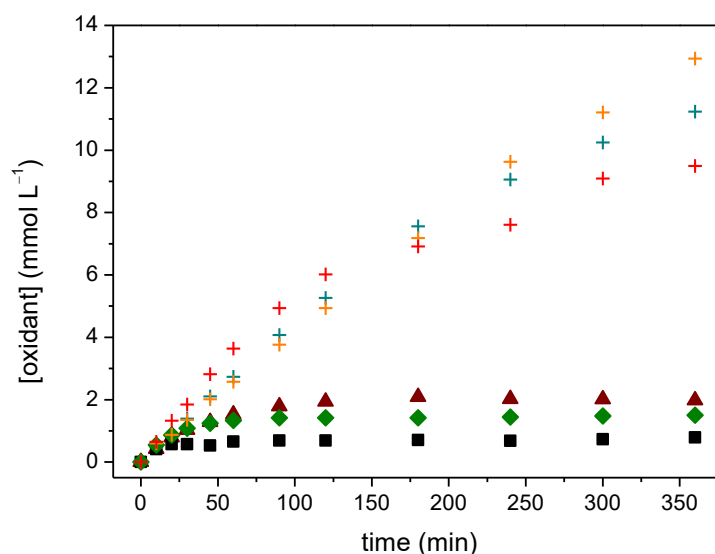


FIGURE 2.9 – Concentration evolution of oxidant species as a function of time for the chemical (H_2O_2 (+), $\text{S}_2\text{O}_8^{2-}$ (+), and HClO (+)) and UVC/Oxidant processes (UVC/ H_2O_2 (♦), UVC/ $\text{S}_2\text{O}_8^{2-}$ (▲), and UVC/ HClO (■)). Conditions: 0.6 mol L^{-1} of oxidant (flow rate 0.1 mL min^{-1}), pH 3, and $38 \text{ }^\circ\text{C}$.

To confirm if the homolysis of the oxidants mediated by UVC will result in the formation of HO^\bullet species (the common radical in the three coupled processes), treatment of solutions containing benzoic acid were also carried out using the UVC AOPs. Due to its electrophilic nature, HO^\bullet species can react with aromatic rings via addition reactions to generate phenolic compounds. Thus, the reaction between benzoic acid and HO^\bullet result in the formation of salicylic acid (substitution in ortho, meta, or para positions). Both benzoic and salicylic acid were monitored by HPLC. Experimental procedure and chromatographic conditions are available in TEXT A2 (APPENDIX A).

FIGURE 2.10 shows the chromatographic profiles of benzoic acid treated samples (100 mg L^{-1}) using the UVC/ H_2O_2 , UVC/ $\text{S}_2\text{O}_8^{2-}$ and UVC/ HClO processes at varying sampling times. As can be observed, salicylic acid was detected in all UVC AOPs, which

confirms that the consumption of the oxidants through homolysis reaction mediated by UVC irradiation is leading to HO^\bullet species. Another interesting point is that the salicylic acid peak in FIGURE 2.10(a)(c) appears after 1 min of reaction for the UVC/ H_2O_2 and UVC/ HClO methods, since HO^\bullet species are produced by a one-step direct photolysis (see eqs. 1 and 6). For the UVC/ $\text{S}_2\text{O}_8^{2-}$ process, FIGURE 2.10(b), salicylic acid was only detected after 3 min of reaction; because photolysis of $\text{S}_2\text{O}_8^{2-}$ leads to $\text{SO}_4^{\bullet-}$ which react with H_2O to produce HO^\bullet , *i.e.*, two-step reaction (see eqs. 2 and 4).

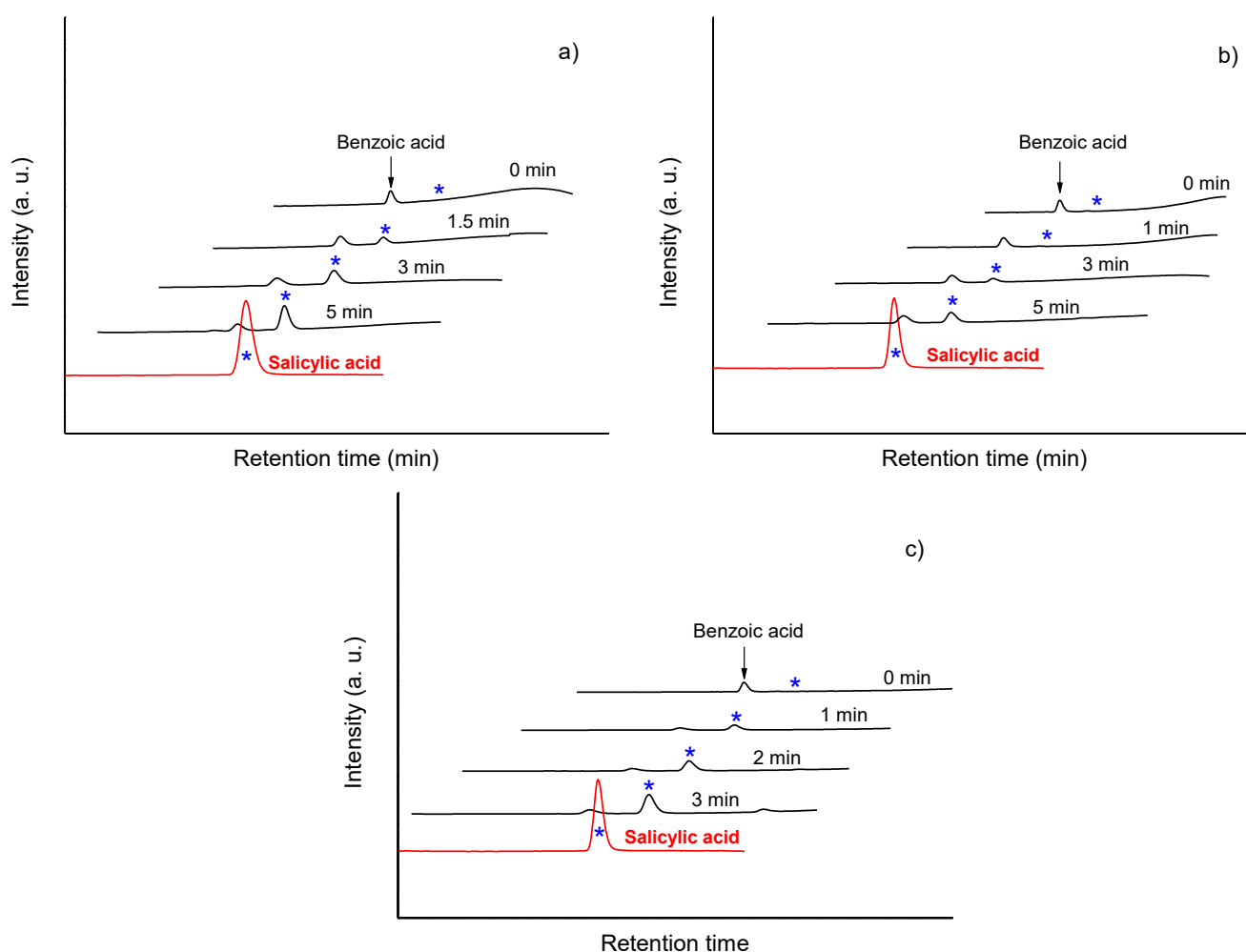


FIGURE 2.10 – Chromatographic profiles of treated samples containing 100 mg L^{-1} of benzoic acid at varying sampling times to show the evolution and formation of benzoic and salicylic acids peaks using the a) UVC/ H_2O_2 , b) UVC/ $\text{S}_2\text{O}_8^{2-}$, and c) UVC/ HClO processes.

On the other hand, as discussed in the work of Liang & Su¹²⁴, benzoic acid has similar reaction rate constants with $\text{SO}_4^{\bullet-}$ and HO^\bullet . In addition, when $\text{SO}_4^{\bullet-}$ species are produced in the reaction media, hydroxybenzoic acids (like salicylic acid) can be generated by a proton abstraction reaction mediated by $\text{SO}_4^{\bullet-}$ followed by a nucleophilic reaction promoted by H_2O .¹²⁵ Thus, in order to try to unravel what kind of radical species are predominantly present in the

reaction medium when using a $\text{S}_2\text{O}_8^{2-}$, quenching experiments using isopropyl alcohol (IPA) and tert-butyl alcohol (TBA) (both at 0.4 mol L^{-1}) were also carried out.

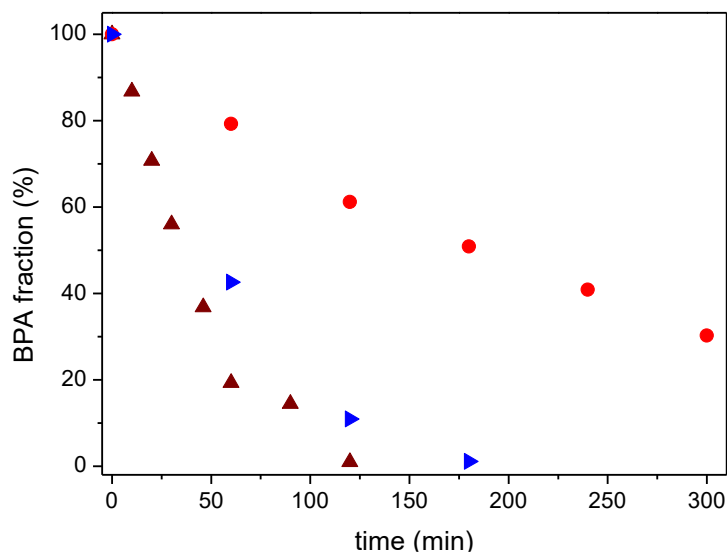


FIGURE 2.11 – Remaining BPA fraction as a function of treatment time for the UVC/ $\text{S}_2\text{O}_8^{2-}$ process in the absence of scavenger (▲), in the presence of IPA (●), and in the presence of TBA (▶). Conditions: 0.6 mol L^{-1} of oxidant (flow rate 0.1 mL min^{-1}), pH 3, and $38 \text{ }^\circ\text{C}$.

Considering the second order rate constants of IPA with HO^\bullet and $\text{SO}_4^{\bullet-}$ ($k_{\text{HO}^\bullet} \sim 10^9 \text{ M}^{-1} \text{ s}^{-1}$ and $k_{\text{SO}_4^{\bullet-}} \sim 10^8 \text{ M}^{-1} \text{ s}^{-1}$) this compound is efficient to quench both generated radicals. In contrast, the rate constant of TBA for HO^\bullet scavenging ($k_{\text{HO}^\bullet} \sim 10^8 \text{ M}^{-1} \text{ s}^{-1}$) is around three orders of magnitude higher than for $\text{SO}_4^{\bullet-}$ ($k_{\text{SO}_4^{\bullet-}} \sim 10^5 \text{ M}^{-1} \text{ s}^{-1}$).¹²⁵ In this sense, results showed in FIGURE 2.11 can be explained based on the effective quenching properties of these alcohols. Thus, the presence of IPA (scavenger for HO^\bullet and $\text{SO}_4^{\bullet-}$) in the UVC/ $\text{S}_2\text{O}_8^{2-}$ system led to a decrease in the degradation rate of BPA, while a lower inhibition to BPA removal using TBA was observed (similar to the condition without scavenger). That behavior implies that the $\text{SO}_4^{\bullet-}$ species are mainly responsible for the removal of BPA in the reaction medium at pH 3, since the TBA reacts predominantly with HO^\bullet . Similar observations were also reported in other works.^{119, 126}

The role of the Cl^\bullet species were not possible to be unraveled in this study as the chemical oxidation reaction between HClO and BPA showed a similar pseudo-first order kinetic constant value as the one for the HClO/UVC process. However, as reported in the work of Nowell & Hoigne¹²⁷ and Watts & Linden¹²⁸, the main produced radical species were HO^\bullet in acidic solutions when using HClO oxidant.

This does not imply that the contribution to BPA degradation of chlorine-derived radicals is negligible, but it probably means that they have a secondary role in the oxidation mechanism (see discussion in section 2.4.3). In fact, recent works have been concentrated on the study the chlorine-derived radicals and their reaction kinetics with some organic contaminants using UVC/free chlorine system. For instance, the kinetic constants of these radicals with the target contaminants have been recently determined by using probe compounds under specific conditions.^{129, 130}

Thus, Cai *et al.*¹³¹ reported that the rate constant of fluconazole (a chlorine-resistant compound) reaction with Cl^\bullet can be calculated by using the probe compounds nitrobenzene and benzoic acid, while 2,4,5 trimethoxybenzoic acid can be used as the probe for the fluconazole reaction with ClO^\bullet . In addition, the role of the reactive chlorine radicals on degradation of some CEC has been explored in a few theoretical studies by using computational quantum chemistry (specifically computational kinetic models).^{131, 132} However, the reaction mechanisms of these chlorine-derived radicals with organic compounds are still unclear.

2.4.3. Identification of oxidation by-products

In order to identify the main intermediate compounds produced during BPA oxidation using distinct UVC AOPs, aliquots were collected at different treatment time intervals to be analyzed through LC–MS/MS. TABLE 2.2 shows the proposed chemical structures for the main oxidation by-products detected, as well as retention times (R.T.) and main fragment ions. Among the detected intermediates, only two compounds, n. **3** and n. **4** (m/z 247 and m/z 259, respectively) appeared in all investigated UVC AOPs and only compound n. **5** (m/z 261a) occur during treatment of BPA using the UVC/ $\text{S}_2\text{O}_8^{2-}$ and UVC/HClO processes. FIGURES A2–A4, in the APPENDIX A, illustrates the integrated chromatographic area of the oxidation by-products reported in TABLE 2.2 as a function of treatment time. As expected for the UVC/ H_2O_2 process and, due to its low mineralization and ϕ values attained (see FIGURES 2.4 and 2.5, respectively), a higher number of oxidation by-products fully hydroxylated were detected, *e.g.*, compounds n. **1**, **2**, **8**, and **9**.

As far as we could ascertain, this is the first report for the occurrence of these intermediates, except for oxidation by-products **1** and **2**, which were found during BPA degradation through the Fenton reaction.¹³³ In contrast, only three intermediates (**3**, **4**, and **5**; two of them with low intensities – see FIGURE A4) occurred for the HClO/UVC method, which also corroborates the high levels of TOC removal and ϕ for BPA, as reported earlier. Moreover, and different from what is reported in the literature regarding the use of chlorine-

based processes for BPA removal¹³⁴⁻¹³⁶, no organochlorine oxidation by-products were detected during measurements. Such behavior could be attributed to the low accumulation of intermediate compounds, precluding their identification through LC-MS/MS considering the high mineralization rate achieved.

In order to confirm the BPA susceptibility regarding the addition reactions mediated by chlorine species, LC-MS/MS analyses were also carried out for the chemical experiment using only HClO (*i.e.*, without UVC irradiation). Contrary to the results for the UVC/HClO process, two organochlorine intermediates (compounds n. **6** and n. **7**) were detected during the chemical process using HClO (FIGURE A5). In addition, throughout the 6 h treatment process the integrated areas for these organochlorine compounds increased (in agreement with the low TOC removed – see FIGURE 2.3(b)), especially for compound n. **6**, which is more toxic than the parent BPA molecule (see discussion below on the toxicity assays).

These data do not imply the absence of chlorination in the BPA molecule during the UVC/HClO process since the degradation rate for the chemical and coupled methods were very similar. Probably in both methods (with and without radiation) at the beginning of reaction detectable amounts of organochlorines are generated (*i.e.*, less than 2 h), but only in the UVC/HClO method they are completely removed after 2 h of treatment. In contrast, the organochlorine by-products produced during the chemical process using HClO were detected even after 6 h treatment (FIGURE A5). In this sense, and to avoid (or minimize) the formation of organochlorine compounds, it is recommended to couple HClO process and UVC radiation.

FIGURES A6-A14, in the APPENDIX A, show the fragmentation route proposed for all intermediates detected. In a general way, most of the oxidation by-products resulted from addition reactions mediated by the electrophilic HO[•] species (as expected for the experiments with benzoic acid) in the methyl substituents and especially in the aromatic rings. The higher polar degree of by-products in relation to the BPA molecule is another characteristic corroborating the proposed oxidation by-products for generating a lower retention time of intermediates during LC-MS/MS analyses as the stationary phase (C-18 column) used is non-polar. The variety of chemical structures identified in this work resulting from hydroxylation reactions confirm the non-selective nature of the HO[•] species (and possibly SO₄^{•-}), as mentioned by other authors.¹³⁷⁻¹⁴⁰

TABLE 2.2 – LC-MS/MS data of the main detected oxidation by-products during treatment of BPA solutions using different UVC AOPs.

n	Molecular mass (Da)	R.T (min)	Molecular ion [M-H] ⁻ (m/z)	Main fragment ions (m/z)	Proposed chemical structure	Previously reported by ref.
1	152 ^{a††}	1.86	151	133 and 107		[133]
2	244 ^{a††}	1.30	243	211, 149, and 133		[133]
3	248 ^{abc}	1.16	247	229, 203, 167, 149, and 119		no
4	260 ^{abc}	1.30	259	244, 215, 179, and 165		no
5	262 ^{abc}	1.18	261a	197 and 119		no
6	262 ^{b^d}	1.49	261b	215 and 119		[117]
7	278 ^d	1.56	277	245, 135, and 119		no
8	324 ^{a†}	1.20	323	279, 243, and 227		no
9	342 ^{a†}	1.25	341	261 and 243		no

a = UVC/H₂O₂; b = UVC/S₂O₈²⁻; c = UVC/HClO; d = HClO.

[†]only detected in 4 h.

^{††}detected in 2 and 4 h.

In the final stages of the BPA molecule oxidation, the production of carboxylic acids clearly indicates that the break of aromatic ring and further oxidation before complete mineralization, *i.e.*, conversion to CO₂. In addition, previous studies demonstrated that when

molecules containing phenolic rings are further oxidized, short chain carboxylic acids, including acetic, formic, fumaric, glyoxylic, maleic, oxalic, and succinic, represented the main detected compounds.^{141, 142} In this work, a large number of short chain carboxylic acids (acetic, butyric, dichloroacetic, formic, glycolic, glyoxylic, malic, malonic, oxalic, propionic, pyruvic, succinic, tartaric, and tartronic acids) were identified through HPLC during BPA oxidation.

FIGURE 2.12 illustrates the concentration evolution of these carboxylic acids as a function of treatment time using distinct UVC AOPs, which shows the occurrence of tartronic acid for all tested UVC AOPs and at high concentration values, especially for the UVC/HClO (~27 mg L⁻¹) process. This latter method also generated the largest number of carboxylic acids, mainly during the first 2 h of experiment; however, most of them were completely removed within 5 h of treatment, even the only chlorinated carboxylic acid detected (dichloroacetic acid). Remaining amounts of acetic acid were still detected after 6 h, which might be responsible for the residual TOC values in the final stages of the experiment, as well as other non-identified carboxylic acids (see Figure 2.12(c)).

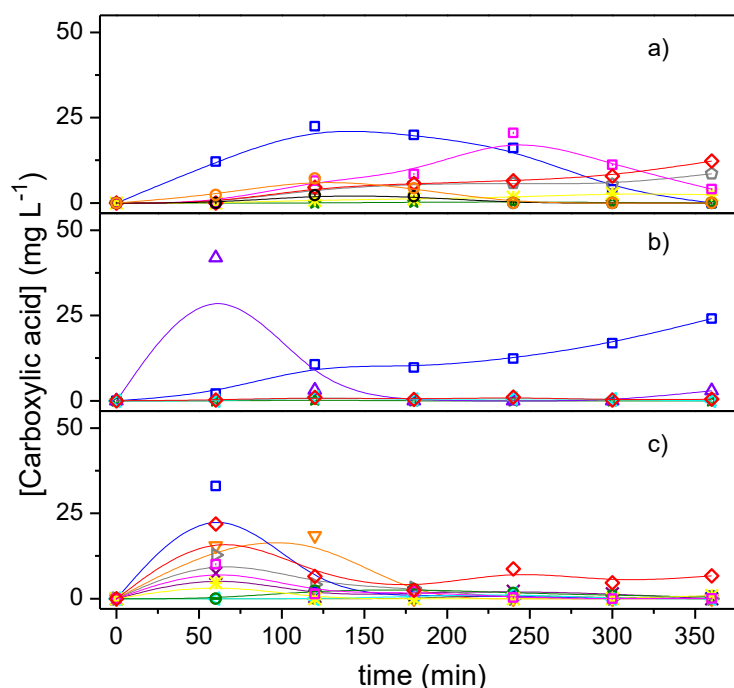


FIGURE 2.12 – Concentration evolution of the main detected carboxylic acids as a function of the treatment time for the a) UVC/H₂O₂, b) UVC/S₂O₈²⁻ and c) UVC/HClO processes: acetic (◇), butyric (○), dichloroacetic (×), formic (◻), glycolic (◁), glyoxylic (△), malic (◊), malonic (⊖), oxalic (▽), propionic (⊙), pyruvic (+), succinic (*), tartaric (▷) and tartronic (◻). Conditions: 0.6 mol L⁻¹ of oxidant (flow rate 0.1 mL min⁻¹), pH 3, and 38 °C.

On the other hand, in the chemical process using HClO, high concentrations of carboxylic acids appeared in the final stages of treatment (mainly acetic, formic, and glyoxylic acids). Moreover and similarly to the treatment using UVC/HClO, dichloroacetic acid was generated and completely removed within 3 h of treatment (see FIGURE 2.13). The UVC/H₂O₂ method produced the highest concentrations of carboxylic acids during the experiment (FIGURE 2.12(a)); however, these acids were not completely removed until 6 h of treatment, corroborating the low mineralization levels attained. Finally, tartronic and glyoxylic acids were the main carboxylic acids produced and detected during treatment using the UVC/S₂O₈²⁻ method. For this process, significantly lower TOC resulted from the complete removal of glyoxylic acid within 3 h of treatment, as can be seen in FIGURE 2.12(b).

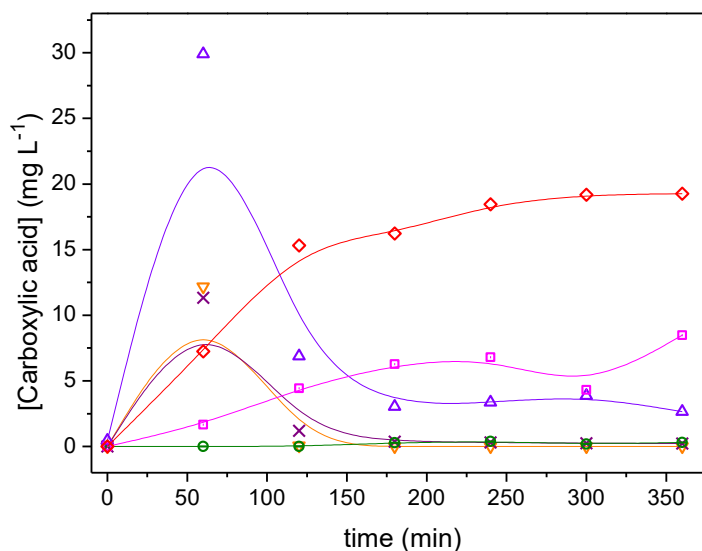


FIGURE 2.13 – Concentration evolution of the main detected carboxylic acids as a function of the treatment time for the chemical process using HClO: acetic (◇), dichloroacetic (×), formic (◻), glyoxylic (△), malonic (⊖), oxalic (▽). Conditions: 0.6 mol L⁻¹ of oxidant (flow rate 0.1 mL min⁻¹), pH 3, and 38 °C.

2.4.4. Toxicity: experimental and theoretical analyses

To assess the environmental compatibility of the UVC AOPs, acute toxicity tests using *A. salina* as the testing organism for a 24 h exposure were carried out during treatment of BPA solutions. The percentage of mortality for *A. salina* decreased during the treatment of BPA solutions and was completely ceased after 4 h using UVC/S₂O₈²⁻ and UVC/HClO processes, as shown in FIGURE 2.14. In the case of the UVC/H₂O₂ method, the toxicity decreased after 2 h of treatment and was completely removed by the end of experiment (6 h).

Considering the estimated value for the LC_{50} for BPA (28.9 mg L^{-1}) using *A. salina* and the time below 2 h required for the BPA concentration to decrease for all tested UVC AOPs (see FIGURE 2.4(a)), the mortality of *A. salina* was expected to cease just after 2 h of treatment if toxicity was only due to the parent molecule. As the time for complete toxicity removal was longer than expected considering the LC_{50} values, treatment of BPA solutions using different UVC AOPs resulted in toxic intermediates whose type and concentration depend on the specific method as well as the complete detoxification of the treated BPA solution.

Pérez-Moya *et al.*¹⁴³ reported a sharp mortality decrease using Vero cells after a 5 min treatment of BPA solutions (30 mg L^{-1}) involving Fenton, Fenton-like, and photo-Fenton processes. However, mortality was 50% higher after further reaction time, probably due to the formation of intermediates that are more toxic than the parent molecule. Other authors found a similar behavior concerning higher toxicity at the beginning of treatment.¹⁴⁴

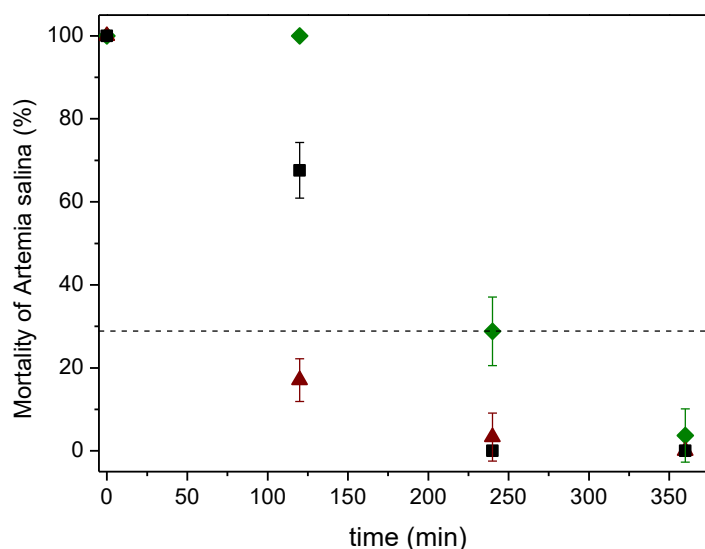


FIGURE 2.14 – Evolution of mortality of *A. salina* (%) as a function of the treatment time for the UVC/H₂O₂ (◆), UVC/S₂O₈²⁻ (▲), and UVC/HClO (■) processes. The dashed line indicates the LC_{50} value (28.9 mg L^{-1}) found for BPA. The error bars refer to the calculated errors for triplicate analyses. Conditions: 0.6 mol L^{-1} of oxidant (flow rate 0.1 mL min^{-1}), pH 3, and $38 \text{ }^{\circ}\text{C}$.

To benefit the understanding of the results obtained during the toxicity tests using *A. salina*, the ECOSAR software was used to estimate the acute and chronic toxicity baseline of BPA and its oxidation by-products (identified through LC-MS/MS analyses) for different aquatic organisms (*fish*, *daphnid*, and *green algae*).

Taking into account the results obtained by using the software and the classification proposed in the Globally Harmonized System of Classification and Labelling of Chemicals (GHS), as seen in TABLES 2.3 and A2 (APPENDIX A), respectively, it is possible to state that:

i) except for the organochlorine compound n. **6**, all the remaining oxidation by-products are less toxic than the BPA molecule;

ii) intermediate compounds n. **1**, **4**, and **5** are not harmful for acute toxicity, but harmful for chronic toxicity, while intermediate n. **2** is harmful for acute and chronic toxicity – these intermediates were found only during the treatment using the UVC/H₂O₂ process;

iii) intermediate compound n. **3** is detrimental for acute and chronic toxicity and appeared during all treatment processes; however, its signal during LC-MS/MS analyses was around 15 times higher in the UVC/H₂O₂ process than UVC/S₂O₈²⁻ and UVC/HClO systems;

iv) the intermediates identified during the HClO chemical process, n. **6** and **7**, are considered very toxic and toxic toward chronic toxicity, respectively;

v) the remaining oxidation by-products showed no acute or chronic toxicity effects.

TABLE 2.3 – Estimated acute and chronic toxicity data for BPA and its initial oxidation by-products (with elucidated structure) predicted by the ECOSAR software. The toxicity values can be classified according to GHS, summarized in TABLE A2.

n	Acute toxicity (10 ³ mg L ⁻¹)			Chronic toxicity (mg L ⁻¹)		
	Fish	Daphnid	Green Algae	Fish	Daphnid	Green Algae
BPA	0.0063	0.0041	0.0058	0.733	0.617	2.12
1	1.10	0.567	0.283	95.91	42.19	59.62
2	0.139	0.080	0.064	13.8	8.18	17.4
3	0.036	0.022	0.023	3.89	2.69	7.09
4	0.399	0.220	0.146	37.8	19.9	36.0
5	1.13	0.594	0.326	101	47.2	72.4
6	0.0019	0.0013	0.0024	0.239	0.234	0.999
7	0.041	0.025	0.026	4.47	3.08	8.09
8	823	327	55.2	52714	11733	6499
9	24600	8390	765	1320000	199000	64650

Legend: Very toxic Toxic Harmful Not harmful

All these results may explain why the UVC/H₂O₂ process demanded a prolonged treatment time to reduce toxicity towards *A. salina* in comparison to the UVC/S₂O₈²⁻ and UVC/HClO processes. In addition, none of the 15 carboxylic acids detected in this work were

considered toxic for acute or chronic exposure for the concentration levels obtained and based on the ECOSAR software estimation. Among the detected carboxylic acids, glyoxylic acid is considered the most toxic ($LC_{50} = 256 \text{ mg L}^{-1}$) for fish in acute exposure.

2.4.5. Economical comparison and energy consumption analysis

An economic comparison to determine the most satisfactory cost-efficiency relationship among the investigated UVC AOPs was performed during BPA degradation based on the total cost per order ($\text{Cost}/O_{\text{TOTAL}} - \$ \text{ m}^{-3} \text{ order}^{-1}$).

According to TABLE 2.4, the $\text{Cost}/O_{\text{TOTAL}}$ values proved significantly lower for the UVC/HClO method than for the UVC/H₂O₂ and UVC/S₂O₈²⁻ processes. Moreover, the $\text{Cost}/O_{\text{TOTAL}}$ for UVC/HClO is ~14 times lower than for UVC/H₂O₂ due to the low oxidation rates attained (and low quantum yield) for the latter process. In the case of the UVC/S₂O₈²⁻ method, the price of the Na₂S₂O₈ oxidant ($\text{Cost}/O_{\text{OX}}$) was higher than the other chemicals, which resulted in high operational costs in comparison to the UVC/HClO process, but a slightly lower than UVC/H₂O₂ costs. This last result is in agreements to the literature reports, *i.e.*, the UVC/S₂O₈²⁻ process is more cost-efficient method than UVC/H₂O₂. However, in this study both values are very close, which is clearly related to the lower price of the Na₂S₂O₈ reagent reported in other studies ($0.74 \text{ \$ kg}^{-1}$)[§] in relation to ours ($13.7 \text{ \$ kg}^{-1}$ from Sigma Aldrich).¹⁴⁵⁻¹⁴⁷ Thus, considering the $\text{Cost}/O_{\text{TOTAL}}$ parameter, *i.e.*, time of treatment using the UVC lamp and price of chemicals, UVC/HClO is the most cost-efficient process for BPA degradation and UVC/S₂O₈²⁻ and UVC/H₂O₂ methods are less recommended. Lu *et al.*¹¹⁵ also reported that the UVC/HClO process is more cost-effective than the UVC/S₂O₈²⁻ method for the degradation of clofibric acid.

TABLE 2.4 – Economic comparison per order of BPA[†] degradation using different UVC AOPs.

Type of cost per order	UVC/H ₂ O ₂	UVC/S ₂ O ₈ ²⁻	UVC/HClO
$\text{Cost}/O_{\text{UVC}} (\text{\$ m}^{-3} \text{ order}^{-1})$	6.87 (3.91)**	3.44 (1.96)**	0.477 (0.272)**
* $\text{Cost}/O_{\text{OX}} (\text{\$ m}^{-3} \text{ order}^{-1})$	0.018	1.74	0.018
$\text{Cost}/O_{\text{TOTAL}} (\text{\$ m}^{-3} \text{ order}^{-1})$	6.89 (3.93)**	5.18 (3.70)**	0.495 (0.290)**

[†]mean values obtained after two repetitions.

*oxidant price (US\$): 0.504 kg^{-1} for H₂O₂ (Synth), $13.7 \text{ \$ kg}^{-1}$ for Na₂S₂O₈ (Sigma Aldrich), and 3.21 kg^{-1} for NaClO (Nalgon).

**values in parentheses refer to calculation taking into account the rated power of the UVC lamp (9W).

Experimental conditions: [BPA] = 0.44 mmol L^{-1} , [oxidant] = 0.6 mol L^{-1} (added in a flow rate of 0.1 mL min^{-1}), pH 3, and $38 \text{ }^{\circ}\text{C}$.

[§]Considering this value ($0.74 \text{ \$ kg}^{-1}$), the $\text{Cost}/O_{\text{TOTAL}}$ of UVC/S₂O₈²⁻ process is $3.53 \text{ \$ m}^{-3} \text{ order}^{-1}$ ($2.05 \text{ \$ m}^{-3} \text{ order}^{-1}$)

Regarding BPA conversion and its oxidation by-products into CO_2 , only the UVC/HClO method was able to remove the content of TOC by one order of magnitude ($\sim 90\%$), therefore, the $\text{Cost}/\text{O}_{\text{TOTAL}}$ value for mineralization using this process remained around $7.8 \text{ \$ m}^{-3} \text{ order}^{-1}$. Such value is significantly higher (~ 30 times) than the one for BPA degradation as the mineralization of complex organic compounds, like BPA and its by-products, requires successive steps of hydroxylation reactions (resulting in a prolonged reaction time). Consequently, there are practically no studies reporting the $\text{Cost}/\text{O}_{\text{TOTAL}}$ for BPA mineralization using UVC AOPs.

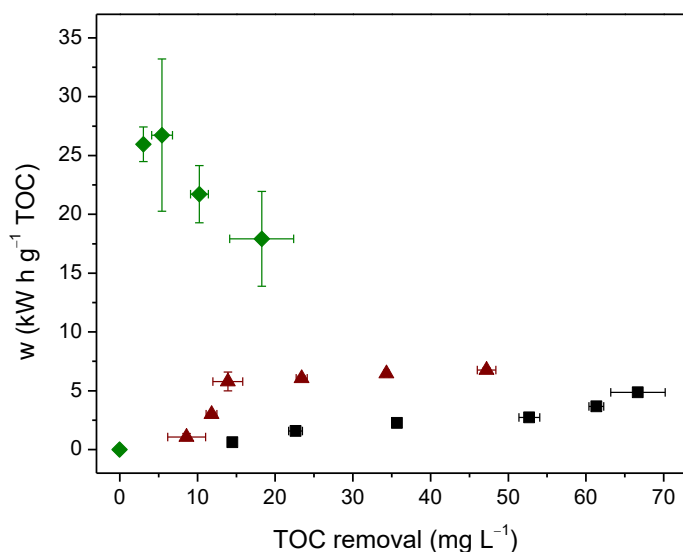


FIGURE 2.15 – Energy consumption per unit mass of removed TOC (w) as a function of TOC removal for the UVC/ H_2O_2 (◆), UVC/ $\text{S}_2\text{O}_8^{2-}$ (▲), and UVC/HClO (■) processes. Conditions: 0.6 mol L^{-1} of oxidant (flow rate 0.1 mL min^{-1}), pH 3, and $38 \text{ }^\circ\text{C}$. Error bars refer to three repetitions.

An alternative treatment to the total cost per unit order (in cases where mineralization removals were lower than 90%) could be the energy consumption per unit mass of removed TOC (w), as showed in the following eq.:

$$w = \frac{Pt}{m} \quad (15)$$

where P is the rated power (9 W), t the time (h), and m the mass (g) of TOC removed after a certain time. As can be observed in FIGURE 2.15, the UVC/HClO process led to the lowest ($\sim 5 \text{ kW h g}^{-1}$) w value.

2.5. CONCLUSIONS

Among the three investigated UVC AOPs in this work, the UVC/HClO showed the best performance for the degradation and mineralization of BPA in comparison to the UVC/S₂O₈²⁻ and UVC/H₂O₂ processes. In all methods, UVC irradiation resulted in a significant improvement of the degradation and mineralization rates and levels due to the homolysis of oxidants and generation of HO[•] and SO₄^{•-} species.

The use of the UVC/HClO method presented only two hydroxylated intermediates, whereas six oxidation by-products were found during treatment of BPA using UVC/H₂O₂, confirming its lower mineralization extent in relation to the UVC/HClO method ($\phi \sim 1$). The LC-MS/MS analyses did not indicate any organochlorine upon the use of the UVC/HClO process, contrasting to the results from the chemical process (only HClO). As both processes showed similar BPA degradation rates, it is speculated that the production of organochlorine intermediates occurs through both methods, but are promptly consumed under UVC irradiation through subsequent hydroxylation reactions.

Toxicity assays using the *A. salina* crustacean proved effective at showing the toxicity evolution of BPA solutions during treatment using distinct UVC AOPs. As expected, the mortality of these organisms was completely ceased using the UVC/HClO treatment process due to the high rates of conversion of BPA and its intermediates to CO₂. In contrast, a high mortality percentage appeared for the UVC/H₂O₂ method, probably due to the oxidation by-products produced as analyzed by comparing between experimental data obtained from the LC-MS/MS analyses and theoretical calculations using the ECOSAR software. Finally, the UVC/HClO represents an interesting option since high organic removal rates can be achieved under a low operating cost.

3. CHAPTER 2: UVC-based removal of microcontaminants and pathogens at pilot plant scale

This chapter is an adaptation of the article “*UVC-based advanced oxidation processes for simultaneous removal of microcontaminants and pathogens from simulated municipal wastewater at pilot plant scale*” by Isaac Sánchez-Montes, Irene Salmerón García, Gracia Rivas Ibáñez, José M. Aquino, María Inmaculada Polo-López, Sixto Malato, and Isabel Oller.

Environmental Science: Water Research & Technology, DOI: 10.1039/d0ew00279h

Environmental
Science
Water Research & Technology



PAPER

View Article Online
View Journal | View Issue



Cite this: *Environ. Sci.: Water Res. Technol.*, 2020, 6, 2553

UVC-based advanced oxidation processes for simultaneous removal of microcontaminants and pathogens from simulated municipal wastewater at pilot plant scale†

Isaac Sánchez-Montes,^a Irene Salmerón García,^b Gracia Rivas Ibáñez,^b José Mario Aquino,^a María Inmaculada Polo-López,^b Sixto Malato^{a,b} and Isabel Oller^{a,b}

3.1. ABSTRACT

UVC-based advanced oxidation processes, using *in situ* production of strong oxidizing radicals, such as HO[•] and SO₄^{•-}, have shown high oxidation rates for OMCs; however, few studies have focused on the simultaneous removal of OMCs and pathogens, like bacteria. Thus, the aim of this work was to assess the degradation of six pharmaceuticals, acetaminophen, caffeine, carbamazepine, trimethoprim, sulfamethoxazole, and diclofenac, in the presence of *Escherichia coli*, *Enterococcus faecalis*, and *Salmonella enteritidis* in a simulated effluent from a municipal wastewater treatment plant by the application of UVC/H₂O₂ and UVC/S₂O₈²⁻ processes at pilot plant scale. The concentration of OMCs and bacteria was monitored along the oxidation processes as well as their regrowth after 24, 48, and 144 h. UVC-based processes were compared in terms of the required treatment time to remove at least 80% of the sum of OMCs, regrowth assessment, and energy consumption. Despite the UVC/H₂O₂ and UVC/S₂O₈²⁻ processes showing similar results, even after using distinct molar concentrations, the UVC/H₂O₂ process did not exhibit bacterial regrowth under dark conditions. A simple model has also been proposed in this work with the main objective of calculating the minimum concentration of oxidants as a function of the radiation absorption at 254 nm in a given photo-reactor setup.

3.2. SHORT INTRODUCTION

Assurance of safe reclaimed water free of chemical and microbiological contaminants is a serious global concern that is increasing with population growth and uncertain climate changes. Wastewater effluents treated by conventional methods can contain a huge amount of microcontaminants (OMCs) and pathogens (mainly pharmaceuticals and bacteria, respectively) that may lead to toxic effects in humans when reaching fresh water sources.^{9, 148-150} In addition, water supplies from non-traditional sources, including treated municipal wastewater, have been proposed as feasible options in recent years.^{30, 31} Unfortunately, consolidated tertiary treatments, such as UVC radiation, ozonation and chlorination are not effective enough or present serious drawbacks in their application to remove OMCs.

Previous studies have investigated the efficiency of different UVC AOPs (even UVC/H₂O₂ and UVC/S₂O₈²⁻) to eliminate pathogens or OMCs from water. However, most of these studies applied such processes at a fundamental level, *i.e.*, at laboratory scale, using pure or distilled water, and under acidic or basic conditions.^{76, 119} Under more realistic experimental conditions, for instance, in complex matrices, such as municipal wastewater, the efficiency of these technologies can be significantly reduced, mainly due to the quenching reactions between the produced free radicals and the dissolved organic matter (DOM) and inorganic ions (HCO₃⁻, SO₄²⁻, Cl⁻, and PO₄³⁻) present in these effluents.^{151, 152}

Moreover, disinfection and degradation processes have been studied independently and only very few works reported on the concomitant achievement of OMC removal and elimination of pathogens. Thus, investigation of UVC AOPs for tertiary treatment of municipal wastewater is worthy and focuses not only on microorganism inactivation, but also on the possibility of attaining simultaneous degradation of OMCs for water reusing purposes, *e.g.*, agricultural applications.

In this context, this work aimed to investigate and compare the use of the UVC/H₂O₂ and UVC/S₂O₈²⁻ processes for the simultaneous removal of OMCs and pathogens from a simulated municipal wastewater effluent at pilot plant scale. *Escherichia coli* (*E.coli*), *Enterococcus faecalis* (*E. faecalis*), and *Salmonella enteritidis* (*S. enteritidis*) were selected as target microorganisms because they are used as pathogen indicators in regulations and guidelines for wastewater disposal and reuse.^{153, 154} Six OMCs, acetaminophen (ACT), caffeine, (CAF), carbamazepine (CBZ), trimethoprim (TMP), sulfamethoxazole (SMX) and diclofenac (DCF), were chosen as target molecules since they are usually detected in municipal wastewater. In addition, this work intends to compare UVC/H₂O₂ and UVC/S₂O₈²⁻ processes

in terms of treatment time, consumption of chemicals, and the influence of the oxidant residual concentration on the bacterial regrowth. Finally, a simple model based on the optical path length of the UVC radiation is proposed to determine the most suitable oxidant concentration to be used in these systems to simultaneously remove OMCs and pathogens.

3.3. MATERIALS AND METHODS

3.3.1. Chemicals

ACT, CBZ, TMP, SMX, and DCF were purchased from Sigma-Aldrich (>99%). Caffeine (CAF) was provided by Fluka (>99%). H₂O₂ (35%), Na₂S₂O₈ (>98%), KI (>99.5%), Na₂S₂O₃ (>99%), bovine liver catalase (a.r.), phosphate-buffered saline (a.r.), acetonitrile (UPLC-grade), and formic acid (UPLC-grade) were purchased from Sigma-Aldrich. All chemicals were used as received. The OMC stock solution for experiments was prepared in methanol at 2.5 g L⁻¹ each to avoid hydrolysis of OMCs and allow spiking low volumes of water with very low quantities of methanol in the pilot plant. Simulated municipal wastewater (SMWW) effluent was used as the wastewater model. The resulting physicochemical properties of the prepared SMWW effluent are shown in TABLE 3.1.

TABLE 3.1 – Physicochemical characterization of SMWW effluent

Parameters	Values
pH	7.6±0.3
Conductivity (mS cm ⁻¹)	1.4±0.1
Turbidity (NTU)	3.4±0.2
DOC (mg L ⁻¹)	15.5±0.6
DIC (mg L ⁻¹)	13.5±1.2

This matrix was prepared after adaption of the procedure described in Zhang *et al.*¹⁵⁵ and in the APHA Standard Methods¹⁵⁶, using the following chemicals:

(i) Inorganics salts: NaHCO₃ (96 mg L⁻¹), MgSO₄ (60 mg L⁻¹), NaCl (580 mg L⁻¹), and K₂HPO₄ (7.0 mg L⁻¹) (Sigma-Aldrich); CaSO₄·2H₂O (60 mg L⁻¹) and (NH₄)₂SO₄ (23.6 mg L⁻¹) (Panreac); KCl (4 mg L⁻¹) (J.T. Baker).

(ii) Organic matter: beef extract (1.8 mg L⁻¹) and peptone (2.7 mg L⁻¹) (Biolife); humic acid (4.2 mg L⁻¹), sodium lignin sulfonate (2.4 mg L⁻¹) and sodium lauryl sulphate (0.9 mg L⁻¹) (Sigma-Aldrich); tannic acid (4.2 mg L⁻¹) and acacia gum powder (4.7 mg L⁻¹) (Panreac).

It is important to remark that SMWW characteristics are highly similar to those of the actual MWWTP effluent and selected OMCs and pathogens to be monitored were spiked at concentrations in the range of those actually found in such effluents.

3.3.2. Analyses

3.3.2.1. Analytical quantification of OMCs

The concentration of OMCs was monitored by ultra-performance liquid chromatography (UPLC) with a UV-DAD detector (Agilent Technologies, Infinity Series 1200) using a Poroshell 120 EC-C18 column as the stationary phase (Agilent Technologies: 50 mm×3.0 mm, 2.7 µm particle) and a mixture of 25 mmol L⁻¹ formic acid and ACN as the mobile phase at 1 mL min⁻¹. A gradient elution mode was used. The initial condition was 100% formic acid 25 mmol L⁻¹, varying in 10 min up to 50% formic acid/ACN; then in 2 min 100% ACN was reached and maintained for another 2 min. Analysis time was set to 14 min, followed by 3 min of post-time for setting the column to initial conditions.

The injection volume and temperature of the column were 50 µL and 30 °C, respectively. Before sample analysis, 9 mL of collected sample were filtered using a 0.22 µm PTFE filter (Millipore) and the filter was washed with 1 mL of ACN to remove any adsorbed compounds. The detection limit (DL) for all the compounds studied was 5 µg L⁻¹. Other information, such as retention time, maximum quantification wavelength and chromatographic area of 100 µg L⁻¹ for each OMC can be seen in APPENDIX B (TABLE B1).

Other parameters were also monitored, such as pH (GLP 22 pH meter, CRISON), conductivity (GLP 31 conductimeter, CRISON), and turbidity (2100 N turbidimeter, HACH). Dissolved organic carbon (DOC) and dissolved inorganic carbon (DIC) were measured using a TOC-VCSN analyzer (Shimadzu) in filtered samples through 0.45 µm nylon filter (AISIMO).

Ion chromatography was used to measure the concentration of various ions in samples previously filtered (0.45 µm nylon filter), using a Metrohm 850 Professional analyzer. For anion determination, a Metrosep A Supp 7150/4.0 column at 45 °C and 3.6 mmol L⁻¹ sodium carbonate at 0.7 mL min⁻¹ were used as the stationary and mobile phase, respectively. A Metrosep C6 150/4.0 column and 1.7 mmol L⁻¹ solutions of nitric acid and dipicolinic acid at 1.2 mL min⁻¹ were used for cation quantification.

The concentration of oxidants was determined by two different methods using a UV-vis Evolution 220 spectrophotometer (Thermo Scientific). H₂O₂ concentration was analyzed spectrophotometrically at 410 nm after adding 0.5 mL of titanium (IV) oxysulfate to 5 mL of a filtered sample (DIN 38402H15). S₂O₈²⁻ concentration was monitored by using an iodometric method adapted from Liang *et al.*¹⁰³ Briefly, 3.5 mL of 50 g L⁻¹ KI solution and 0.5

mL of 5 g L^{-1} NaHCO_3 solution were added to 1 mL of previously filtered sample, allowed to react for 15 min, and then the absorbance at 352 nm was measured.

3.3.2.2. Bacterial quantification analyses

Selected strains of bacteria were provided by Spanish Culture Collection (CECT): *E. coli* (O157:H7) (CECT 4972), *E. faecalis* (CECT 5143), and *S. enteritidis* (CECT 4155). These strains were used to prepare the microbial suspensions spiked in the SMWW effluent. A colony-forming unit of *E. coli*, *E. faecalis*, and *S. enteritidis* were inoculated in 14 mL of nutrient broth (a mixture of NaCl, beef extract, and peptone), Luria-Bertani broth (Sigma-Aldrich), and tryptone soya broth (OXOID), respectively, and grown aerobically in a rotary shaker (90 rpm) at 37°C for 20 h.

The microbial suspensions were then centrifuged at 3000 rpm (704 g) for 15 min (J.P. Selecta) and then the microbial pellet was re-suspended in sterilized phosphate-buffered saline (PBS) solution to give a stock suspension containing approximately 10^{11} CFU per 100 mL. An aliquot of 100 μL of each bacterial suspension was added to the SMWW effluent to obtain an initial concentration of 10^5 CFU per 100 mL.

Bacterial quantification was performed by the standard plate counting method using specific culture media: Chromocult[®] (Merck), Slanetz–Bartley agar (1% TTC) (Scharlau), and Salmonella Shigella agar (Scharlau) for *E. coli*, *E. faecalis*, and *S. enteritidis*, respectively. When the bacterial concentration expected was lower than 2×10^2 CFU per 100 mL, samples were processed by the membrane filtration method. For each bacterium, 100 mL of sample were filtered using a $0.45 \mu\text{m}$ -pore-size cellulose nitrate membrane (Sartorius) and a Microfil filtration system (Millipore). Then, the obtained membranes were plated in the corresponding medium and incubated at 37°C . *E. coli* colonies were counted after 24 h; *E. faecalis* and *S. enteritidis* samples were counted after 48 h. The detection limit (DL) of this technique is 1 CFU per 100 mL, taking into account the minimum disinfection level required by the Spanish legislation for reusing reclaimed wastewater (RD 1620/2007).¹⁵⁷ A control sample (without treatment) for each bacterium was plated before and after the experiment to guarantee the strain's good quality.

When oxidant reagents were used, a proportional volume of bovine liver catalase solution (0.1 g L^{-1}) or sodium thiosulfate (10 mmol L^{-1}) was added to the samples in order to quench residual H_2O_2 and $\text{S}_2\text{O}_8^{2-}$, respectively. Regrowth of bacteria was quantified in predetermined samples stored at room temperature for 24, 48, and 144 h (6 days) (quencher was not added for this analysis). Disinfection experiments were carried out in duplicate and

average values were plotted. The inactivation kinetics of each bacterium observed during the UVC-based treatments were calculated by using Chick–Watson's equation.¹⁵⁸ In this case, the data were fitted using a double log-linear kinetic model characterized by a fast inactivation in the first stage (k_1) followed by a slow second inactivation stage (k_2):

$$\text{Log}\left(\frac{N}{N_0}\right) = -k_1 t ; t = [0, t_1] \quad (16)$$

$$\text{Log}\left(\frac{N}{N_0}\right) = -k_2 t ; t = [t_1, t_2] \quad (17)$$

where N and N_0 are the values of bacteria concentration at time t (min) and prior to the experiment in CFU per 100 mL.

3.3.3. UVC pilot plant description and experimental procedure

UVC, UVC/H₂O₂, and UVC/S₂O₈²⁻ experiments were carried out by using a UVC pilot plant. FIGURE 3.1(a–b) shows a schematic configuration of the photo-reactor containing the UVC lamp and a real image of the pilot plant. Briefly, the pilot plant consists of three medium pressure UVC lamps (230 W with radiation emission at 254 nm) protected by quartz tubes ($\varnothing_{\text{int,L}} = 3.70$ cm) and axially located in a stainless steel cylindrical photo-reactor ($\varnothing_{\text{int,C}} = 8.89$ cm). The flexible design of the system allows the use of one, two or three lamps in batch or continuous flow mode. In this study, a single lamp was used in batch mode (recirculation flow rate 36 L min⁻¹) with a total volume of 80 L.

Total irradiated surface of the photo-reactor (one lamp; $S_p = 0.34$ m²) and the illuminated volume (one lamp; $V_{\text{illu}} = 6.21$ L) were calculated according to eqs. (18) and (19) taking into account the specific characteristics of the lamp and its chamber. From FIGURE 3.1(a), $r_{\text{int,C}}$ is the internal radius of the chamber and L_L and $r_{\text{int,L}}$ are the height and internal radius of the lamp, respectively.

$$S_p (\text{m}^2) = 2\pi r_{\text{int,C}} L_L \quad (18)$$

$$V_{\text{illu}} (\text{L}) = \pi L_L (r_{\text{int,C}}^2 - r_{\text{int,L}}^2) \quad (19)$$

To compare the energy consumption of these processes with other photochemical based systems, the accumulative UVC energy per liter (Q_{UVC} ; kJ L⁻¹) was calculated according to eq. (20). For that, the incident energy rate on a surface per unit area

(irradiance; W m^{-2}) emitted by the UVC lamp was continuously monitored using a detector (ProMinent) placed in the inner wall of the cylindrical photochemical reactor.

$$Q_{\text{UVC}} (\text{kJ L}^{-1}) = \text{Dose} (\text{kJ m}^{-2}) \frac{S_p (\text{m}^2)}{V_T (\text{L})} \quad (20)$$

where Dose is the product of emitted irradiance by the UVC lamp (W m^{-2}) multiplied by the illumination time fraction (s). S_p is the total irradiated surface of the photo-reactor (m^2) and V_T is the total water volume (L). Details of the irradiance profile of the UVC lamp (maximum 84.8 W m^{-2}) measured in distilled water are shown in FIGURE B1 (APPENDIX B).

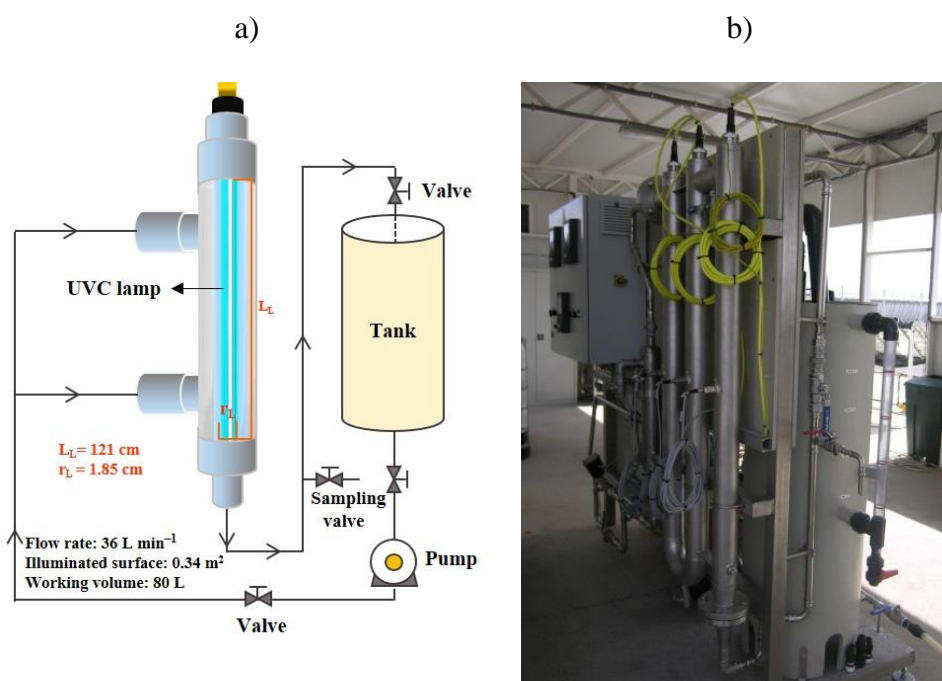


FIGURE 3.1 – UVC pilot plant: a) UVC photo-reactor scheme and main characteristics and b) real image of the experimental setup of the plant.

In UVC AOPs experiments, the system's reservoir was filled with 80 L of SMWW effluent and the required quantity of a stock solution of OMCs was added to obtain an initial concentration of $100 \mu\text{g L}^{-1}$ of each compound. The sum of these concentrations for the six selected OMCs ($\sum C_0$) is considered higher but very close to the range normally found in effluents of municipal wastewater treatment plants.^{89, 159-161}

Then, each bacterial stock was added to obtain 10^5 CFU per 100 mL per bacterium. After 15 min of homogenization (UVC lamp switched off), an initial sample was taken to check the initial concentration of both OMCs and bacteria. Then, H_2O_2 (5, 15, 25, 35,

and 50 mg L⁻¹) or S₂O₈²⁻ (20, 40, and 100 mg L⁻¹) was added to the reservoir tank. After homogenization (10 min), another sample was collected to verify the effect of the oxidants on the concentration of OMCs and bacteria in the dark (any significant variation in initial concentrations was observed in either of the experiments performed). Then the UVC lamp was switched on and the experiment started. Samples were collected at predetermined and regular time intervals to analyze simultaneously the degradation of OMCs, inactivation of bacteria and reagent evolution along all the UVC-based experiments performed in this study.

3.4. RESULTS AND DISCUSSION

3.4.1. UVC treatment

The obtained results of simultaneous inactivation of bacteria and degradation of OMCs using only UVC light in the SMWW effluent are depicted in FIGURE 3.2. A high inactivation rate of *E. coli*, *E. faecalis*, and *S. enteritidis* was obtained under UVC irradiation. The strong effect of the UVC light observed on bacterial inactivation is based on the occurrence of very specific damage on DNA and other essential components, such as proteins, lipids, membrane, etc., that inhibits its duplication and consequently bacterial reproduction. The typical UVC damage induces the formation of thymine–thymine cyclobutane cys–syn thymine–thymine photodimers and pyrimidine (6–4) pyrimidone photoproducts (TT (6–4) photoproducts).¹⁶²

No significant differences in the irradiation time required (60 min) to reach the detection limit (DL) and in the calculated pseudo-first order kinetic constants (k) of bacterial inactivation were observed. A double log-linear kinetic characterized by a fast inactivation in the first stage (k_1) followed by a slow second inactivation stage (k_2) was observed for all bacteria (see FIGURE 3.2). The k_1 for *E. coli*, *E. faecalis*, and *S. enteritidis* were $3.5 \pm 0.6 \times 10^{-1}$, $3.6 \pm 0.5 \times 10^{-1}$, and $3.3 \pm 0.7 \times 10^{-1} \text{ min}^{-1}$, respectively, while the second stage, k_2 , was around $0.23 \pm 0.02 \times 10^{-1} \text{ min}^{-1}$ for all pathogens. Clearly, the inactivation process is governed by the first stage.

In addition, for all bacteria, the accumulative UVC energy needed to reduce 5 log the initial concentration ($10^5 \text{ CFU } 100 \text{ mL}^{-1}$) was around 1.2 kJ L^{-1} and 0.09 kJ L^{-1} for a 3.5 log reduction (around 8 min of illumination). Similarly, Rodríguez-Chueca *et al.*¹⁶³ did not observe differences in the energy consumption for *E. coli* and *E. faecalis* inactivation under UVC irradiation using real and simulated wastewater. In that paper, a 3.5 log reduction in bacteria concentration demanded 0.057 kJ L^{-1} of UVC energy, working in continuous flow

mode but at laboratory scale. The upper energy consumption reported in the present work might come from the scaling-up to pilot plant scale as well as differences in the reactor design setup.

Increase of temperature resulting from operation of the UVC lamp was also monitored during all experiments and the maximum-recorded temperature value remained around 30 °C. This temperature value did not affect the bacterial viability since temperatures higher than 45 °C are necessary to produce thermal damages on the investigated bacteria.^{164, 165} In addition, this temperature interval should not increase the efficiency of UVC/H₂O₂ or UVC/S₂O₈²⁻ processes, as temperatures higher than 40 °C and 50 °C, respectively, are normally required.^{166, 167}

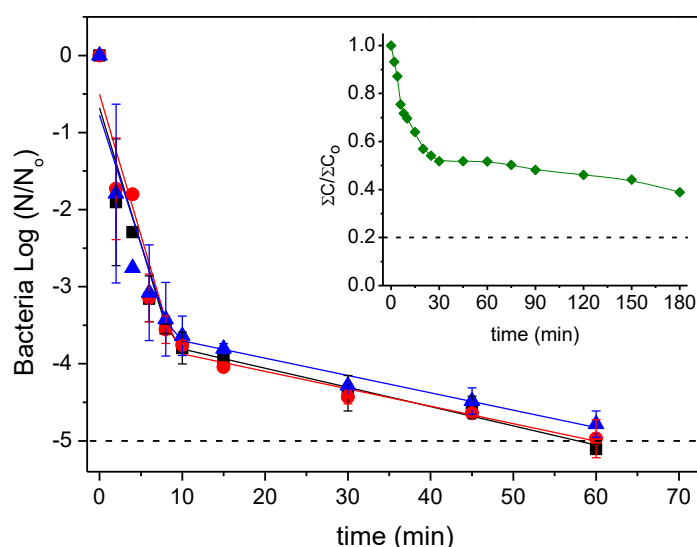


FIGURE 3.2 – Simultaneous bacterial inactivation and total OMC degradation (inset) under UVC irradiation in SMWW effluent as a function of treatment time: *E. coli* (■), *E. faecalis* (●), *S. enteritidis* (▲), and $\sum C_i/\sum C_0$ (◆). Dashed lines (---) refer to detection limit of bacteria (DL = 1 CFU per 100 mL⁻¹) and 80% removal of total OMCs.

Under certain conditions, the mechanisms of self-repair of microorganisms reverse the DNA damage produced by light absorption.⁴³ As the UVC process does not generate residual oxidants, reactivation of injured microorganisms is expected if favorable conditions are presented; such as the presence of nutrients related to wastewater (*e.g.*, DOM and inorganic salts) that provide a food source for bacteria, allowing them to metabolize and reproduce.¹⁶⁸

Therefore, bacterial regrowth was analyzed in selected samples of experiments stored in the dark after 24, 48, and 144 h (6 days) at room temperature. Although an apparent complete inactivation of *E. coli*, *E. faecalis*, and *S. enteritidis* was attained within 60 min under UVC irradiation, regrowth assessment in samples collected after 75 min of UVC treatment was

carried out for all bacterial strains. *E. coli* had an exponential increase in the concentration of viable bacteria after 48 and 144 h in the dark, with values of 2.3 and 3.5 log, respectively. In contrast, the regrowth assessment for *S. enteritidis* decreased from 1.1 log in 48 h to 0.2 log after 144 h, probably due to the lack of essential nutrients for its viability. Regrowth assessment for *E. faecalis* was not carried out in the stored samples after 24 and 48 h, but it was observed (1 log) after 144 h. These regrowth tests offer a good evaluation of the effectiveness of a process and the ability to handle post-treated effluents, which could remain stored in the dark several days before its further reuse. In this sense, UVC technology is not fully recommended for municipal wastewater effluent disinfection, even less for reclaimed final purposes.

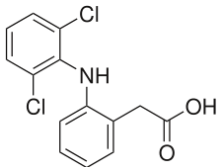
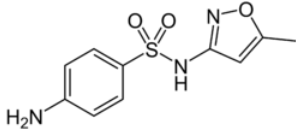
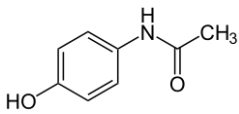
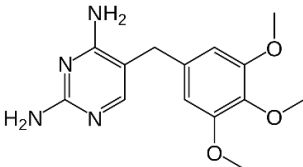
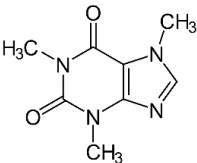
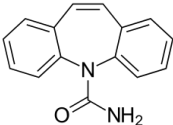
On the other hand, the inset in FIGURE 3.2 shows the degradation profile for the sum of OMC concentrations ($\sum C_t / \sum C_0$) in the SMWW effluent during the UVC process, where $\sum C_t$ and $\sum C_0$ are the sums at time t and prior to the experiment, respectively. For analysis purposes and considering, as an example, environmental regulations already established in Switzerland for OMC elimination from MWWTPs, experiments were performed with the aim of removing 80% of total OMCs.^{169, 170} UVC irradiation significantly decreased the total amount of OMCs (60%) in the effluent after 180 min (3.8 kJ L⁻¹ accumulated UVC radiation required); however, it was not enough to attain the degradation target of 80%. Clearly, some OMCs demanded a longer irradiation time (and so higher accumulative UVC energy) to be oxidized than that required for reaching complete bacterial inactivation, but others were slightly affected by UVC irradiation.

However, it is important to highlight that though complete elimination of the sum of OMCs was not achieved, some of them attained degradation percentages higher than 75%. This behavior is in agreement with the different absorption capacities of UVC light by the organic compounds, measured by the quantum yield and the molar absorption coefficient at 254 nm. These two fundamental parameters govern the direct photolysis rate; thus, molecules with moderate values of these parameters will be more sensitive to degradation under UVC irradiation. Chemical structures, photochemical properties (absorbance, quantum yields, and molar absorption coefficients) at 254 nm, and degradation percentages of these OMCs can be seen in TABLE 3.2. FIGURE B2 (APPENDIX B) also shows the UV absorption spectrums of these compounds.

In this sense, DCF and SMX, with having high values of these parameters at 254 nm, were substantially removed (<DL) at the beginning of the experiment, *i.e.*, in 20 min (0.3 kJ L⁻¹ accumulative UVC energy) and 30 min (0.6 kJ L⁻¹ accumulative UVC energy),

respectively. On the other hand, 75% of ACT was removed only after 180 min (3.8 kJ L⁻¹ of accumulative UVC energy), while CBZ, CAF, and TMP showed the lowest degradation percentages (20%, 30%, and 40%, respectively) since they have low molar absorption and quantum yield.

TABLE 3.2 – Photochemical properties of OMCs (at 254 nm) and experimental degradation percentages under UVC irradiation.

OMCs	Chemical structure	*A ₂₅₄	†ε ₂₅₄ (10 ³ M ⁻¹ cm ⁻¹)	†Φ ₂₅₄ (10 ⁻² mol Es ⁻¹)	*Degradation (%)
DCF		0.023	6.1	22.2	~100% (20 min)
SMX		0.064	16.5	5.8	~100% (30 min)
ACT		0.056	6.6	4.6	75% (180 min)
TMP		0.017	2.9	0.6	40% (180 min)
CAF		0.022	4.2	0.3	30% (180 min)
CBZ		0.026	5.5	0.2	20% (180 min)

A₂₅₄ = absorbance at 254 nm

ε₂₅₄ (M⁻¹ cm⁻¹) = molar absorptivity coefficient at 254 nm

Φ₂₅₄ (mol Es⁻¹) = quantum yield at 254 nm

*Experimental values obtained in this study

†Reference = Yu *et al.*¹⁷¹

These results are in accordance with the findings of Yu *et al.*¹⁷¹, which classified several pollutants based on their relative reactivity towards UVC direct photolysis. DCF and SMX were considered easily photodegraded by UVC light with no additional oxidants, whereas CAF, CBZ, and TMP were classified as photo-resistant but highly reactive with HO[•] radicals.

Cerreta *et al.*¹⁷² also reported that SMX was almost completely removed in natural and distilled water after 30 min of treatment (90%; 0.7 kJ L⁻¹ accumulative UVC energy) using only UVC, while only 18% of CBZ degradation was observed after 120 min (2.7 kJ L⁻¹ accumulative UVC energy).

Other parameters, such as pH, conductivity, turbidity, DOC, DIC, and ion concentration were also monitored but had an insignificant variation throughout the experiments, as expected. It is important to mention that specifically, a decrease in the organic load (measured by DOC) is expected to provoke an increase of light penetration in the system. Consequently, this might result in an improvement of UVC-based AOPs efficiency considering OMC removal and bacterial inactivation.

3.4.2. UVC/H₂O₂ treatment for simultaneous bacterial inactivation and OMCs degradation

Fast inactivation rates of *E. coli*, *E. faecalis*, and *S. enteritidis* were observed for UVC/H₂O₂ experiments in all concentrations investigated (5–50 mg L⁻¹), as it can be observed in FIGURE 3.3. Similar to the UVC results, double log-linear kinetics was observed for all bacterial inactivation. However, in comparison with these results, the addition of H₂O₂ did not entail an improvement in the disinfection process since the pseudo-first order inactivation kinetic constants (k_1 and k_2) did not show a significant increase (see TABLE 3.3).

Only at higher H₂O₂ concentrations (25, 35, and 50 mg L⁻¹), it was observed a slight increase in the inactivation kinetic constants and a reduction in the irradiation time to attain the DL. In particular, for 25 mg L⁻¹ H₂O₂, bacterial inactivation was very fast in the first stage, so it was not possible to fit the curve to calculate k_1 . According to these results, the main inactivation mechanism came from the effect of UVC radiation rather than from damage produced by HO[•] generated through H₂O₂ activation.

Similarly, Pablos *et al.*¹⁷³ and Yoon *et al.*¹⁷⁴ suggested that the germicidal effect of UVC absorption by bacterial DNA in *E. coli* K12 and DH5 α strains, respectively, is the main inactivation mechanism and no significant differences were observed in the values of k for UVC and UVC/H₂O₂. Moussavi *et al.*¹⁷⁵ also reported that the enhancement on inactivation of *E. coli* by adding H₂O₂ was hardly noticeable compared to UVC in the treatment of hospital wastewater. In contrast, Rubio *et al.*¹⁷⁶ reported a significant enhancement in *E. coli* K12 inactivation in natural water after addition of H₂O₂ compared to the use of only UVC light. The k increased 150% for the combined process.

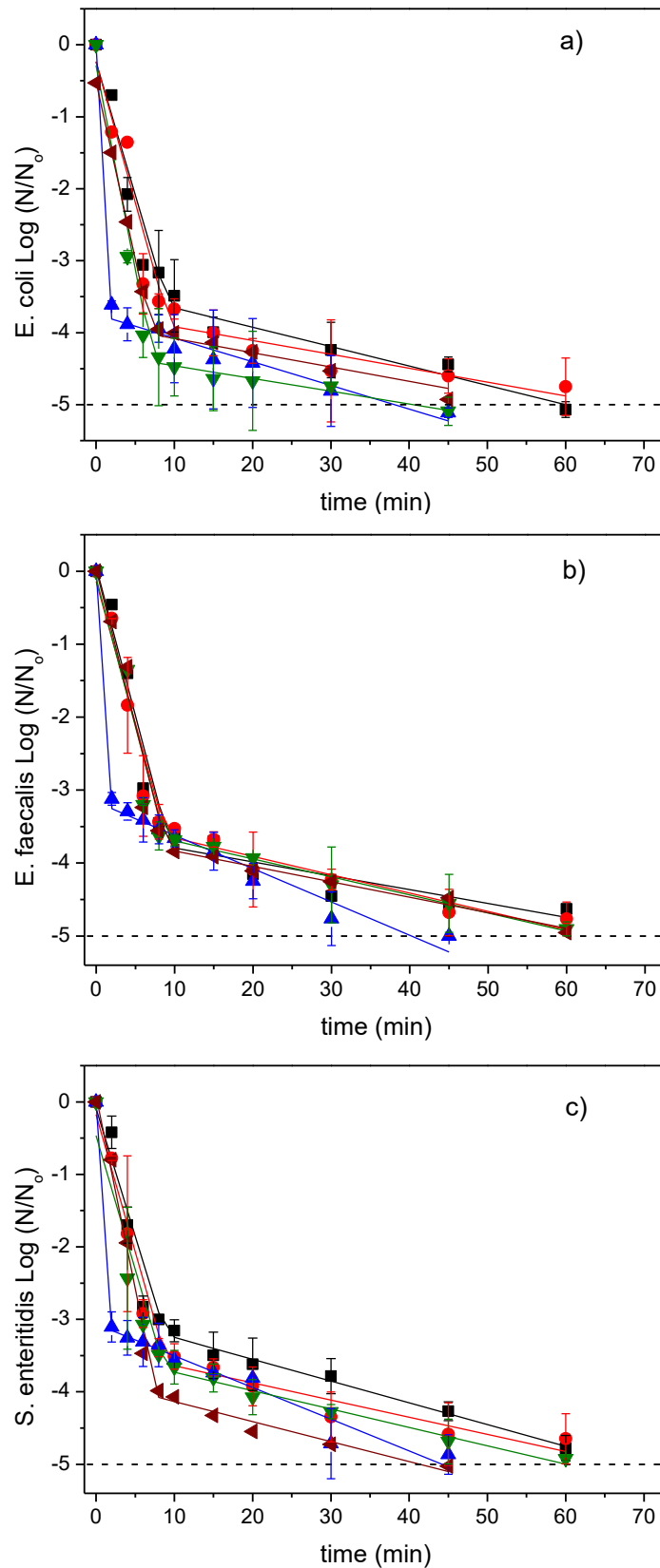


FIGURE 3.3 – Effect of different H₂O₂ concentration ([H₂O₂]) on the a) *E. coli*, b) *E. faecalis*, and c) *S. enteritidis* inactivation by UVC/H₂O₂ as a function of treatment time in SMWW effluent. [H₂O₂] = 5 (■), 15 (●), 25 (▲), 35 (▼), and 50 mg L⁻¹ (◄). Dashed lines (---) refer to detection limit (DL = 1 CFU per 100 mL⁻¹).

Moreover, Moreno-Andrés *et al.*¹⁷⁷ indicated that the addition of H₂O₂ (10 mg L⁻¹) to the UVC system improved the disinfection efficiency of *E. faecalis* in salty water. Probably, the sum of the effects of UVC irradiation and HO^{*} species was the major route for bacterial inactivation in those studies, and in other cases HO^{*} species compensated for the absorption of photons at 254 nm by H₂O₂. The inactivation efficiency of microorganisms using this process may also depend on many factors, such as the hydrodynamic parameters of the photo-reactor, power of the UVC lamp (or UVC energy dose), light path length of the photo-reactor, water matrix, oxidant concentration, type of bacterial strains, etc.

TABLE 3.3 – Pseudo-first order kinetic constants (*k*) for simultaneous inactivation of bacteria and OMCs degradation in a SMWW effluent by a UVC/H₂O₂ process.

Process UVC/H ₂ O ₂ (mg L ⁻¹)	Bacteria – <i>k</i> ₁ / <i>k</i> ₂ (10 ⁻¹ min ⁻¹)			Total OMCs – <i>k</i> (10 ⁻² min ⁻¹)		
	<i>E. coli</i>	<i>E. faecalis</i>	<i>S. enteritidis</i>	($\sum C_t/\sum C_0$)	time ^a (min)	Q _{UVC} ^b (kJ L ⁻¹)
0	3.5±0.6 (0.86) / 0.24±0.02 (0.97)	3.6±0.5 (0.90) / 0.23±0.02 (0.96)	3.3±0.7 (0.87) / 0.22±0.02 (0.97)	0.5 (0.82) only 60%	180	3.8
5	3.7±0.5 (0.90) / 0.27±0.04 (0.90)	4.0±0.5 (0.93) / 0.19±0.04 (0.81)	3.5±0.5 (0.90) / 0.30±0.02 (0.98)	1.2 (0.94)	120	2.5
15	3.9±0.6 (0.88) / 0.19±0.04 (0.77)	3.9±0.5 (0.91) / 0.25±0.04 (0.89)	3.8±0.4 (0.94) / 0.24±0.04 (0.86)	3.0 (0.97)	52	1.0
25	ND / 0.33±0.03 (0.93)	ND / 0.45±0.4 (0.95)	ND / 0.44±0.04 (0.94)	5.7 (0.99)	24	0.4
35	5.6±0.9 (0.93) / 0.18±0.02 (0.91)	4.1±0.7 (0.89) / 0.25±0.01 (0.98)	3.8±0.7 (0.87) / 0.25±0.02 (0.97)	7.0 (0.99)	21	0.4
50	4.8±0.9 (0.88) / 0.26±0.03 (0.96)	4.2±0.5 (0.92) / 0.21±0.01 (0.97)	5.3±0.4 (0.97) / 0.27±0.03 (0.93)	10.0 (0.99)	17	0.3

^avalues refer to the attainment of 80% removal of total OMCs except for the UVC alone experiment, in which only 60% of total OMCs removal was attained.

^baccumulative UVC energy required to attain 80% removal of total OMCs
values in parentheses refers to coefficient of determination (R²)

ND = not determined

Moreno-Andrés¹⁷⁷ also reported a detrimental effect on bacterial inactivation due to the addition of a high concentration of H₂O₂ (100 mg L⁻¹) based on the competition for the absorption of photons at 254 nm between bacteria and the oxidant. This detrimental effect was not observed under the operating conditions used in this work, which would probably appear at higher concentrations of H₂O₂ or longer light path length in which the competition for photon absorption would be significantly higher (see section 3.4.4).

It is important to note that the photolysis percentage of H₂O₂ was only 10% after 60 min independently of the concentration used. This means a consumption rate of 0.008, 0.045, and 0.076 mg H₂O₂ L⁻¹ min⁻¹ for 5, 25 and 50 mg L⁻¹, respectively, which explain the poor contribution of low H₂O₂ concentrations on bacterial inactivation in comparison with the UVC effect. In this case, for concentrations between 25 and 50 mg L⁻¹, high residual concentrations

of this oxidant were present in the treated wastewater. This suggests that the slight enhancement on bacterial inactivation observed at high concentrations might be due to a small fraction of HO^\bullet generated or to the direct disinfectant effect of H_2O_2 , since it is well known that at high concentrations this oxidant has a toxic effect on bacterial viability. Rodríguez-Chueca *et al.*¹⁶⁴ reported 6 log and 1.5 log reduction of *E. coli* and *E. faecalis*, respectively, after 180 min in the dark using 50 mg L^{-1} of H_2O_2 . At lower concentrations (20 mg L^{-1}) this effect is not significant on inactivation of *E. coli* O157:H7 and *S. enteritidis*, as reported by Nahim-Granados *et al.*¹⁵⁹

As discussed in the UVC reference experiment, bacterial regrowth was monitored in the treated samples due to their self-repair capacity in the dark. In the presence of H_2O_2 , regrowth was not observed after the treatment (sample withdrawn after 75 min) under any of the conditions tested ($5\text{--}50 \text{ mg L}^{-1}$) and for all times analyzed (24, 48 and 144 h). H_2O_2 concentration in all experiments remained constant in the dark until 144 h of storage. Therefore, the remaining H_2O_2 has a possible further bacteriostatic effect, preventing bacterial repair/reproduction during the storage or through the distribution system. Other studies report assessment of bacterial regrowth but only after 24 and 48 h.^{164, 178, 179}

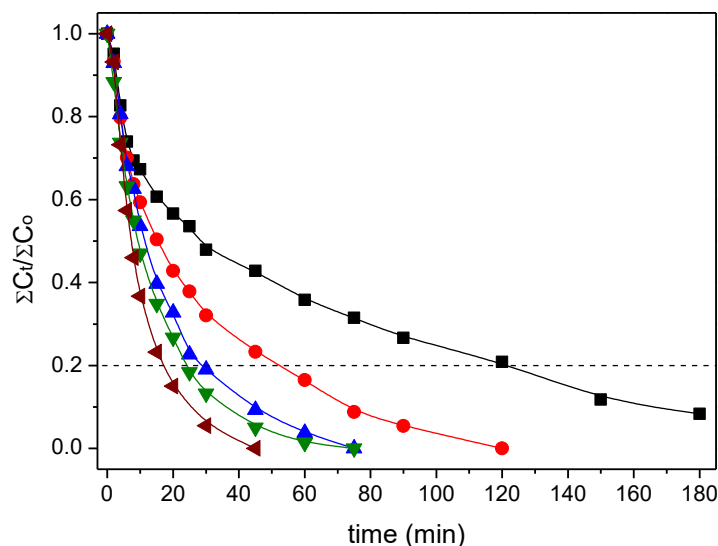


FIGURE 3.4 – Effect of different H_2O_2 concentration ($[\text{H}_2\text{O}_2]$) on the total OMC degradation by UVC/ H_2O_2 as a function of treatment time in SMWW effluent. $[\text{H}_2\text{O}_2] = 5$ (■), 15 (●), 25 (▲), 35 (▼), and 50 mg L^{-1} (◄). Dashed line (---) refers to 80% removal of total OMCs.

The effect of H_2O_2 concentration on OMC degradation was also evaluated as can be seen in FIGURE 3.4. The use of H_2O_2 in combination with UVC irradiation increased the removal of all target compounds compared with UVC alone, especially those that are photo-

stable, CAF, CBZ, and TMP, resulting in a degradation rate of over 80% for the sum of OMCs under all investigated conditions. This effect was mainly caused by the effect of HO^\bullet generated in H_2O_2 activation at 254 nm (see eq. (1)). Illumination time (and accumulative UVC energy) required to achieve 80% OMC degradation decreased with the increase in H_2O_2 concentration, *e.g.*, from 120 min (2.5 kJ L^{-1} accumulative UVC energy required) with 5 mg L^{-1} to 17 min (0.3 kJ L^{-1} accumulated UVC energy) with $50 \text{ mg L}^{-1} \text{ H}_2\text{O}_2$ (TABLE 3.3).

Clearly, UVC/ H_2O_2 at 5 mg L^{-1} required a higher UVC energy dose to degrade OMCs than that required for reaching complete bacterial inactivation. Pseudo-first order kinetic constants (k) corresponding to these experiments are also shown in TABLE 3.3. It was noticed that the degradation kinetic constants of this process were strongly dependent on the initial concentration of the oxidant. That behavior can be observed in FIGURE 3.5, which shows a linear relationship between kinetic constants and initial concentrations of H_2O_2 .

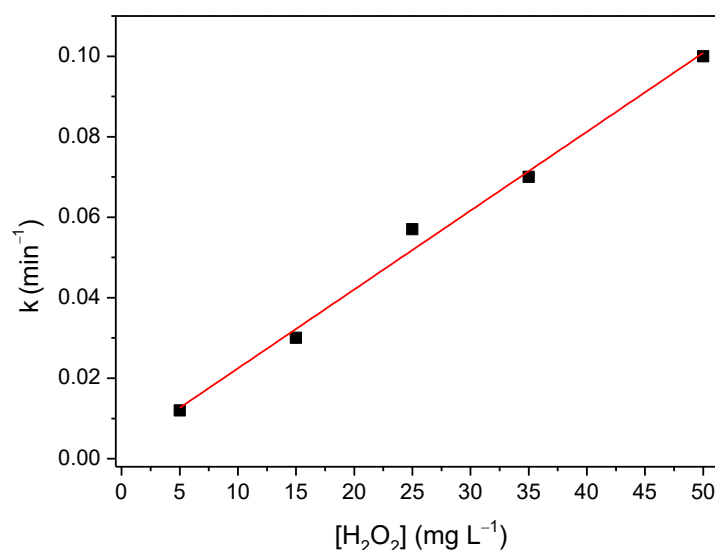


FIGURE 3.5 – Pseudo-first order kinetic constant (k ; ■) as a function of H_2O_2 concentration ($[\text{H}_2\text{O}_2]$) for UVC/ H_2O_2 process. The obtained slope and R^2 for the linear regression were $0.00196 \text{ L (mg min)}^{-1}$ and 0.990, respectively.

Despite this, it is important also to highlight that while kinetic constants increased proportionally with H_2O_2 till 0.1 min^{-1} for $50 \text{ mg L}^{-1} \text{ H}_2\text{O}_2$, the illumination time required to reach 80% of degradation varied slightly when using 35 and $25 \text{ mg L}^{-1} \text{ H}_2\text{O}_2$ and ranged from 21 to 24 min, respectively. In addition, oxidant residual concentrations after treatment were 49 and 23 mg L^{-1} for 50 and $25 \text{ mg L}^{-1} \text{ H}_2\text{O}_2$, respectively, showing a limitation caused by the light path length and therefore by the photo-reactor configuration, which will be addressed in section 3.4.4.

For a better understanding of the effect of the UVC/H₂O₂ process on OMC removal, the degradation profile of each compound and the oxidant consumption are detailed in FIGURE B3. Moreover, TABLE B2 shows the calculated k for each contaminant as a function of H₂O₂ concentration used.

CAF, TMP, and CBZ, which did not exhibit a high photodegradation percentage (20–40%), were significantly removed using 5 mg L⁻¹ H₂O₂ under UVC irradiation, attaining removal rates of over 80% after 180 min and with a H₂O₂ consumption close to 1.0 mg L⁻¹. For this condition, only 0.8 mg L⁻¹ H₂O₂ and 2.5 kJ L⁻¹ were required to eliminate 80% of the total OMCs. A higher increase in the degradation rate was observed for UVC/H₂O₂ with 25 mg L⁻¹, reaching 80% of removal in 24 min and consuming 2.3 mg L⁻¹ of the oxidant. As expected, 80% of total OMCs was quickly achieved using 50 mg L⁻¹ (17 min; 0.3 kJ L⁻¹ accumulated UVC energy) with a H₂O₂ consumption of 1.3 mg L⁻¹. It is important to note that for the same process, the degradation kinetic constant for the photo-stable compounds did not show significant differences, which confirm the non-selectivity of the generated HO[•] species by the H₂O₂ homolysis. On the other hand, DOC decreased around 10% only for high concentrations of H₂O₂ (25–50 mg L⁻¹).

3.4.3. UVC/S₂O₈²⁻ treatment for simultaneous bacterial inactivation and OMCs degradation

E. coli, *E. faecalis*, and *S. enteritidis* inactivation by the UVC/ S₂O₈²⁻ process is shown in FIGURE 3.6. As it can be observed, *E. coli* was quickly inactivated under the two investigated conditions, improving significantly the pseudo-first order kinetic constants obtained with the UVC process (see TABLE 3.4). Due to the high rate of *E. coli* inactivation under these conditions, it was not possible to calculate the kinetic constants k_1 (first stage). DL was achieved only after 10 min (0.1 kJ L⁻¹ accumulated UVC energy) and 15 min (0.2 kJ L⁻¹ accumulated UVC energy) for 40 and 20 mg L⁻¹ S₂O₈²⁻, respectively.

Several studies attributed the bacterial inactivation in the UVC/S₂O₈²⁻ system to the selectivity and reactivity of generated SO₄^{•-} species (see eq. (2)), which reacts with macromolecules that are present in the cell wall. Michael-Kordatou *et al.*¹⁸⁰ reported a significant enhancement (around 200%) to reduce 5-log of *E. coli* in urban wastewater after the addition of S₂O₈²⁻. Popova *et al.*¹⁸¹ also reported an increase (>130%) in the rate constant to eliminate *E. coli* when using the UVC/S₂O₈²⁻ process.

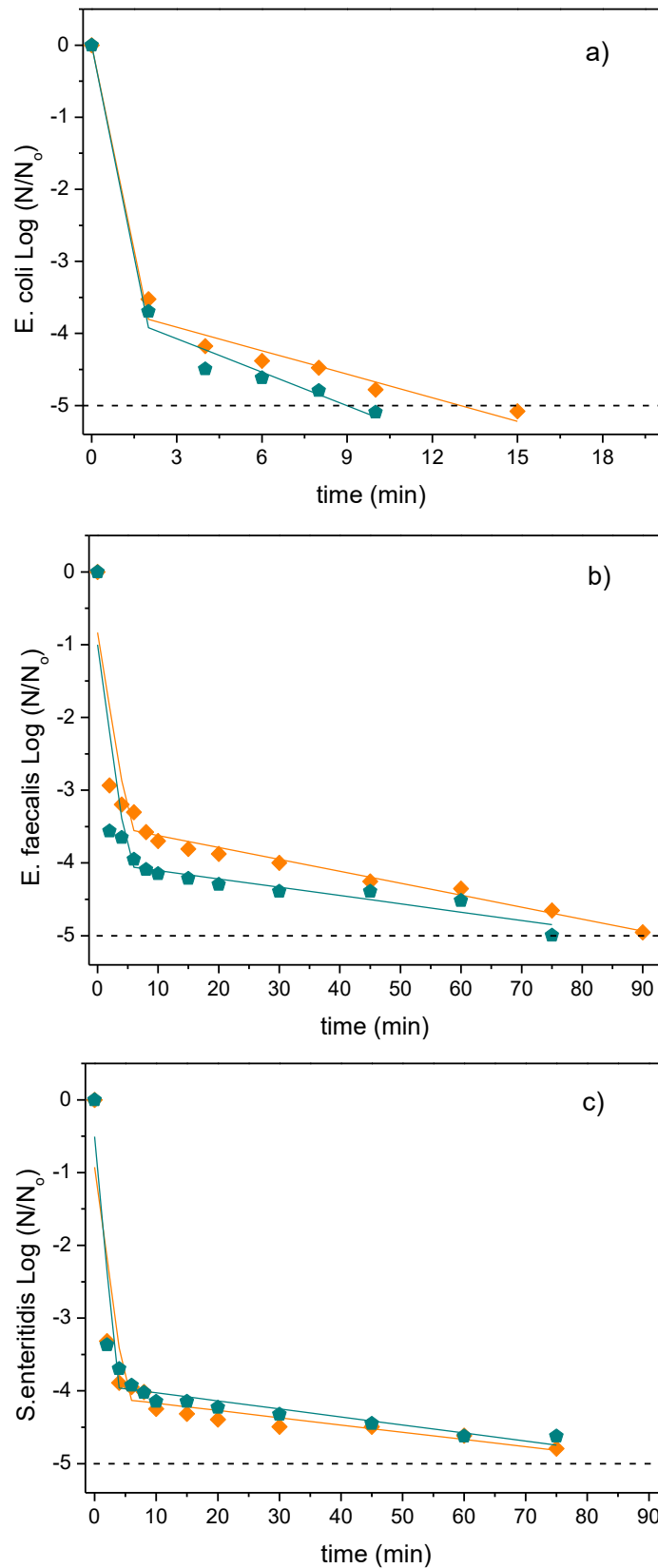


FIGURE 3.6 – Effect of different $\text{S}_2\text{O}_8^{2-}$ concentration ($[\text{S}_2\text{O}_8^{2-}]$) on the a) *E. coli*, b) *E. faecalis*, and c) *S. enteritidis* inactivation by UVC/ $\text{S}_2\text{O}_8^{2-}$ as a function of treatment time in SMWW effluent. $[\text{S}_2\text{O}_8^{2-}] = 20$ (◆) and 40 mg L^{-1} (◆). Dashed lines (---) refer to detection limit (DL = 1 CFU per 100 mL^{-1}).

On the other hand, comparison with systems based on the generation of HO[•], such as UVC/H₂O₂, is difficult to address. From a purely chemical approach, the best option is to compare the efficiency of these systems using an equivalent molar ratio of both oxidants, but the high S₂O₈²⁻ molar mass implies very high concentrations in terms of mass per unit of volume.¹⁷⁹ This would lead to a drastic increase in the operating costs of this process. In this sense, the focus of this study was to assess the behavior of this system under realistic conditions, rather than strictly compare kinetics with UVC/H₂O₂. It must be highlighted that H₂O₂ and S₂O₈²⁻ selected concentrations were in the range of those successfully studied in previous research works.^{163, 179} In addition, other factors such as the stronger selective oxidation capability towards macromolecules/biomolecules of the cell membrane and the half-life of the produced radical can favor a stronger action of SO₄^{•-}.

Wordofa *et al.*¹⁸² showed that exposure to SO₄^{•-} promoted the loss of cell viability of *E. coli* O157:H7 5 times faster than when HO[•] was used. This unique feature of SO₄^{•-} is possibly associated with its highly selective reactivity towards electron-rich moieties on the surface of *E. coli* O157:H7 cell membranes, such as flagella, proteins, and extracellular polymeric substances. Moreover, Serna-Galvis *et al.*¹⁸³ also attributed the microorganism inactivation by UVC/S₂O₈²⁻ to the already commented high interaction of SO₄^{•-} with organic macromolecules of the cell wall.

As can be seen in FIGURE 3.6(b–c), the UVC/S₂O₈²⁻ system was less effective on *E. faecalis* and *S. enteritidis* inactivation. Both bacteria were inactivated within 75–90 min (1.2–1.5 kJ L⁻¹ accumulated UVC energy, respectively) for the two tested concentrations. Clearly, this result indicates a different inactivation mechanism, probably related to structural differences and cellular composition between these bacteria. In particular, *E. faecalis*, which required 90 and 75 min to attain the DL using 20 and 40 mg L⁻¹ of S₂O₈²⁻, respectively, has a structural difference with *E. coli* regarding the cell wall components. *E. faecalis* has a thicker cell wall in which the major component is the peptidoglycan layer. In contrast, *E. coli* has a thin layer of peptidoglycan together with an outer membrane that results in a more complex structure. These differences make Gram-negative bacteria (*e.g.*, *E. coli*) more sensitive than Gram-positive (*e.g.*, *E. faecalis*) with respect to UV-based treatments.^{178, 184} Although both *E. coli* and *S. enteritidis* are Gram-negative bacteria, the latter one showed higher resistance to inactivation, which could be due to the presence of different sugars and sugar linkages that form the lipopolysaccharide, the major component of the Gram-negative bacterial outer membrane.¹⁸⁵

Wordofa *et al.*¹⁸² also reported that the efficiency of these processes are dependent on the specific composition of macromolecules for each bacterial group. Another possible mechanism is related to the detrimental effect on bacteria inactivation based on the competition for the absorption of photons at 254 nm between bacteria and oxidant, since $S_2O_8^{2-}$ has a high capacity of light absorption at this wavelength.⁷¹ While some fundamental investigations on the inactivation of different microorganisms by $SO_4^{\bullet-}$ have been established, the molecular mechanisms of inactivation, particularly the interaction of $SO_4^{\bullet-}$ with biomolecules, are far from complete comprehension.

TABLE 3.4 – Pseudo-first order kinetic constants (k) for simultaneous inactivation of bacteria and OMC degradation in a SMWW effluent by the UVC/ $S_2O_8^{2-}$ process.

UVC/ $S_2O_8^{2-}$ (mg L ⁻¹)	Bacteria – k_1/k_2 (10 ⁻¹ min ⁻¹)			Total OMCs – k (10 ⁻² min ⁻¹)		
	<i>E. coli</i>	<i>E. faecalis</i>	<i>S. enteritidis</i>	($\sum C_t/\sum C_0$)	time ^a (min)	Q _{UVC} ^b (kJ L ⁻¹)
0	3.5±0.6 (0.86) / 0.24±0.02 (0.97)	3.6±0.5 (0.90) / 0.23±0.02 (0.96)	3.3±0.7 (0.87) / 0.22±0.02 (0.97)	0.5 (0.82) only 60%	180	3.8
20	ND / 1.1±0.1 (0.87)	5.1±2.1 (0.53) / 0.2±0.01 (0.95)	6.2±2.7 (0.59) / 0.1±0.02 (0.80)	1.6 (0.99)	90	1.8
40	ND / 1.5±0.3 (0.84)	6.0±2.8 (0.52) / 0.1±0.01 (0.87)	6.0±2.7 (0.57) / 0.1±0.01 (0.92)	4.2 (0.98)	45	0.9
100	NM	NM	NM	11.6 (0.98)	24	0.4

^avalues refer to the attainment of 80% removal of total OMCs except for the UVC alone experiment, in which only 60% of total OMCs removal was attained

^baccumulative UVC energy required to attain 80% removal of total OMCs values in parentheses refers to coefficient of determination (R^2)

ND = not determined

NM = not measured

Bacterial regrowth assessment was carried out after 24, 48, and 144 h after the treatment was finished. Regrowth for all bacteria was detected for 20 and 40 mg L⁻¹ $S_2O_8^{2-}$, but much lower compared with that using only the UVC treatment. In particular, *E. faecalis* and *S. enteritidis* had a maximum regrowth of around 0.7 log after 48 h under both conditions, but it was not detected (<DL) after 144 h of storage. In contrast, *E. coli* regrowth was significant, increasing the concentration of viable bacteria after 24 and 48 h in the dark, until 1.3 and 1.9 log, respectively, remaining almost constant after 144 h. This means that the residual concentration of $S_2O_8^{2-}$, 18 mg L⁻¹ (for the initial concentration of 20 mg L⁻¹) and 28 mg L⁻¹ (for the initial concentration of 40 mg L⁻¹) did not prevent bacterial regrowth since $S_2O_8^{2-}$ has no bactericidal effect by itself.

To check this, several experiments (data not shown) were carried out putting in contact bacteria with $S_2O_8^{2-}$ in different concentrations (up to 50 mg L⁻¹) and in the dark. No

significant effect was observed on the viability of bacteria. This fact is explained due to the size and charge of $S_2O_8^{2-}$, which can limit the diffusion through the cell membrane, avoiding the inactivation *via* Fenton-like reaction, as in the case of H_2O_2 .¹⁸⁶ Moreno-Andrés *et al.*¹⁷⁸ observed regrowth (after 48) for *E. coli* and *E. faecalis* bacteria in distilled water after UVC/ $S_2O_8^{2-}$ treatment, even when using a higher oxidant concentration (200 mg L^{-1}) than the used in the present study.

The UVC/ $S_2O_8^{2-}$ system was also effective in removing 80% of the sum of OMCs (FIGURE 3.7), but in slightly longer treatment times than those obtained with UVC/ H_2O_2 . This result could be justified by the use of $S_2O_8^{2-}$ in a molar concentration lower than that of H_2O_2 . Therefore, it is important to stress that similar treatment time (24 min; 0.4 kJ L^{-1} accumulated UVC energy) was required to eliminate 80% of the sum of OMCs with 25 mg L^{-1} UVC/ H_2O_2 and 100 mg L^{-1} UVC/ $S_2O_8^{2-}$, that means 0.73 mmol L^{-1} and 0.52 mmol L^{-1} , respectively.

Starling *et al.*¹⁸⁷ reported an increase in the removal rates for photo-stable compounds CAF and CBZ in 2 L of a real surface water by using UVC/ $S_2O_8^{2-}$ (1 mmol L^{-1}), resulting in more than 90% degradation with an UVC energy of 5.9 and 11.8 J L^{-1} , respectively. In contrast, DOC concentration had a very slight variation throughout the experiments, even when using the higher $S_2O_8^{2-}$ concentration (100 mg L^{-1}).

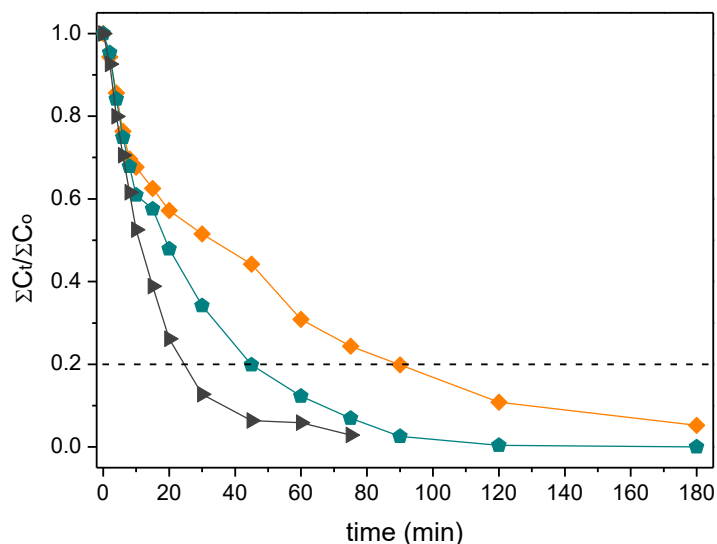


FIGURE 3.7 – Effect of different $S_2O_8^{2-}$ concentration ($[S_2O_8^{2-}]$) on the total OMC degradation by UVC/ $S_2O_8^{2-}$ as a function of treatment time in SMWW effluent. $[S_2O_8^{2-}] = 20$ (◆), 40 (◆), and 100 mg L^{-1} (▶). Dashed line (---) refers to 80% removal of total OMCs.

Similar to the UVC/H₂O₂ process, increase in the oxidant concentration also increased OMC removal rates (k), achieving 80% of total degradation after 90 min (1.8 kJ L⁻¹ accumulated UVC energy) when using 20 mg L⁻¹ S₂O₈²⁻ and only 24 min (0.4 kJ L⁻¹ accumulated UVC energy) for 100 mg L⁻¹ (TABLE 3.4). This confirms that the generation of SO₄^{•-} plays a major role in the degradation of the six OMCs; FIGURE 3.8 shows a linear relationship between the degradation kinetic constants with the initial concentration of S₂O₈²⁻. In addition, similar evolution curves for pseudo-first order kinetic constants for OMC removal were obtained compared to UVC/H₂O₂ experiments, confirming that it was not necessary to check more S₂O₈²⁻ concentrations.

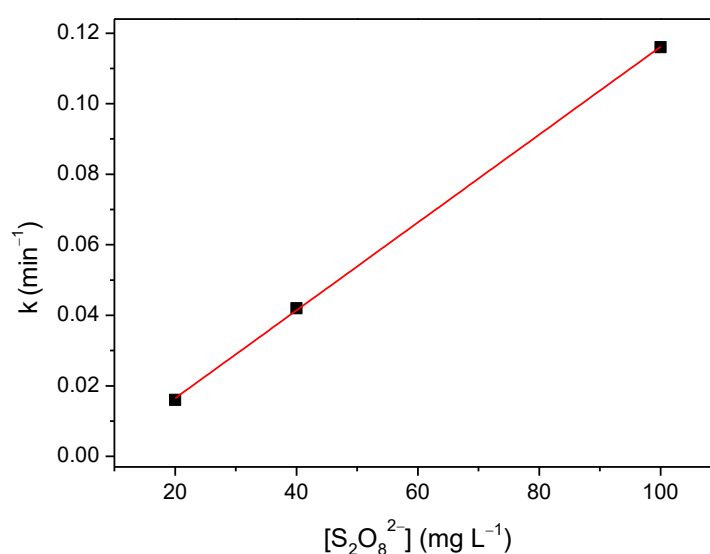


FIGURE 3.8 – Pseudo-first order kinetic constant (k ; ■) as a function of S₂O₈²⁻ concentration ([S₂O₈²⁻]) for UVC/S₂O₈²⁻ process. The obtained slope and R² for the linear regression were 0.00125 L (mg min)⁻¹ and 0.999, respectively

On the other hand, in APPENDIX B, FIGURE B4 shows the degradation profile of each contaminant and the S₂O₈²⁻ consumption for all conditions studied, as well as the degradation kinetic constants (this last parameter is shown in TABLE B3). As expected, the degradation curves had a similar profile as UVC/H₂O₂. No significant increase in the degradation rates of DCF and SFX were observed; however, TMP was slowly oxidized with regard to the rest of the OMCs, contrary to what occurred when UVC/H₂O₂ was applied (see degradation kinetic constants in TABLE B3).

This behavior is explained by the different reaction rates of SO₄^{•-} with specific functional groups of organic molecules. Wojnárovits *et al.*¹⁸⁸ reported that electron-donating substituents increase the rate constants and electron-withdrawing substituents decrease it. In this sense, -OR and -NH₂ (electron-withdrawing substituents) present in the molecular

structure of TMP affect the efficiency of $\text{SO}_4^{\bullet-}$ to degrade this compound. ACT also showed lower kinetic constants due to the effect of these substituents in its structure ($-\text{OH}$ and $-\text{NHCOR}$). Once again, this confirms the selective character of generated $\text{SO}_4^{\bullet-}$ species against the non-selective character of HO^\bullet generated in UVC/ H_2O_2 . As expected, consumption rates increased with $\text{S}_2\text{O}_8^{2-}$ initial concentration, attaining 0.04, 0.15, and 0.20 mg $\text{S}_2\text{O}_8^{2-} \text{L}^{-1} \text{min}^{-1}$ for 20, 40 and 100 mg L^{-1} , respectively.

3.4.4. Preliminary model to determine the maximum yield of oxidant for UVC based system

As reported in this study and in others from the literature, the UVC/ H_2O_2 and UVC/ $\text{S}_2\text{O}_8^{2-}$ processes are very efficient for removing contaminants in aqueous medium. Nevertheless, critical oxidant concentrations seem to be attained and experiments carried out beyond these values are not effective in oxidizing organic compounds. Distinct critical concentrations of H_2O_2 have been reported as the most suitable since the optimum oxidant concentration is highly dependent on the nature of the target contaminant, water matrix, hydrodynamic parameters of the photo-reactor, and power of the UVC lamp.

As can be seen in FIGURES 3.9-3.10, the illumination time required for the removal of 80% of the sum of OMCs is shown to be close to 9 min, remaining constant with the increase in the concentration of the oxidant used (H_2O_2 and $\text{S}_2\text{O}_8^{2-}$, respectively), *i.e.*, the maximum oxidant concentration to be used in this system was reached. Moreover, the first order kinetic constant (k) showed that adding H_2O_2 and $\text{S}_2\text{O}_8^{2-}$ above 150 and 200 mg L^{-1} , respectively, did not produce any enhancement in the efficiency of the treatment (see FIGURES B5-B6). This means that increasing the concentration of the oxidant is not always linked to a treatment improvement due to the self-scavenging reactions (as discussed in section 2.4.1 and shown in TABLE A1) and/or due to the limitations associated to the experimental configuration of the photo-reactors.

Consequently, the optical path length of the photo-reactor could play an important role in the efficiency of these processes, determining the amount of generated radicals. In this sense, the Beer–Lambert law that relates the absorbance with the optical path length and the oxidant concentration can be used to determine the most suitable oxidant quantity for a given photo-reactor setup, as shown in the following eq.:

$$[\text{Ox}] = \frac{A_{254}}{\varepsilon_{254} \ell} \quad (21)$$

where $[Ox]$ is the oxidant concentration ($mg\ L^{-1}$), A_{254} is the absorbance of the solution at 254 nm (including the matrix effect), ϵ_{254} is the molar absorptivity coefficient of oxidants at 254 nm ($mg^{-1}\ L\ cm^{-1}$), and ℓ is the optical path length of the photo-reactor (cm). Here, $A_{254} = 0.186$ (measured at 254 nm) and $\ell = 2.595\ cm$ (from FIGURE 3.1, $\ell = r_{int,C} - r_{int,L}$).

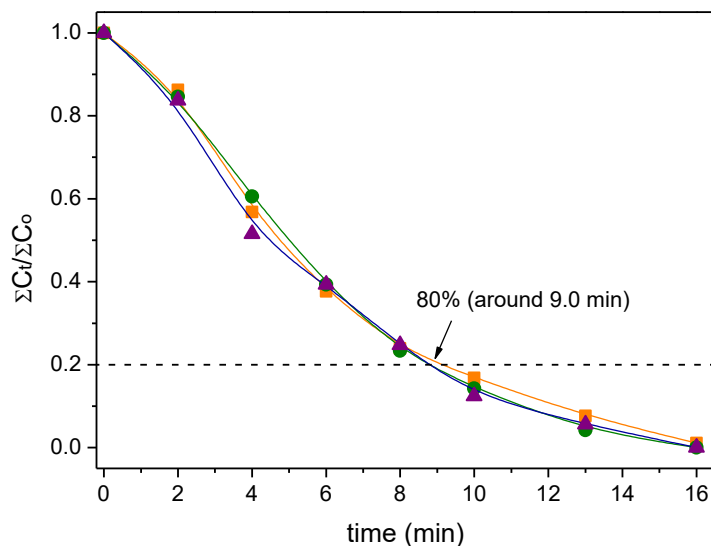


FIGURE 3.9 – Effect of high H_2O_2 concentration ($[H_2O_2]$) on the total OMC degradation under UVC irradiation as a function of treatment time in SMWW effluent: $[H_2O_2] = 150$ (□), 300 (●), and $600\ mg\ L^{-1}$ (▲). Dashed line (---) refers to 80% removal of total OMCs.

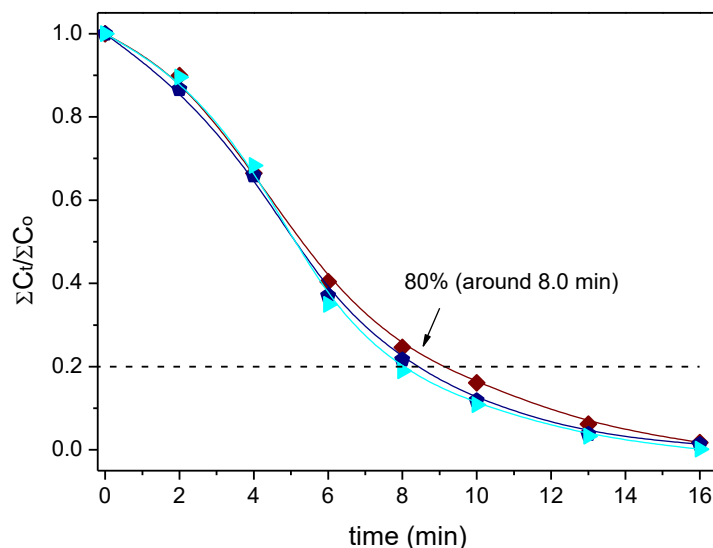


FIGURE 3.10 – Effect of high $S_2O_8^{2-}$ concentration ($[S_2O_8^{2-}]$) on the total OMC degradation under UVC irradiation as a function of treatment time in SMWW effluent. $[S_2O_8^{2-}] = 200$ (◆), 250 (◆), and $300\ mg\ L^{-1}$ (▶). Dashed line (---) refers to 80% removal of total OMCs.

Taking these parameters into account, the H_2O_2 concentration calculated with eq. (21) is $126\ mg\ L^{-1}$ ($3.70\ mmol\ L^{-1}$) using the molar absorptivity coefficient of H_2O_2 at

254 nm calculated for this system ($5.7 \times 10^{-4} \text{ mg}^{-1} \text{ L cm}^{-1}$). This represents a good approximation considering that the experimental concentration for the UVC/H₂O₂ process to attain saturation was 150 mg L⁻¹.

As discussed above, the quantum yield of S₂O₈²⁻ is 2.8 times higher than that of H₂O₂, so the molar concentration to reach saturation using this oxidant is probably proportional to this factor or lower, *i.e.*, 1.32 mmol L⁻¹ (or 253 mg of S₂O₈²⁻ L⁻¹). The obtained experimental concentration to attain saturation was 200 mg L⁻¹ (or 1.04 mmol L⁻¹). Additionally, there are many factors to be considered for modelling these systems, such as secondary reactions (including self-scavenging reactions), scavengers present in the matrix, nature of the target contaminants, etc. Therefore, the objective of this rough study was only to check the feasibility of a simple equation allowing us to predict the saturation concentration of the oxidants under the specific experimental conditions used in this investigation.

3.5. CONCLUSIONS

The simultaneous elimination of OMCs and *E. coli*, *E. faecalis*, and *S. enteritidis* bacteria were attained at pilot plant scale by UVC/H₂O₂ and UVC/S₂O₈²⁻ processes. UVC alone was not suitable due to subsequent bacteria regrowth accompanied by a very slow and incomplete removal of OMCs.

UVC/H₂O₂ led to a successful bacterial inactivation (without subsequent regrowth) and a simultaneous degradation of OMCs up to 99%. By adding 25–50 mg L⁻¹ H₂O₂, 4 log of *E. coli*, *E. faecalis*, and *S. enteritidis* bacterial inactivation and OMC degradation rate higher than 80% were attained in less than 30 min. In the case of the UVC/S₂O₈²⁻ process, quicker *E. coli* inactivation was attained due to the possible reaction of generated SO₄⁻ with macromolecules in the cell wall. However, regrowth of bacteria was not prevented even when using 50 mg L⁻¹ in the dark, possibly due to the limitation of S₂O₈²⁻ diffusion through the cell membrane. When using 20–40 mg L⁻¹ S₂O₈²⁻, 4 log of *E. coli*, *E. faecalis*, and *S. enteritidis* bacterial inactivation was attained in less than 10 min, but achieving more than 80% OMC degradation took a longer treatment time than in the UVC/H₂O₂ process. OMCs exhibited removal rates proportional to the oxidant concentration used both for UVC/H₂O₂ and for UVC/S₂O₈²⁻.

The use of a simple model based on the Beer–Lambert law and taking into account the molar absorptivity of oxidants, as well as water absorbance (matrix effect) and optical length of the photo-reactor, enabled estimation of the maximum concentration of

oxidants required to attain maximum oxidation rates in the specific UVC pilot plant used in this study. Further improvements, such as scavenging reactions and water matrix effects, must be considered for a better understanding of the UVC-based processes.

Nevertheless, it has been demonstrated that UVC/H₂O₂ and UVC/S₂O₈²⁻ are able to produce an effluent with enough quality to be reused for several purposes, with agriculture as one of the most suitable end-uses as it is the highest consumer of freshwater worldwide. However, it is important to highlight that UVC/S₂O₈²⁻ process would need a slight addition of bactericidal species to avoid bacterial regrowth along water storage or reclaimed water distribution systems.

4. GENERAL CONCLUSIONS AND PERSPECTIVES FOR FUTURE STUDIES

This thesis aimed to investigate and compare the efficiency of different UVC AOPs to remove CEC and/or inactivate pathogens from water matrices under distinct experimental conditions.

In the first part of this study (laboratory scale), the activation of the oxidants under UVC irradiation led to the generation of high oxidation power radicals (*i.e.*, HO[•] and SO₄^{•-}), which were detected by the measurements of oxidants concentration evolution, generation of salicylic acids (HO[•] detection), and the use of scavengers. In all UVC AOPs, these species (HO[•] and SO₄^{•-}) were responsible for a significant increase in the oxidation rates of BPA in comparison to the photochemical and chemicals methods.

The UVC/HClO process demonstrated the best performance for the degradation and mineralization of BPA, as well as a lower quantity of oxidation by-products generated (*i.e.*, only two by-products hydroxylated detected). Moreover, LC-MS/MS analyses did not indicate any organochlorine resulting from the use of the UVC/HClO process, contrasting with the results obtained by using HClO (without UVC irradiation). However, as both processes showed similar BPA degradation rates, it is speculated that the production of organochlorine intermediates has happened in both methods (*i.e.*, UVC/HClO and HClO), but this production was promptly consumed under UVC irradiation after subsequent hydroxylation reactions. Doubtlessly, the role of UVC light avoiding (or minimizing) the formation of organochlorine by-products in the UVC/HClO process is worth to be investigated in future studies and applications.

On the other hand, the toxicity evolution of BPA solutions before and during the treatment using different UVC AOPs was successfully monitored by using the microcrustacean *A. salina*. Due to the high BPA conversion rate attained and its intermediates to CO₂ using UVC/HClO, the mortality percentage of *A. salina* was completely ceased during this process, whereas a high mortality percentage was observed using UVC/H₂O₂ method. This latter behavior was most likely due to oxidation by-products generated which have a theoretical detrimental effect on acute and chronic toxicity calculated using the ECOSAR software.

From an economic point of view, the UVC/HClO process is the most cost-effective process among the processes studied in this thesis. This cost-effectiveness was sort of expected because this UVC/HClO system needed the shortest reaction time to remove BPA. Moreover, the cheaper cost of free chlorine and its high accessibility, when comparing to the other

oxidants, makes this process an interesting and low-budget option. Finally, by taking into account the environmental and economical parameters here discussed, the UVC/HClO method represents a viable alternative since high organic removal rates can be achieved without organochlorine by-products generation and under a low operating cost.

Despite all this, some scientific challenges need to be elucidated before putting this system (*i.e.*, UVC/HClO) in use in real applications. For instance, the reaction mechanisms of several chlorine-derived radicals (*e.g.*, Cl^\bullet , ClO^\bullet , $\text{Cl}_2^{\bullet-}$, etc.) with organic compounds are far from complete comprehension. In fact, to date, it is being a difficult task to create proper experimental conditions to determine the oxidation mechanism and the kinetic constants (with probe compounds) related to the reaction between all chlorine-derived radicals and organic pollutants.

In addition, based on a recent study pertaining of my research project, it was observed that the interaction between HClO at high concentrations and UVC light generates chlorate ions (ClO_3^-) through radical propagation reactions, having such compounds been considered toxic in several environmental legislations. To the best of our knowledge, this observation has been vaguely studied and explained in the literature, and only few studies have reported the generation of chlorine oxyanions species (ClO_4^- , ClO_3^- , and ClO_2^-) in UVC/free chlorine systems. Therefore, more in-depth studies are needed to unveil what is behind such chlorine-based processes.

Another major concern related to chlorine-based processes is the poor oxidation efficiency in a complex matrix (*e.g.*, municipal wastewater, containing microcontaminants, pathogens, inorganic ions, and dissolved organic matter). Hence, it is known that the reaction between free ammonia present in wastewater (*i.e.*, NH_4^+ and NH_3) and free chlorine (mainly HClO) leads to the formation of toxic inorganic chloramines. In addition, the interaction of free chlorine with dissolved organic matter (DOM) may drive to the generation of carcinogenic disinfection by-products, such as trihalomethane and haloacetic acids. In parallel, and considering real situations, a much higher concentration of this oxidant would be required in comparison to a simpler system. In this sense, improved technologies, such as UVC/ H_2O_2 and UVC/ $\text{S}_2\text{O}_8^{2-}$, are recommended, at least at present, to remove contaminants from complex matrices.

Thus, in the second part of this study, the simultaneous elimination of six OMCs and three different bacteria by the UVC/ H_2O_2 and UVC/ $\text{S}_2\text{O}_8^{2-}$ processes was successfully investigated in a simulated municipal wastewater effluent at pilot plant scale. Although the

required limits for water reuse in agriculture were reached using only UVC radiation (considering only microbial targets) and they were in accordance with some international regulations (*e.g.*, Spanish RD1620/2007), UVC treatment alone was not suitable due to a slow and incomplete removal of OMCs. As previously discussed, OMCs pose a potential hazard for the environment and receptors of reclaimed water, for instance, an accumulation of OMCs in fruits and raw-eaten vegetables might happen in crops by the use of reclaimed water in agricultural activities. This observation is truly relevant because it shows that the same process can be effective in microorganism inactivation but inadequate for the degradation of persistent organic contaminants.

However, such a problem has been overcome by the use of UVC/H₂O₂ process, which led simultaneously to up 99% degradation of all OMCs and bacterial inactivation without subsequent regrowth. Regarding the latter, this can be explained due to the internal Fenton reaction between the endogenous iron and the H₂O₂ diffused through the cell membrane, *i.e.*, residual H₂O₂ concentration has an important role (bacteriostatic effect) for the disinfection process. In the case of the UVC/S₂O₈²⁻ process, more than 80% of OMC degradation was obtained. However, bacterial regrowth was not prevented even when using 50 mg L⁻¹ in the dark, possibly due to diffusion limitations of S₂O₈²⁻ (considering its size and charge) through the cell membrane. It is important to highlight that bacterial regrowth is an important parameter to be concerned when it comes to water reclamation, since this water can remain stored by several days, including at the distribution systems before its final disposal.

On the other hand, wastewater regulations establish different possibilities for reusing the reclaimed water depending on their quality, microbiological characteristics, and physicochemical parameters. According to these parameters, reclaimed water coming from the UVC/H₂O₂ process might represent a great alternative to be utilized in agriculture purposes, since this activity demands the highest level of freshwater when compared to other anthropogenic activities. In addition, it has been demonstrated that the UVC/S₂O₈²⁻ process was able to produce effluents with enough quality to be reused for several purposes. However, it is important to highlight that this process requires a slight addition of sanitizers in to avoid possible regrowth of unwanted pathogens after the treatment.

Finally, the optimum oxidant concentration to be used in the UVC-based processes is a very important parameter to achieve the maximum theoretical efficiency of these technologies. However, the development of such model to determine this critical oxidant concentration is not a simple task, because the optimal concentration depends on several factors

such as water matrix, scavenging species, geometric parameters of the photo-reactor, photochemical properties of the oxidants, power of the UVC lamp, among others. Despite of this, a simple model based on the Beer–Lambert law enabled reasonable estimation of the oxidant concentration required to attain the maximum oxidation rates (*i.e.*, shortest reaction time). All this effort made it clear that further investigations are necessary to better understand the main parameters that should limit the performance of UVC-based methods.

5. REFERENCES

1. WORLD ECONOMIC FORUM. Global Risks 2015. 10th Ed., Geneva, Switzerland, 2015.
2. ERCIN, A. E. & HOEKSTRA, A. Y. "Water footprint scenarios for 2050: a global analysis". *Environ. Int.*, **64**: 71, 2014.
3. VÖRÖSMARTY, C. J.; GREEN, P.; SALISBURY, J.; LAMMERS, R. B. "Global water resources: vulnerability from climate change and population growth". *Science*, 289 (5477): 284, 2000.
4. MEKONNEN, M. M. & HOEKSTRA, A. Y. "Four billion people facing severe water scarcity". *Sci. Adv.*, 2 (2): e1500323, 2016.
5. HOEKSTRA, A. Y.; MEKONNEN, M. M.; CHAPAGAIN, A. K.; MATHEWS, R. E.; RICHTER, B. D. "Global monthly water scarcity: blue water footprints versus blue water availability". *PLoS One*, 7 (2): e32688, 2012
6. UNITED NATIONS – Population Division. World Population Prospects 2019: Highlights, Department of Economic and Social Affairs. New York, USA, 2019.
7. FAO. The wealth of waste: the economics of wastewater use in agriculture. Water Report, **35**, 2010.
8. SCHEWE, J.; HEINKE, J.; GERTEN, D.; HADDELAND, I.; ARNELL, N. W.; CLARK, D. B.; DANKERS, R.; EISNER, S.; FEKETE, B. M.; COLÓN-GONZÁLEZ, F. J.; GOSLING, S. N.; KIM, H.; LIU, X.; MASAKI, Y.; PORTMANN, F. T.; SATOH, Y.; STACKE, T.; TANG, Q.; WADA, Y.; WISSER, D.; ALBRECHT, T.; FRIELER, K.; PIONTEK, F.; WARSZAWSKI, L.; KABAT, P. "Multimodel assessment of water scarcity under climate change". *PNAS*, 111 (9): 3245, 2014
9. CAICEDO, C.; ROSENWINKEL, K. H.; EXNER, M.; VERSTRAETE, W.; SUCHENWIRTH, R.; HARTEMANN, P.; NOGUEIRA, R. "Legionella occurrence in municipal and industrial wastewater treatment plants and risks of reclaimed wastewater reuse: review". *Water Res.*, **149**: 21, 2019.
10. WANG, J.; CHU, L.; WOJNÁROVITS, L.; TAKÁCS, E. "Occurrence and fate of antibiotics, antibiotic resistant genes (ARGs) and antibiotic resistant bacteria (ARB) in municipal wastewater treatment plant: an overview". *Sci. Total Environ.*, **744**: 140997, 2020.
11. BEXFIELD, L. M.; TOCCALINO, P. L.; BELITZ, K.; FOREMAN, W. T.; FURLONG, E. T. "Hormones and pharmaceuticals in groundwater used as a source of drinking water across the United States". *Environ. Sci. Technol.*, 53 (6): 2950, 2019.
12. SUI, Q.; CAO, X.; LU, S.; ZHAO, W.; QIU, Z.; YU, G. "Occurrence, sources and fate of pharmaceuticals and personal care products in the groundwater: a review". *Emerg. Cont.*, 1 (1): 14, 2015.
13. KARBALAEI, S.; HANACHI, P.; WALKER, T. R.; COLE, M. "Occurrence, sources, human health impacts and mitigation of microplastic pollution". *Environ. Sci. Pollut. Res.*, 25 (36): 36046, 2018.
14. NOGUEIRA, E. N.; DORES, E. F. G. C.; PINTO, A. A.; AMORIM, R. S. S.; RIBEIRO, M. L.; LOURENCETTI, C. "Currently used pesticides in water matrices in Central-Western Brazil". *J. Brazil Chem. Soc.*, **23**: 1476, 2012.
15. CIZMAS, L.; SHARMA, V. K.; GRAY, C. M.; MCDONALD, T. J. "Pharmaceuticals and personal care products in waters: occurrence, toxicity, and risk". *Environ. Chem. Lett.*, 13 (4): 381, 2015.
16. HARADA, A.; KOMORI, K.; NAKADA, N.; KITAMURA, K.; SUZUKI, Y. "Biological effects of PPCPs on aquatic lives and evaluation of river waters affected by different wastewater treatment levels". *Water Sci. Technol.*, 58 (8): 1541, 2008.
17. GERBA, C. P. "Environmental microbiology". IN: *Environmentally Transmitted Pathogens*. Elsevier Inc., 3rd Ed., 2015. p. 509-550.

18. NEIL, K. P.; YODER, J. S.; HALL, A. J.; BOWEN, A. "Enteric diseases transmitted through food, water, and zoonotic exposures". IN: Principles and Practice of Pediatric Infectious Diseases. LONG, S. S.; PROBER, C. G.; FISCHER, M. (Eds.), Elsevier Inc., 5th Ed., 2018. p. 397-409.
19. FAO. The State of the World's Land and Water Resources for Food and Agriculture (SOLAW) – Managing Systems at Risk. Rome and Earthscan. London, 2011.
20. GRIFFITHS, J. K. "Waterborne diseases". IN: International Encyclopedia of Public Health. HEGGENHOUGEN, H. K. (Ed), Oxford, Academic Press, 2008. p. 551-563.
21. SADOFF, C.W., HALL, J.W., GREY, D., AERTS, J.C.J.H., AIT-KADI, M., BROWN, C., COX, A., DADSON, S., GARRICK, D., KELMAN, J., MCCORNICK, P., RINGLER, C., ROSEGRANT, M., WHITTINGTON, D. AND WIBERG, D. "Securing Water, Sustaining Growth: Report of the GWP/OECD Task Force on Water Security and Sustainable Growth". University of Oxford, UK, 2015. p. 1-180.
22. VÖRÖSMARTY, C. J.; MCINTYRE, P. B.; GESSNER, M. O.; DUDGEON, D.; PRUSEVICH, A.; GREEN, P.; GLIDDEN, S.; BUNN, S. E.; SULLIVAN, C. A.; LIERMANN, C. R.; DAVIES, P. M. "Global threats to human water security and river biodiversity". Nature, 467 (7315): 555, 2010.
23. WE ARE WATER FOUNDATION. "Brazil, so much water and yet so little (2017)". Accessed in (07/24/2020): https://www.wearewater.org/en/brazil-so-much-water-and-yet-so-little_286801.
24. SISTEMA NACIONAL DE INFORMAÇÕES SOBRE SANEAMENTO. "24º Diagnóstico dos Serviços de Água e Esgoto". Ministério do Desenvolvimento Regional, Brasília, Brasil, 2019.
25. WATER.ORG. "Brazil's water and sanitation crisis (2017)". Accessed in (07/24/2020): <https://water.org/our-impact/where-we-work/brazil/>.
26. DE SOUSA, D. N. R.; MOZETO, A. A.; CARNEIRO, R. L.; FADINI, P. S. "Spatio-temporal evaluation of emerging contaminants and their partitioning along a Brazilian watershed". Environ. Sci. Pollut. Res., 25 (5): 4607, 2018.
27. CAMPANHA, M. B.; AWAN, A. T.; DE SOUSA, D. N. R.; GROSSELI, G. M.; MOZETO, A. A.; FADINI, P. S. "A 3-year study on occurrence of emerging contaminants in an urban stream of São Paulo State of Southeast Brazil". Environ. Sci. Pollut. Res., 22 (10): 7936, 2015.
28. DE SOUSA, D. N. R.; MOZETO, A. A.; CARNEIRO, R. L.; FADINI, P. S. "Electrical conductivity and emerging contaminant as markers of surface freshwater contamination by wastewater". Sci. Total Environ., **484**: 19, 2014
29. JARDIM, W. F.; MONTAGNER, C. C.; PESCARA, I. C.; UMBUZEIRO, G. A.; DI DEA BERGAMASCO, A. M.; ELDRIDGE, M. L.; SODRÉ, F. F. "An integrated approach to evaluate emerging contaminants in drinking water". Sep. Purif. Technol., **84**: 3, 2012
30. SALGOT, M. & FOLCH, M. "Wastewater treatment and water reuse". Curr. Opin. Environ. Sci. Health, **2**: 64, 2018.
31. ROCCARO, P. "Treatment processes for municipal wastewater reclamation: The challenges of emerging contaminants and direct potable reuse". Curr. Opin. Environ. Sci. Health, **2**: 46, 2018.
32. COMMISSION IMPLEMENTING DECISION [2018/840/EU](https://eur-lex.europa.eu/legal-content/EN/TXT/?uri=CELEX%3A32018D0840). Accessed in (07/21/2020): <https://eur-lex.europa.eu/legal-content/EN/TXT/?uri=CELEX%3A32018D0840>.
33. REGULATION [2020/741/EU](https://eur-lex.europa.eu/eli/reg/2020/741/eu). Accessed in (07/21/2020): <https://eur-lex.europa.eu/eli/reg/2020/741/oj>.
34. MINISTÉRIO DO MEIO AMBIENTE - Conselho Nacional de Recursos Hídricos, Moção nº 40. Diario Oficial da União, 2006.

35. FAPESP/CONFAP/Water JPI/JPI Oceans/JPI AMR. "Aquatic Pollutants: Risks posed to human health and the environment by pollutants and pathogens present in water resources". Accessed in (07/25/2020): <http://www.fapesp.br/en/14014>.
36. UNITED NATIONS. "Sustainable Development Goals to 2030". Accessed in (07/25/2020): <https://www.un.org/sustainabledevelopment/>.
37. TERCEIRA CHAMADA DE PROPOSTAS. "Acordo de Cooperação FAPESP/SABESP". Accessed in (07/25/2020): <http://www.fapesp.br/13985#3>.
38. MIKLOS, D. B.; REMY, C.; JEKEL, M.; LINDEN, K. G.; DREWES, J. E.; HÜBNER, U. "Evaluation of advanced oxidation processes for water and wastewater treatment – a critical review". *Water Res.*, **139**: 118, 2018.
39. KÜMMERER, K. "Antibiotics in the aquatic environment – a review – Part I". *Chemosphere*, 75 (4): 417, 2009.
40. PARK, K.-Y.; CHOI, S.-Y.; LEE, S.-H.; KWEON, J.-H.; SONG, J.-H. "Comparison of formation of disinfection by-products by chlorination and ozonation of wastewater effluents and their toxicity to *Daphnia magna*". *Environ. Pollut.*, **215**: 314, 2016.
41. LI, C.; WANG, D.; XU, X.; WANG, Z. "Formation of known and unknown disinfection by-products from natural organic matter fractions during chlorination, chloramination, and ozonation". *Sci. Total Environ.*, **587-588**: 177, 2017.
42. ZHANG, X.-L.; YANG, H.-W.; WANG, X.-M.; FU, J.; XIE, Y. F. "Formation of disinfection by-products: effect of temperature and kinetic modeling". *Chemosphere*, 90 (2): 634, 2013.
43. GUO, M.-T. & KONG, C. "Antibiotic resistant bacteria survived from UV disinfection: safety concerns on genes dissemination." *Chemosphere*, **224**: 827, 2019.
44. FRAIESE, A.; CESARO, A.; BELGIORNO, V.; SANROMÁN, M. A.; PAZOS, M.; NADDEO, V. "Ultrasonic processes for the advanced remediation of contaminated sediments". *Ultrason. Sonochem.*, **67**: 105171, 2020
45. GOGATE, P. R.; THANEKAR, P. D.; OKE, A. P. "Strategies to improve biological oxidation of real wastewater using cavitation based pre-treatment approaches". *Ultrason. Sonochem.*, **64**: 105016, 2020.
46. PINCHAI, C.; MONNOT, M.; LEFÈVRE, S.; BOUTIN, O.; MOULIN, P. "Membrane filtration coupled with wet air oxidation for intensified treatment of biorefractory effluents". *Water Sci. Technol.*, 80 (12): 2338, 2019.
47. BRILLAS, E. "A review on the photoelectro-Fenton process as efficient electrochemical advanced oxidation for wastewater remediation. Treatment with UV light, sunlight, and coupling with conventional and other photo-assisted advanced technologies". *Chemosphere*, **250**: 126198, 2020.
48. RADJENOVIC, J. & SEDLAK, D. L. "Challenges and opportunities for electrochemical processes as next-generation technologies for the treatment of contaminated water". *Environ. Sci. Technol.*, 49 (19): 11292, 2015.
49. SANTOS, G. O. S.; EGUILUZ, K. I. B.; SALAZAR-BANDA, G. R.; SAEZ, C.; RODRIGO, M. A. "Photoelectrolysis of clopyralid wastes with a novel laser-prepared MMO-RuO₂TiO₂ anode". *Chemosphere*, **244**: 125455, 2020.
50. SANTOS, G. O. S.; DÓRIA, A. R.; VASCONCELOS, V. M.; SÁEZ, C.; RODRIGO, M. A.; EGUILUZ, K. I. B.; SALAZAR-BANDA, G. R. "Enhancement of wastewater treatment using novel laser-made Ti/SnO₂-Sb anodes with improved electrocatalytic properties". *Chemosphere*, **259**: 127475, 2020.
51. SÁNCHEZ-MONTES, I.; FUZER NETO, J. R.; SILVA, B. F.; SILVA, A. J.; AQUINO, J. M.; ROCHA-FILHO, R. C. "Evolution of the antibacterial activity and oxidation intermediates during the electrochemical degradation of norfloxacin in a flow cell with a PTFE-doped β-PbO₂ anode: critical comparison to a BDD anode". *Electrochim. Acta*, **284**: 260, 2018.

52. SOUZA, F. L.; LANZA, M. R. V.; LLANOS, J.; SÁEZ, C.; RODRIGO, M. A.; CAÑIZARES, P. "A wind-powered BDD electrochemical oxidation process for the removal of herbicides". *J. Environ. Manag.*, **158**: 36, 2015.
53. PAN, Z.; SONG, C.; LI, L.; WANG, H.; PAN, Y.; WANG, C.; LI, J.; WANG, T.; FENG, X. "Membrane technology coupled with electrochemical advanced oxidation processes for organic wastewater treatment: recent advances and future prospects". *Chem. Eng. J.*, **376**: 120909, 2019.
54. MONTES, I. J. S.; SILVA, B. F.; AQUINO, J. M. "On the performance of a hybrid process to mineralize the herbicide tebuthiuron using a DSA[®] anode and UVC light: A mechanistic study". *Appl. Catal. B-Environ.*, **200**: 237, 2017.
55. BABAEI, A. A.; GHANBARI, F. "COD removal from petrochemical wastewater by UV/hydrogen peroxide, UV/persulfate and UV/percarbonate: biodegradability improvement and cost evaluation". *J. Water Reuse Desal.*, **6** (4): 484, 2016.
56. XIAO, R.; LIU, K.; BAI, L.; MINAKATA, D.; SEO, Y.; KAYA GÖKTAŞ, R.; DIONYSIOU, D. D.; TANG, C.-J.; WEI, Z.; SPINNEY, R. "Inactivation of pathogenic microorganisms by sulfate radical: present and future". *Chem. Eng. J.*, **371**: 222, 2019.
57. HOKANSON, D. R.; LI, K.; TRUSSELL, R. R. "A photolysis coefficient for characterizing the response of aqueous constituents to photolysis". *Front. Env. Sci. Eng.*, **10** (3): 428, 2016.
58. CRITTENDEN, J. C.; HU, S.; HAND, D. W.; GREEN, S. A. "A kinetic model for H₂O₂/UV process in a completely mixed batch reactor". *Water Res.*, **33** (10): 2315, 1999.
59. MIRALLES-CUEVAS, S.; DAROWNA, D.; WANAG, A.; MOZIA, S.; MALATO, S.; OLLER, I. "Comparison of UV/H₂O₂, UV/S₂O₈²⁻, solar/Fe(II)/H₂O₂ and solar/Fe(II)/S₂O₈²⁻ at pilot plant scale for the elimination of micro-contaminants in natural water: an economic assessment". *Chem. Eng. J.*, **310**: 514, 2017.
60. PÉREZ, M. H.; PEÑUELA, G.; MALDONADO, M. I.; MALATO, O.; FERNÁNDEZ-IBÁÑEZ, P.; OLLER, I.; GERNJAK, W.; MALATO, S. "Degradation of pesticides in water using solar advanced oxidation processes". *Appl. Catal. B-Environ.*, **64** (3): 272, 2006.
61. MIKLOS, D. B.; HARTL, R.; MICHEL, P.; LINDEN, K. G.; DREWES, J. E.; HÜBNER, U. "UV/H₂O₂ process stability and pilot-scale validation for trace organic chemical removal from wastewater treatment plant effluents". *Water Res.*, **136**: 169, 2018.
62. GUAN, R.; YUAN, X.; WU, Z.; JIANG, L.; LI, Y.; ZENG, G. "Principle and application of hydrogen peroxide based advanced oxidation processes in activated sludge treatment: a review". *Chem. Eng. J.*, **339**: 519, 2018.
63. WEEKS, J. L. & MATHESON, M. S. "The primary quantum yield of hydrogen peroxide decomposition". *J. Ame. Chem. Soc.*, **78** (7): 1273, 1956.
64. LIAO, C.-H. & GUROL, M. D. "Chemical oxidation by photolytic decomposition of hydrogen peroxide". *Environ. Sci. Technol.*, **29** (12): 3007, 1995.
65. YU, X.-Y. & BARKER, J. R. "Hydrogen peroxide photolysis in acidic aqueous solutions containing chloride ions. II. Quantum yield of HO[•](aq) radicals". *J. Phys. Chem. A*, **107** (9): 1325, 2003.
66. TULLY, F. P.; RAVISHANKARA, A. R.; THOMPSON, R. L.; NICOVICH, J. M.; SHAH, R. C.; KREUTTER, N. M.; WINE, P. H. "Kinetics of the reactions of hydroxyl radical with benzene and toluene". *J. Phys. Chem.*, **85** (15): 2262, 1981.
67. GUERRA-RODRÍGUEZ, S.; RODRÍGUEZ, E.; SINGH, D. N.; RODRÍGUEZ-CHUECA, J. J. "Assessment of sulfate radical-based advanced oxidation processes for water and wastewater treatment: a review". *Water*, **10** (12): 1828, 2018.
68. WACŁAWEK, S.; LUTZE, H. V.; GRÜBEL, K.; PADIL, V. V. T.; ČERNÍK, M.; DIONYSIOU, D. D. "Chemistry of persulfates in water and wastewater treatment: a review". *Chem. Eng. J.*, **330**: 44, 2017.

69. LIU, K.; BAI, L.; SHI, Y.; WEI, Z.; SPINNEY, R.; GÖKTAŞ, R. K.; DIONYSIOU, D. D.; XIAO, R. "Simultaneous disinfection of *E. faecalis* and degradation of carbamazepine by sulfate radicals: an experimental and modelling study". *Environ. Pollut.*, **263**: 114558, 2020.
70. YANG, Q.; CHOI, H.; CHEN, Y.; DIONYSIOU, D. D. "Heterogeneous activation of peroxymonosulfate by supported cobalt catalysts for the degradation of 2,4-dichlorophenol in water: the effect of support, cobalt precursor, and UV radiation". *Appl. Catal. B-Environ.*, **77** (3): 300, 2008.
71. LI, W.; JAIN, T.; ISHIDA, K.; LIU, H. "A mechanistic understanding of the degradation of trace organic contaminants by UV/hydrogen peroxide, UV/persulfate and UV/free chlorine for water reuse". *Environ. Sci. Water Res. Technol.*, **3** (1): 128, 2017.
72. WANG, J. & WANG, S. "Activation of persulfate (PS) and peroxymonosulfate (PMS) and application for the degradation of emerging contaminants". *Chem. Eng. J.*, **334**: 1502, 2018.
73. OH, W.-D.; DONG, Z.; LIM, T.-T. "Generation of sulfate radical through heterogeneous catalysis for organic contaminants removal: current development, challenges and prospects". *Appl. Catal. B-Environ.*, **194**: 169, 2016.
74. LUO, S.; WEI, Z.; DIONYSIOU, D. D.; SPINNEY, R.; HU, W.-P.; CHAI, L.; YANG, Z.; YE, T.; XIAO, R. "Mechanistic insight into reactivity of sulfate radical with aromatic contaminants through single-electron transfer pathway". *Chem. Eng. J.*, **327**: 1056, 2017.
75. JIANG, C.; JI, Y.; SHI, Y.; CHEN, J.; CAI, T. "Sulfate radical-based oxidation of fluoroquinolone antibiotics: kinetics, mechanisms and effects of natural water matrices". *Water Res.*, **106**: 507, 2016.
76. XIAO, R.; LUO, Z.; WEI, Z.; LUO, S.; SPINNEY, R.; YANG, W.; DIONYSIOU, D. D. "Activation of peroxymonosulfate/persulfate by nanomaterials for sulfate radical-based advanced oxidation technologies". *Curr. Opin. Chem. Eng.*, **19**: 51, 2018.
77. SZABO, J. & MINAMYER, S. "Decontamination of biological agents from drinking water infrastructure: a literature review and summary". *Environ. Int.*, **72**: 124, 2014.
78. LI, W.; ZHANG, J.; WANG, F.; QIAN, L.; ZHOU, Y.; QI, W.; CHEN, J. "Effect of disinfectant residual on the interaction between bacterial growth and assimilable organic carbon in a drinking water distribution system". *Chemosphere*, **202**: 586, 2018.
79. UYSAL, T.; YILMAZ, S.; TURKOGLU, M.; SADIKOGLU, M. "Investigation of some disinfection chemicals and water quality parameters in swimming pools in the city center and districts of Canakkale, Turkey". *Environ. Monitor. Asses.*, **189** (7): 338, 2017.
80. FENG, Y.; SMITH, D. W.; BOLTON, J. R. "Photolysis of aqueous free chlorine species (HOCl and OCl⁻) with 254 nm ultraviolet light". *J. Environ. Eng. Sci.* **6** (3): 277, 2007.
81. STANBURY, D. M. "Reduction potentials involving inorganic free radicals in aqueous solution". IN: *Advances in Inorganic Chemistry*. SYKES, A. G. (Ed), Academic Press, Vol. 33, 1989. p. 69-138.
82. GREBEL, J. E.; PIGNATELLO, J. J.; MITCH, W. A. "Effect of halide ions and carbonates on organic contaminant degradation by hydroxyl radical-based advanced oxidation processes in saline waters". *Environ. Sci. Technol.*, **44** (17): 6822, 2010.
83. CHUANG, Y.-H.; CHEN, S.; CHINN, C. J.; MITCH, W. A. "Comparing the UV/monochloramine and UV/free chlorine advanced oxidation processes (AOPS) to the UV/hydrogen peroxide aop under scenarios relevant to potable reuse". *Environ. Sci. Technol.*, **51** (23): 13859, 2017.
84. GWENZI, W. & CHAUKURA, N. "Organic contaminants in African aquatic systems: current knowledge, health risks, and future research directions. *Sci. Total Environ.*, **619-620**: 1493, 2018.
85. VALCÁRCEL, Y.; VALDEHÍTA, A.; BECERRA, E.; LÓPEZ DE ALDA, M.; GIL, A.; GORGA, M.; PETROVIC, M.; BARCELÓ, D.; NAVAS, J. M. "Determining the presence of chemicals with suspected endocrine activity in drinking water from the Madrid region (Spain)

- and assessment of their estrogenic, androgenic and thyroidal activities". *Chemosphere*, **201**: 388, 2018.
86. LEE, H.-S.; JUNG, D.-W.; HAN, S.; KANG, H.-S.; SUH, J.-H.; OH, H.-S.; HWANG, M.-S.; MOON, G.; PARK, Y.; HONG, J.-H.; KOO, Y. E. "Veterinary drug, 17 β -trenbolone promotes the proliferation of human prostate cancer cell line through the Akt/AR signaling pathway". *Chemosphere*, **198**: 364, 2018.
87. PETRIE, B.; BARDEN, R.; KASPRZYK-HORDERN, B. "A review on emerging contaminants in wastewaters and the environment: current knowledge, understudied areas and recommendations for future monitoring". *Water Res.*, **72**: 3, 2015.
88. SALIMI, M.; ESRAFILI, A.; GHOLAMI, M.; JONIDI JAFARI, A.; REZAEI KALANTARY, R.; FARZADKIA, M.; KERMANI, M.; SOBHI, H. R. "Contaminants of emerging concern: a review of new approach in AOP technologies". *Environ. Monitor. Asses.*, **189** (8): 414, 2017.
89. TRAN, N. H.; REINHARD, M.; GIN, K. Y.-H. "Occurrence and fate of emerging contaminants in municipal wastewater treatment plants from different geographical regions-a review". *Water Res.*, **133**: 182, 2018.
90. WARD, J. L. & BLUM, M. J. "Exposure to an environmental estrogen breaks down sexual isolation between native and invasive species". *Evol. Appl.*, **5** (8): 901, 2012.
91. USEPA. Endocrine Disruptor Screening Program: What is Endocrine Disruption? Accessed in (7/28/2020): <https://www.epa.gov/endocrine-disruption/what-endocrine-disruption>.
92. LIMA, D. R. S.; TONUCCI, M. C.; LIBÂNIO, M.; AQUINO, S. F. D. "Fármacos e desreguladores endócrinos em águas brasileiras: ocorrência e técnicas de remoção". *Engen. San. Amb.*, **22**: 1043, 2017.
93. COLEDAM, D. A. C.; SÁNCHEZ-MONTES, I.; SILVA, B. F.; AQUINO, J. M. "On the performance of HOCl/Fe²⁺, HOCl/Fe²⁺/UVA, and HOCl/UVC processes using in situ electrogenerated active chlorine to mineralize the herbicide picloram". *Appl. Catal. B-Environ.*, **227**: 170, 2018.
94. AO, X. & LIU, W. "Degradation of sulfamethoxazole by medium pressure UV and oxidants: peroxymonosulfate, persulfate, and hydrogen peroxide". *Chem. Eng. J.*, **313**: 629, 2017.
95. BUXTON, G. V.; GREENSTOCK, C. L.; HELMAN, W. P.; ROSS, A. B. "Critical review of rate constants for reactions of hydrated electrons, hydrogen atoms and hydroxyl radicals (HO \cdot /O \cdot^-) in aqueous solution". *J. Phys. Chem. Ref. Data*, **17** (2): 513, 1988.
96. BECK, G. "Elektrische leitfähigkeitsmessungen zum nachweis geladener zwischenprodukte der pulsradolyse". *Int. J. Rad. Phy. Chem.*, **1** (3): 361, 1969.
97. SEHESTED, K.; RASMUSSEN, O. L.; FRICKE, H. "Rate constants of OH with HO₂, O²⁻, and H₂O₂⁺ from hydrogen peroxide formation in pulse-irradiated oxygenated water". *J. Phys. Chem.*, **72** (2): 626, 1968.
98. V. BUXTON, G.; BYDDER, M.; ARTHUR SALMON, G. "The reactivity of chlorine atoms in aqueous solution Part II. The equilibrium SO₄⁻+Cl⁻Cl^{Nsbd}+SO₄²⁻". *Phy. Chem. Chem. Phy.*, **1** (2): 269, 1999.
99. HUIE, R. E. & CLIFTON, C. L. "Rate constants for hydrogen abstraction reactions of the sulfate radical, SO₄⁻. Alkanes and ethers". *Int. J. Chem. Kinet.* **21** (8): 611, 1989.
100. HAYON, E.; TREININ, A.; WILF, J. "Electronic spectra, photochemistry, and autoxidation mechanism of the sulfite-bisulfite-pyrosulfite systems. SO₂⁻, SO₃⁻, SO₄⁻, and SO₅⁻ radicals". *J. Ame. Chem. Soc.*, **94** (1): 47, 1972.
101. ENNIS, C. A. & BIRKS, J. W. "Rate constants for the reactions hydroxyl + hypochlorous acid .fwdarw. water + chlorine oxide (ClO) and hydrogen + hypochlorous acid .fwdarw. products". *J. Phys. Chem.*, **92** (5): 1119, 1988.

102. JAYSON, G. G.; PARSONS, B. J.; SWALLOW, A. J. "Some simple, highly reactive, inorganic chlorine derivatives in aqueous solution. Their formation using pulses of radiation and their role in the mechanism of the Fricke dosimeter". *J. Chem. Soc., Faraday Trans. 1*, 69 (0): 1597, 1973.
103. LIANG, C.; HUANG, C.-F.; MOHANTY, N.; KURAKALVA, R. M. "A rapid spectrophotometric determination of persulfate anion in ISCO". *Chemosphere*, 73 (9): 1540, 2008.
104. CHAI, X. S.; HOU, Q. X.; LUO, Q.; ZHU, J. Y. "Rapid determination of hydrogen peroxide in the wood pulp bleaching streams by a dual-wavelength spectroscopic method". *Anal. Chim. Acta*, 507 (2): 281, 2004.
105. GUERRA, R. "Ecotoxicological and chemical evaluation of phenolic compounds in industrial effluents". *Chemosphere*, 44 (8): 1737, 2001.
106. PUNZI, M.; NILSSON, F.; ANBALAGAN, A.; SVENSSON, B.-M.; JÖNSSON, K.; MATTIASSON, B.; JONSTRUP, M. "Combined anaerobic–ozonation process for treatment of textile wastewater: removal of acute toxicity and mutagenicity". *J. Hazard. Mater.*, **292**: 52, 2015.
107. VANHAECKE, P.; PERSOONE, G.; CLAUS, C.; SORGELOOS, P. "Proposal for a short-term toxicity test with *Artemia nauplii*". *Ecotox. Environ. Safe.*, 5 (3): 382, 1981.
108. HAMILTON, M. A.; RUSSO, R. C.; THURSTON, R. V. "Trimmed Spearman-Kärber method for estimating median lethal concentrations in toxicity bioassays". *Environ. Sci. Technol.*, 11 (7): 714-719, 1977.
109. BERETSOU, V. G.; PSOMA, A. K.; GAGO-FERRERO, P.; AALIZADEH, R.; FENNER, K.; THOMAIDIS, N. S. "Identification of biotransformation products of citalopram formed in activated sludge". *Water Res.*, **103**: 205, 2016.
110. BURDEN, N.; MAYNARD, S. K.; WELTJE, L.; WHEELER, J. R. "The utility of QSARs in predicting acute fish toxicity of pesticide metabolites: a retrospective validation approach". *Regul. Tox. Pharma.*, **80**: 241, 2016.
111. CARPINTEIRO, I.; RODIL, R.; QUINTANA, J. B.; CELA, R. "Reaction of diazepam and related benzodiazepines with chlorine. Kinetics, transformation products and in-silico toxicological assessment". *Water Res.*, **120**: 280, 2017.
112. YANG, Y.; LU, X.; JIANG, J.; MA, J.; LIU, G.; CAO, Y.; LIU, W.; LI, J.; PANG, S.; KONG, X.; LUO, C. "Degradation of sulfamethoxazole by UV, UV/H₂O₂ and UV/persulfate (PDS): formation of oxidation products and effect of bicarbonate". *Water Res.*, **118**: 196, 2017.
113. ZHANG, R.; YANG, Y.; HUANG, C.-H.; LI, N.; LIU, H.; ZHAO, L.; SUN, P. "UV/H₂O₂ and UV/PDS treatment of trimethoprim and sulfamethoxazole in synthetic human urine: transformation products and toxicity". *Environ. Sci. Technol.*, 50 (5): 2573, 2016.
114. MIWA, D. W.; MALPASS, G. R. P.; MACHADO, S. A. S.; MOTHEO, A. J. "Electrochemical degradation of carbaryl on oxide electrodes". *Water Res.*, 40 (17): 3281, 2006.
115. LU, X.; SHAO, Y.; GAO, N.; CHEN, J.; DENG, H.; CHU, W.; AN, N.; PENG, F. "Investigation of clofibric acid removal by UV/persulfate and UV/chlorine processes: kinetics and formation of disinfection byproducts during subsequent chlor(am)ination". *Chem. Eng. J.*, **331**: 364, 2018.
116. JAMES, R. B.; KEITH, G. B.; WILLIAM, T.; CHADWICK, A. T. "Figures-of-merit for the technical development and application of advanced oxidation technologies for both electric- and solar-driven systems". *IUPAC Technical Report*, 73 (4): 627, 2001.
117. YAMAMOTO, T. & YASUHARA, A. "Chlorination of bisphenol A in aqueous media: formation of chlorinated bisphenol A congeners and degradation to chlorinated phenolic compounds". *Chemosphere*, 46 (8): 1215, 2002.

118. LANE, R. F.; ADAMS, C. D.; RANDTKE, S. J.; CARTER, R. E. "Chlorination and chloramination of bisphenol A, bisphenol F, and bisphenol A diglycidyl ether in drinking water". *Water Res.*, **79**: 68, 2015.
119. SHARMA, J.; MISHRA, I. M.; KUMAR, V. "Degradation and mineralization of Bisphenol A (BPA) in aqueous solution using advanced oxidation processes: UV/H₂O₂ and UV/S₂O₈²⁻ oxidation systems". *J. Environ. Manag.*, **156**: 266, 2015.
120. SÁNCHEZ-POLO, M.; ABDEL DAIEM, M. M.; OCAMPO-PÉREZ, R.; RIVERA-UTRILLA, J.; MOTA, A. J. "Comparative study of the photodegradation of bisphenol A by HO, SO₄⁻ and CO₃⁻/HCO₃ radicals in aqueous phase". *Sci. Total Environ.*, **463-464**: 423, 2013.
121. ZHU, Y.; WU, M.; GAO, N.; CHU, W.; LI, K.; CHEN, S. "Degradation of phenacetin by the UV/chlorine advanced oxidation process: kinetics, pathways, and toxicity evaluation". *Chem. Eng. J.*, **335**: 520, 2018.
122. YIN, K.; DENG, Y.; LIU, C.; HE, Q.; WEI, Y.; CHEN, S.; LIU, T.; LUO, S. "Kinetics, pathways and toxicity evaluation of neonicotinoid insecticides degradation via UV/chlorine process". *Chem. Eng. J.*, **346**: 298, 2018.
123. KONG, X.; JIANG, J.; MA, J.; YANG, Y.; LIU, W.; LIU, Y. "Degradation of atrazine by UV/chlorine: efficiency, influencing factors, and products". *Water Res.*, **90**: 15, 2016.
124. LIANG, C. & SU, H.-W. "Identification of sulfate and hydroxyl radicals in thermally activated persulfate. *Ind. Eng. Chem. Res.*, 48 (11): 5558, 2009.
125. ZRINYI, N. & PHAM, A. L.-T. "Oxidation of benzoic acid by heat-activated persulfate: effect of temperature on transformation pathway and product distribution". *Water Res.*, **120**: 43, 2017.
126. YOON, S. H.; JEONG, S.; LEE, S. "Oxidation of bisphenol A by UV/S₂O₈²⁻: comparison with UV/H₂O₂". *Environ. Technol.*, **33** (1-3):123, 2012.
127. NOWELL, L. H. & HOIGNÉ, J. "Photolysis of aqueous chlorine at sunlight and ultraviolet wavelengths–II. Hydroxyl radical production". *Water Res.*, **26** (5): 599, 1992.
128. WATTS, M. J. & LINDEN, K. G. "Chlorine photolysis and subsequent OH radical production during UV treatment of chlorinated water". *Water Res.*, **41** (13): 2871, 2007.
129. WU, Z.; GUO, K.; FANG, J.; YANG, X.; XIAO, H.; HOU, S.; KONG, X.; SHANG, C.; YANG, X.; MENG, F.; CHEN, L. "Factors affecting the roles of reactive species in the degradation of micropollutants by the UV/chlorine process". *Water Res.*, **126**: 351, 2017.
130. GUO, K.; WU, Z.; SHANG, C.; YAO, B.; HOU, S.; YANG, X.; SONG, W.; FANG, J. "Radical chemistry and structural relationships of PPCP degradation by UV/chlorine treatment in simulated drinking water". *Environ. Sci. Technol.*, **51** (18): 10431, 2017.
131. CAI, W.-W.; PENG, T.; YANG, B.; XU, C.; LIU, Y.-S.; ZHAO, J.-L.; GU, F.-L.; YING, G.-G. "Kinetics and mechanism of reactive radical mediated fluconazole degradation by the UV/chlorine process: experimental and theoretical studies". *Chem. Eng. J.*, **402**: 126224, 2020.
132. MINAKATA, D.; KAMATH, D.; MAETZOLD, S. "Mechanistic insight into the reactivity of chlorine-derived radicals in the aqueous-phase UV-chlorine advanced oxidation process: quantum mechanical calculations". *Environ. Sci. Technol.*, **51** (12): 6918, 2017.
133. POERSCHMANN, J.; TROMMLER, U.; GÓRECKI, T. "Aromatic intermediate formation during oxidative degradation of Bisphenol A by homogeneous sub-stoichiometric Fenton reaction". *Chemosphere*, **79** (10): 975, 2010.
134. LI, H.; LONG, Y.; WANG, Y.; ZHU, C.; NI, J. "Electrochemical degradation of bisphenol A in chloride electrolyte–Factor analysis and mechanisms study". *Electrochim. Acta*, **222**: 1144, 2016.
135. LI, H.; LONG, Y.; ZHU, X.; TIAN, Y.; YE, J. "Influencing factors and chlorinated byproducts in electrochemical oxidation of bisphenol A with boron-doped diamond anodes". *Electrochim. Acta*, **246**: 1121, 2017.
136. OUTSIU, A.; FRONTISTIS, Z.; RIBEIRO, R. S.; ANTONOPOULOU, M.; KONSTANTINOU, I. K.; SILVA, A. M. T. FARIA, J. L.; GOMES, H. T.; MANTZAVINOS,

- D. "Activation of sodium persulfate by magnetic carbon xerogels (CX/CoFe) for the oxidation of bisphenol A: process variables effects, matrix effects and reaction pathways". *Water Res.*, **124**: 97, 2017.
137. RAJAB, M.; HEIM, C.; LETZEL, T.; DREWES, J. E.; HELMREICH, B. "Oxidation of bisphenol A by a boron-doped diamond electrode in different water matrices: transformation products and inorganic by-products". *Int. J. Environ. Sci. Technol.*, 13 (11): 2539, 2016.
138. KOPINKE, F.-D. & GEORGI, A. "What controls selectivity of hydroxyl radicals in aqueous solution? Indications for a cage effect". *Am. J. Phys. Chem.*, 121 (41): 7947, 2017.
139. MOUSSET, E.; OTURAN, N.; OTURAN, M. A. "An unprecedented route of OH radical reactivity evidenced by an electrocatalytic process: ipso-substitution with perhalogenocarbon compounds". *Appl. Catal. B-Environ.*, **226**: 135, 2018.
140. GARCIA-SEGURA, S. & BRILLAS, E. "Applied photoelectrocatalysis on the degradation of organic pollutants in wastewaters". *Photochem. Photobiol. C Rev.*, **31**: 1, 2017.
141. CHU, W.; KWAN, C. Y.; CHAN, K. H.; KAM, S. K. "A study of kinetic modelling and reaction pathway of 2,4-dichlorophenol transformation by photo-fenton-like oxidation". *J. Hazard. Mater.*, 121 (1): 119, 2005.
142. MOLKENTHIN, M.; OLMEZ-HANCI, T.; JEKEL, M. R.; ARSLAN-ALATON, I. "Photo-Fenton-like treatment of BPA: effect of UV light source and water matrix on toxicity and transformation products". *Water Res.*, 47 (14): 5052, 2013.
143. PÉREZ-MOYA, M.; KAISTO, T.; NAVARRO, M.; DEL VALLE, L. J. "Study of the degradation performance (TOC, BOD, and toxicity) of bisphenol A by the photo-Fenton process". *Environ. Sci. Pollut. Res.*, 24 (7): 6241, 2017.
144. LU, N.; LU, Y.; LIU, F.; ZHAO, K.; YUAN, X.; ZHAO, Y.; LI, Y.; QIN, H.; ZHU, J. "H₃PW₁₂O₄₀/TiO₂ catalyst-induced photodegradation of bisphenol A (BPA): kinetics, toxicity and degradation pathways". *Chemosphere*, 91 (9): 1266, 2013.
145. KHAN, J. A.; HE, X.; SHAH, N. S.; KHAN, H. M.; HAPESHI, E.; FATTA-KASSINOS, D.; DIONYSIOU, D. D. "Kinetic and mechanism investigation on the photochemical degradation of atrazine with activated H₂O₂, S₂O₈²⁻ and HSO₅⁻". *Chem. Eng. J.*, **252**: 393, 2014.
146. DENG, J.; SHAO, Y.; GAO, N.; XIA, S.; TAN, C.; ZHOU, S.; HU, X. "Degradation of the antiepileptic drug carbamazepine upon different UV-based advanced oxidation processes in water". *Chem. Eng. J.*, **222**: 150, 2013.
147. XIAO, Y.; ZHANG, L.; ZHANG, W.; LIM, K.-Y.; WEBSTER, R. D.; LIM, T.-T. "Comparative evaluation of iodoacids removal by UV/persulfate and UV/H₂O₂ processes". *Water Res.*, **102**: 629, 2016.
148. GALINDO-MIRANDA, J. M.; GUÍZAR-GONZÁLEZ, C.; BECERRIL-BRAVO, E. J.; MOELLER-CHÁVEZ, G.; LEÓN-BECERRIL, E.; VALLEJO-RODRÍGUEZ, R. "Occurrence of emerging contaminants in environmental surface waters and their analytical methodology – a review". *Water Supply*, 19 (7): 1871, 2019.
149. BIEL-MAESO, M.; BAENA-NOGUERAS, R. M.; CORADA-FERNÁNDEZ, C.; LARA-MARTÍN, P. A. "Occurrence, distribution and environmental risk of pharmaceutically active compounds (PhACs) in coastal and ocean waters from the Gulf of Cadiz (SW Spain)". *Sci. Total Environ.*, **612**: 649, 2018.
150. ZHANG, Q.; YANG, S.; XIE, B.; ZHANG, J.; DENG, C.; HU, R. "Environmental and human health risk assessment of antibiotic residues in drinking water sources: case study of a fast-developing megacity in southern China". *Water Supply*, 20 (2): 499, 2019.
151. KUDLEK, E.; DUDZIAK, M.; BOHDZIEWICZ, J. "Influence of inorganic ions and organic substances on the degradation of pharmaceutical compound in water matrix". *Water*, 8 (11): 532, 2016.
152. A. MALVESTITI, J. & F. DANTAS, R. "Influence of industrial contamination in municipal secondary effluent disinfection by UV/H₂O₂". *Environ. Sci. Pollut. Res.*, 26 (13): 13286, 2019.

153. USEPA. Guidelines for Water Reuse (EPA/600/R-12/618). Washington, DC, USA, 2012.
154. ISO. Guidelines for Treated Wastewater Use for Irrigation Projects, Vol. 16075, Geneva, Switzerland, 2015.
155. ZHANG, R.; VIGNESWARAN, S.; NGO, H.; NGUYEN, H. "A submerged membrane hybrid system coupled with magnetic ion exchange (MIEX[®]) and flocculation in wastewater treatment". *Desalination*, 216 (1): 325, 2007.
156. APHA. Standard Methods for the Examination of Water and Wastewater. EATON A. D. & GREENBERG A. E. (Eds.), Maryland, United Book Press Inc., 20th ed., 1998.
157. ROYAL DECREE 1620/2007. "Concerns of the Legal Regime for the Reuse of Treated Water". BOE n° 294, Madrid, Spain, 2007.
158. MARUGÁN, J.; VAN GRIEKEN, R.; SORDO, C.; CRUZ, C. "Kinetics of the photocatalytic disinfection of *Escherichia coli* suspensions". *Appl. Catal. B-Environ.*, 82 (1): 27, 2008.
159. NAHIM-GRANADOS, S.; RIVAS-IBÁÑEZ, G.; ANTONIO SÁNCHEZ PÉREZ, J.; OLLER, I.; MALATO, S.; POLO-LÓPEZ, M. I. "Synthetic fresh-cut wastewater disinfection and decontamination by ozonation at pilot scale". *Water Res.*, **170**: 115304, 2020.
160. COSTA, E. P.; ROCCAMANTE, M.; AMORIM, C. C.; OLLER, I.; SÁNCHEZ PÉREZ, J. A.; MALATO, S. "New trend on open solar photoreactors to treat micropollutants by photo-Fenton at circumneutral pH: increasing optical pathway". *Chem. Eng. J.*, **385**: 123982, 2020.
161. MARTÍNEZ-PIERNAS, A. B.; POLO-LÓPEZ, M. I.; FERNÁNDEZ-IBÁÑEZ, P.; AGÜERA, A. "Validation and application of a multiresidue method based on liquid chromatography-tandem mass spectrometry for evaluating the plant uptake of 74 microcontaminants in crops irrigated with treated municipal wastewater". *J. Chrom. A*, 1534: 10, 2018.
162. HARRIS, G. D.; ADAMS, V. D.; SORENSEN, D. L.; CURTIS, M. S. "Ultraviolet inactivation of selected bacteria and viruses with photoreactivation of the bacteria". *Water Res.*, 21 (6): 687, 1987.
163. RODRÍGUEZ-CHUECA, J.; GARCÍA-CAÑIBANO, C.; LEPISTÖ, R. J.; ENCINAS, Á.; PELLINEN, J.; MARUGÁN, J. "Intensification of UV-C tertiary treatment: disinfection and removal of micropollutants by sulfate radical based advanced oxidation processes. *J. Hazard. Mater.*, **372**: 94, 2019.
164. RODRÍGUEZ-CHUECA, J.; POLO-LÓPEZ, M. I.; MOSTEO, R.; ORMAD, M. P.; FERNÁNDEZ-IBÁÑEZ, P. "Disinfection of real and simulated urban wastewater effluents using a mild solar photo-Fenton". *Appl. Catal. B-Environ.*, **150-151**: 619, 2014.
165. NAHIM-GRANADOS, S.; SÁNCHEZ PÉREZ, J. A.; POLO-LOPEZ, M. I. "Effective solar processes in fresh-cut wastewater disinfection: inactivation of pathogenic *E. coli* O157:H7 and *Salmonella enteritidis*". *Catal. Today*, **313**: 79, 2018.
166. YANG, S.; WANG, P.; YANG, X.; SHAN, L.; ZHANG, W.; SHAO, X.; NIU, R. "Degradation efficiencies of azo dye Acid Orange 7 by the interaction of heat, UV and anions with common oxidants: persulfate, peroxymonosulfate and hydrogen peroxide". *J. Hazard. Mater.*, 179 (1): 552, 2010.
167. JOHNSON, R. L.; TRATNYEK, P. G.; JOHNSON, R. O. B. "Persulfate persistence under thermal activation conditions". *Environ. Sci. Technol.*, 42 (24): 9350, 2008.
168. GIANNAKIS, S.; DARAKAS, E.; ESCALAS-CAÑELLAS, A.; PULGARIN, C. "Elucidating bacterial regrowth: effect of disinfection conditions in dark storage of solar treated secondary effluent". *J. Photoch. Photobio. A*, **290**: 43, 2014.
169. FEO. Gewässerqualität: Revision der Gewässerschutzverordnung. Switzerland, 2017.
170. BOURGIN, M.; BECK, B.; BOEHLER, M.; BOROWSKA, E.; FLEINER, J.; SALHI, E.; TEICHLER, R.; VON GUNTEN, U.; SIEGRIST, H.; MCADELL, C. S. "Evaluation of a full-scale wastewater treatment plant upgraded with ozonation and biological post-treatments:

- Abatement of micropollutants, formation of transformation products and oxidation by-products". *Water Res.*, **129**: 486, 2018.
171. YU, H.-W.; PARK, M.; WU, S.; LOPEZ, I. J. JI, W.; SCHEIDELER, J.; SNYDER, S. A. "Strategies for selecting indicator compounds to assess attenuation of emerging contaminants during UV advanced oxidation processes". *Water Res.*, **166**: 115030, 2019.
172. CERRETA, G.; ROCCAMANTE, M. A.; OLLER, I.; MALATO, S.; RIZZO, L. "Contaminants of emerging concern removal from real wastewater by UV/free chlorine process: a comparison with solar/free chlorine and UV/H₂O₂ at pilot scale". *Chemosphere*, **236**: 124354, 2019
173. PABLOS, C.; MARUGÁN, J.; VAN GRIEKEN, R.; SERRANO, E. "Emerging micropollutant oxidation during disinfection processes using UV-C, UV-C/H₂O₂, UV-A/TiO₂ and UV-A/TiO₂/H₂O₂". *Water Res.*, **47** (3): 1237, 2013.
174. YOON, Y.; CHUNG, H. J.; WEN DI, D. Y.; DODD, M. C.; HUR, H.-G.; LEE, Y. "Inactivation efficiency of plasmid-encoded antibiotic resistance genes during water treatment with chlorine, UV, and UV/H₂O₂". *Water Res.*, **123**: 783, 2017.
175. MOUSSAVI, G.; FATHI, E.; MORADI, M. "Advanced disinfecting and post-treating the biologically treated hospital wastewater in the UVC/H₂O₂ and VUV/H₂O₂ processes: performance comparison and detoxification efficiency". *Process Saf. Environ.*, **126**: 259, 2019.
176. RUBIO, D.; NEBOT, E.; CASANUEVA, J. F.; PULGARIN, C. "Comparative effect of simulated solar light, UV, UV/H₂O₂ and photo-Fenton treatment (UV-Vis/H₂O₂/Fe²⁺,³⁺) in the *Escherichia coli* inactivation in artificial seawater". *Water Res.*, **47** (16): 6367, 2013.
177. MORENO-ANDRÉS, J.; ROMERO-MARTÍNEZ, L.; ACEVEDO-MERINO, A.; NEBOT, E. "Determining disinfection efficiency on *E. faecalis* in saltwater by photolysis of H₂O₂: implications for ballast water treatment". *Chem. Eng. J.*, **283**: 1339, 2016.
178. MORENO-ANDRÉS, J.; RIOS QUINTERO, R.; ACEVEDO-MERINO, A.; NEBOT, E. "Disinfection performance using a UV/persulfate system: effects derived from different aqueous matrices". *Photochem. Photobiol. Sci.*, **18** (4): 878, 2019.
179. ZENG, F.; CAO, S.; JIN, W.; ZHOU, X.; DING, W.; TU, R.; HAN, S.-F.; WANG, C.; JIANG, Q.; HUANG, H.; DING, F. "Inactivation of chlorine-resistant bacterial spores in drinking water using UV irradiation, UV/hydrogen peroxide and UV/peroxymonosulfate: Efficiency and mechanism". *J. Clean. Prod.*, **243**: 118666, 2020.
180. MICHAEL-KORDATOU, I.; IACOVOU, M.; FRONTISTIS, Z.; HAPESHI, E.; DIONYSIOU, D. D.; FATTA-KASSINOS, D. "Erythromycin oxidation and ERY-resistant *Escherichia coli* inactivation in urban wastewater by sulfate radical-based oxidation process under UV-C irradiation". *Water Res.*, **85**: 346, 2015.
181. POPOVA, S.; MATAFONOVA, G.; BATOEV, V. "Simultaneous atrazine degradation and *E. coli* inactivation by UV/S₂O₈²⁻/Fe²⁺ process under KrCl excilamp (222 nm) irradiation". *Ecotox. Environ. Safe.*, **169**:169, 2019.
182. WORDOFA, D. N.; WALKER, S. L.; LIU, H. Sulfate radical-induced disinfection of pathogenic *Escherichia coli* O157:H7 via iron-activated persulfate. *Environ. Sci. Technol. Lett.*, **4** (4): 154, 2017.
183. SERNA-GALVIS, E. A.; SALAZAR-OSPINA, L.; JIMÉNEZ, J. N.; PINO, N. J.; TORRES-PALMA, R. A. "Elimination of carbapenem resistant *Klebsiella pneumoniae* in water by UV-C, UV-C/persulfate and UV-C/H₂O₂. Evaluation of response to antibiotic, residual effect of the processes and removal of resistance gene". *J. Environ. Chem. Eng.*, **8** (1): 102196, 2020.
184. VAN GRIEKEN, R.; MARUGÁN, J.; PABLOS, C.; FURONES, L.; LÓPEZ, A. "Comparison between the photocatalytic inactivation of Gram-positive *E. faecalis* and Gram-negative *E. coli* faecal contamination indicator microorganisms". *Appl. Catal. B-Environ.*, **100** (1): 212, 2010.

185. WANG, W.; PERPELOV, A. V.; FENG, L.; SHEVELEV, S. D.; WANG, Q.; SENCHENKOVA, S.; APOS; N, Y.; HAN, W.; LI, Y.; SHASHKOV, A. S.; KNIREL, Y. A.; REEVES, P. R.; WANG, L. "A group of *Escherichia coli* and *Salmonella enterica* O antigens sharing a common backbone structure". *Microbiology*, 153 (7): 2159, 2007.
186. GIANNAKIS, S.; POLO LÓPEZ, M. I.; SPUHLER, D.; SÁNCHEZ PÉREZ, J. A.; FERNÁNDEZ IBÁÑEZ, P.; PULGARIN, C. "Solar disinfection is an augmentable, in situ-generated photo-Fenton reaction–Part I: a review of the mechanisms and the fundamental aspects of the process". *Appl. Catal. B-Environ.*, **199**:199, 2016.
187. STARLING, M. C. V. M.; SOUZA, P. P.; LE PERSON, A.; AMORIM, C. C.; CRIQUET, J. "Intensification of UV-C treatment to remove emerging contaminants by UV-C/H₂O₂ and UV-C/S₂O₈²⁻: susceptibility to photolysis and investigation of acute toxicity". *Chem. Eng. J.*, **376**: 20856, 2019.
188. WOJNÁROVITS, L. & TAKÁCS, E. "Rate constants of sulfate radical anion reactions with organic molecules: a review". *Chemosphere*, **220**: 1014, 2019.

APPENDIX A

This appendix includes: 02 TEXTS, 02 TABLES, and 14 FIGURES.

TEXT A1 – Fluency rate calculation of the UVC lamp

The fluency rate of the UVC lamp used in the photochemical and UVC AOPs experiments was measured using a FieldMaxII radiometer. For that, the UVC lamp was positioned inside a quartz tube and the fluency rate value (20.2 mW cm^{-2}) was obtained after fitting their evolution as a function of distance. This value refers to a distance of 1 cm from the tube.

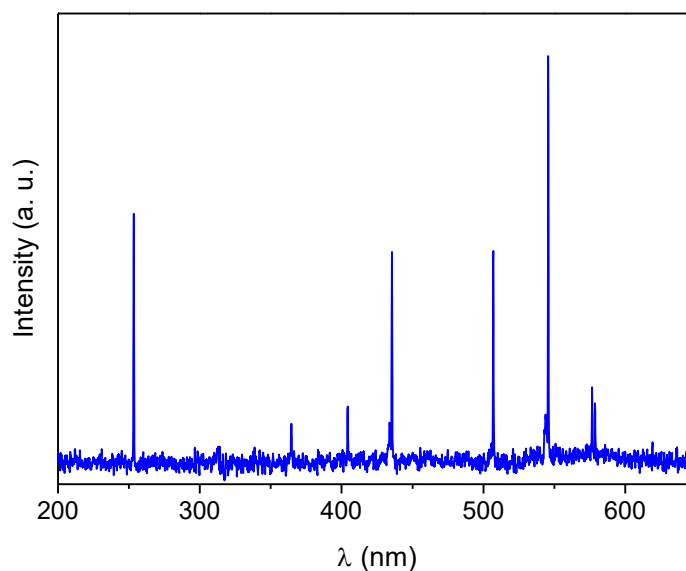


FIGURE A1 – Characteristic spectra of the UVC lamp used in the photochemical and UVC AOPs experiments.

TABLE A1 – Radical self-scavenging reactions involved in the UVC/H₂O₂, UVC/S₂O₈²⁻, and UVC/HClO processes.

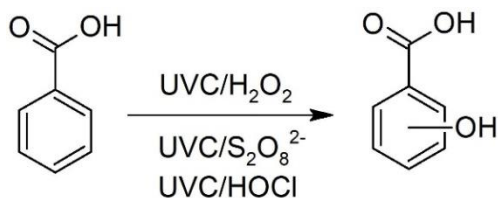
Reactions	Rate constants	References
$2\text{HO}\cdot \rightarrow \text{H}_2\text{O}_2$	$k = 5.5 \times 10^9 \text{ M}^{-1} \text{ s}^{-1}$	[1]
$\text{H}_2\text{O}_2 + \text{HO}\cdot \rightarrow \text{H}_2\text{O} + \text{HO}_2\cdot \leftrightarrow \text{O}_2\cdot^- + \text{H}^+$	$k = 2.7 \times 10^7 \text{ M}^{-1} \text{ s}^{-1}$	[1]
$\text{HO}\cdot + \text{O}_2\cdot^- \rightarrow \text{HO}^- + \text{O}_2$	$k = 8.0 \times 10^9 \text{ M}^{-1} \text{ s}^{-1}$	[1]
$\text{HO}\cdot + \text{HO}_2\cdot \rightarrow \text{H}_2\text{O} + \text{O}_2$	$k = 6.0 \times 10^9 \text{ M}^{-1} \text{ s}^{-1}$	[1]
$\text{SO}_4\cdot^- + \text{S}_2\text{O}_8^{2-} \rightarrow \text{SO}_4^{2-} + \text{S}_2\text{O}_8\cdot^-$	$k = 1.5 \times 10^3 \text{ M}^{-1} \text{ s}^{-1}$	[2]
$\text{SO}_4\cdot^- + \text{SO}_4\cdot^- \rightarrow \text{S}_2\text{O}_8^{2-}$	$k = 4.4 \times 10^8 \text{ M}^{-1} \text{ s}^{-1}$	[3]
$\text{SO}_4\cdot^- + \text{H}_2\text{O} \rightarrow \text{HSO}_4^- + \text{HO}\cdot$	$k < 3 \times 10^8 \text{ s}^{-1}$	[3]
$\text{HOCl} + \text{HO}\cdot \rightarrow \text{ClO}\cdot + \text{H}_2\text{O}$	$k = 1.1 \times 10^8 \text{ M}^{-1} \text{ s}^{-1}$	[4]
$\text{Cl}\cdot + \text{Cl}^- \leftrightarrow \text{Cl}_2$	$k_1 = 2.1 \times 10^{10} \text{ M}^{-1} \text{ s}^{-1}$ $k_{-1} = 1.1 \times 10^5 \text{ s}^{-1}$	[5]
$\text{HO}\cdot + \text{Cl}^- \rightarrow \text{HClO}\cdot^-$	$k_1 = 4.3 \times 10^9 \text{ M}^{-1} \text{ s}^{-1}$ $k_{-1} = 6.1 \times 10^9 \text{ s}^{-1}$	[5]
$\text{HClO}\cdot^- + \text{H}^+ \leftrightarrow \text{Cl}\cdot + \text{H}_2\text{O}$	$k_1 = 2.1 \times 10^{10} \text{ M}^{-1} \text{ s}^{-1}$ $k_{-1} = 1.3 \times 10^3 \text{ M}^{-1} \text{ s}^{-1}$	[5]

Note: k_{-1} refers to the inverse reaction.

- [1] G. V. Buxton, C.L. Greenstock, W.P. Helman, A.B. Ross, Critical review of rate constants for reactions of hydrated electrons, hydrogen atoms and hydroxyl radicals (HO[•]/O^{•-}) in aqueous solution, *J. Phys. Chem.*, **17**: 513, 1988.
- [2] G. V. Buxton, M. Bydder, G. Arthur Salmon, The reactivity of chlorine atoms in aqueous solution Part II. The equilibrium $\text{SO}_4\cdot^- + \text{Cl}^- \rightleftharpoons \text{Cl}\cdot + \text{SO}_4^{2-}$, *Phys. Chem. Chem. Phys.*, **1**: 269, 1999.
- [3] E. Hayon, A. Treinin, J. Wilf, Electronic spectra, photochemistry, and autoxidation mechanism of the sulfite-bisulfite-pyrosulfite systems. SO₂^{•-}, SO₃^{•-}, SO₄^{•-}, and SO₅^{•-} radicals, *J. Am. Chem. Soc.*, **94**: 47, 1972.
- [4] C.A. Ennis, J.W. Birks, Rate constants for the reactions OH + HClO → H₂O + ClO and H + HClO → products, *J. Phys. Chem.*, **92**: 1119, 1988.
- [5] G.G. Jayson, B.J. Parsons, A.J. Swallow, Some simple, highly reactive, inorganic chlorine derivatives in aqueous solution. Their formation using pulses of radiation and their role in the mechanism of the Fricke dosimeter, *J. Chem. Soc. Faraday Trans.*, **69**: 1597, 1973.

TEXT A2 – Hydroxyl radical identification using the benzoic and salicylic acids couple

The reaction between benzoic acid and HO[•] result in the formation of salicylic acid (substitution in ortho, meta, or para positions), as can be seen in the following scheme:



Thus, the evolution of benzoic and salicylic acid concentrations were monitored by HPLC using a core shell C-18 reversed phase (Phenomenex[®]: 150 mm×4.6 mm, 5 μm particle size, 100 Å) as the stationary phase and a mixture of aqueous 0.1 % (V/V) formic acid (eluent A) and acetonitrile (eluent B) as the mobile phase at 1 mL min⁻¹ using a gradient elution protocol: from 20% to 80% of eluent B in 10 min, and then back to 20% in 2 min. The injection volume of the treated samples was 25 μL and the UV detection was set at 300 nm (detection of the ortho and meta substitution isomers).

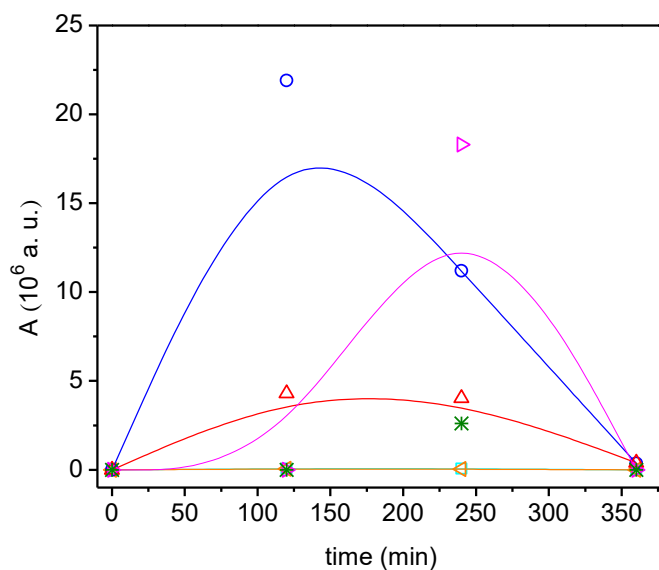


FIGURE A2 – Integrated chromatographic area of m/z 151 (\square), m/z 243 (\triangleleft), m/z 247 (\circ), m/z 259 (\triangle), m/z 323 (\blacktriangleright), and m/z 342 ($*$) by-products as a function of the treatment time for the UVC/ H_2O_2 process: Conditions: 0.6 mol L^{-1} of oxidant (flow rate 0.1 mL min^{-1}), pH 3, and $38 \text{ }^\circ\text{C}$.

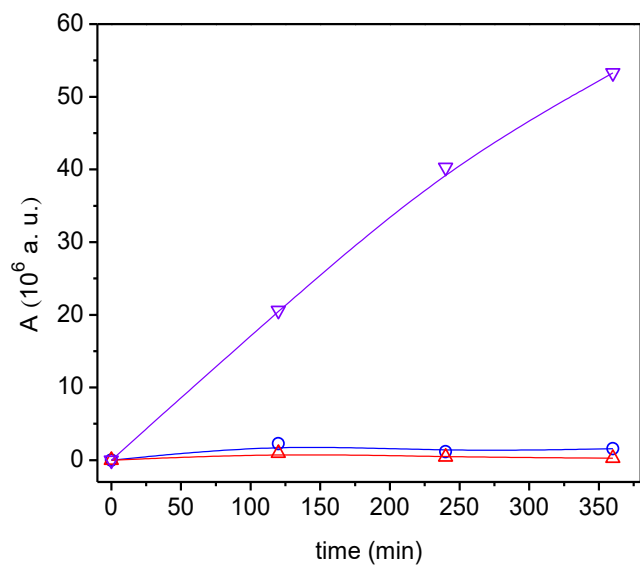


FIGURE A3 – Integrated chromatographic area of m/z 247 (\circ), m/z 259 (\triangle), and m/z 261a (∇) by-products as a function of the treatment time for the UVC/ $\text{S}_2\text{O}_8^{2-}$ process: Conditions: 0.6 mol L^{-1} of oxidant (flow rate 0.1 mL min^{-1}), pH 3, and $38 \text{ }^\circ\text{C}$.

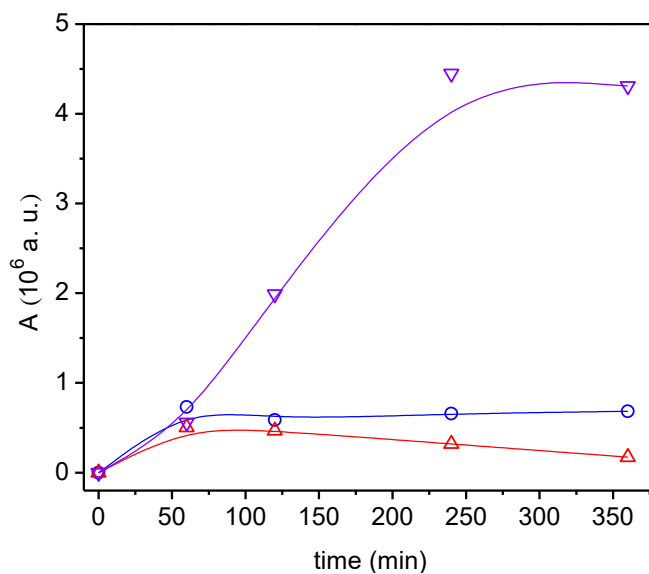


FIGURE A4 – Integrated chromatographic area of m/z 247 (\circ), m/z 259 (\triangle), and m/z 261a (∇) by-products as a function of the treatment time for the UVC/HClO process: Conditions: 0.6 mol L^{-1} of oxidant (flow rate 0.1 mL min^{-1}), pH 3, and $38 \text{ }^\circ\text{C}$.

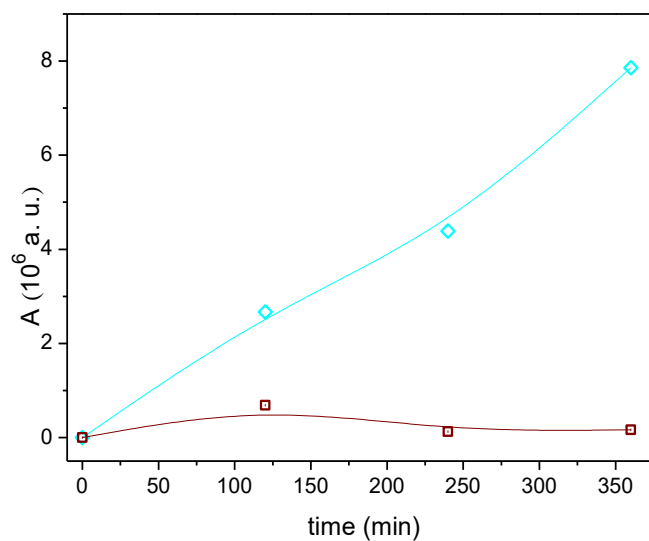
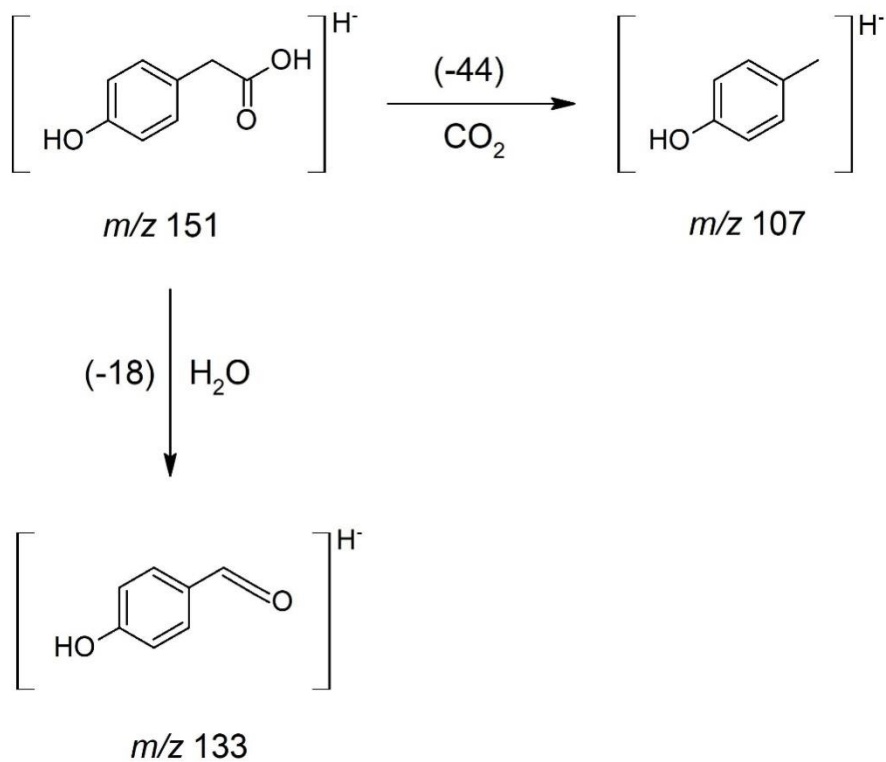
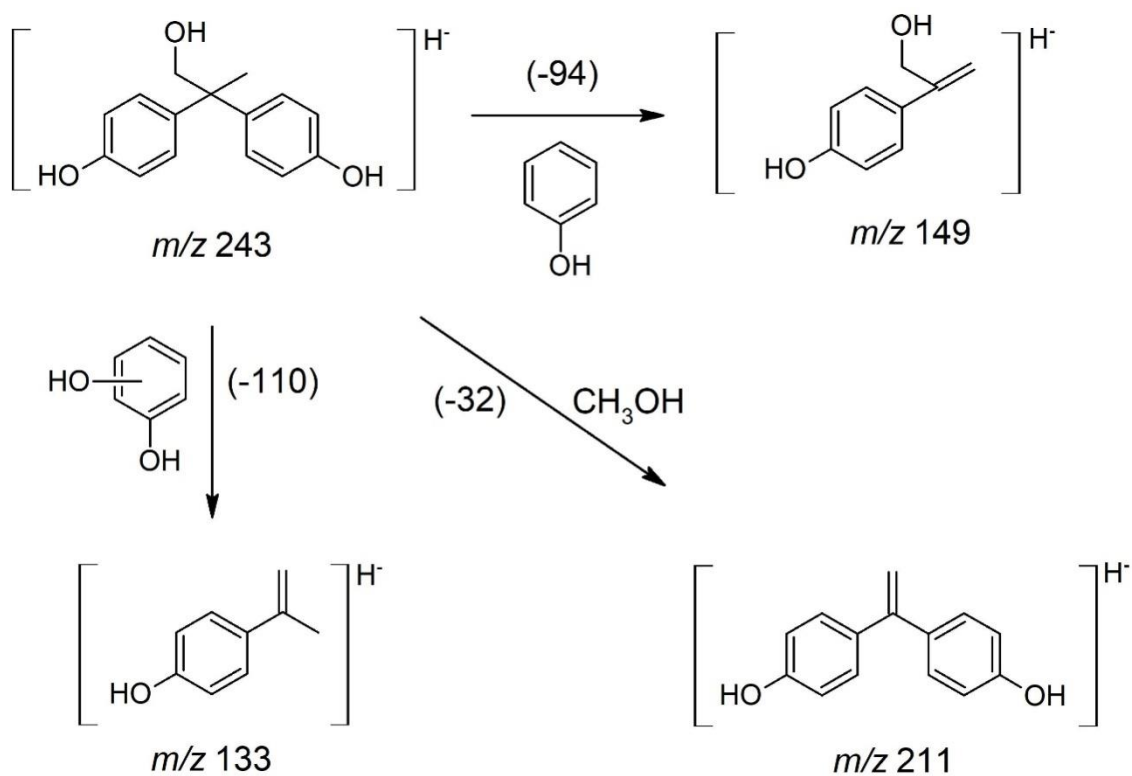
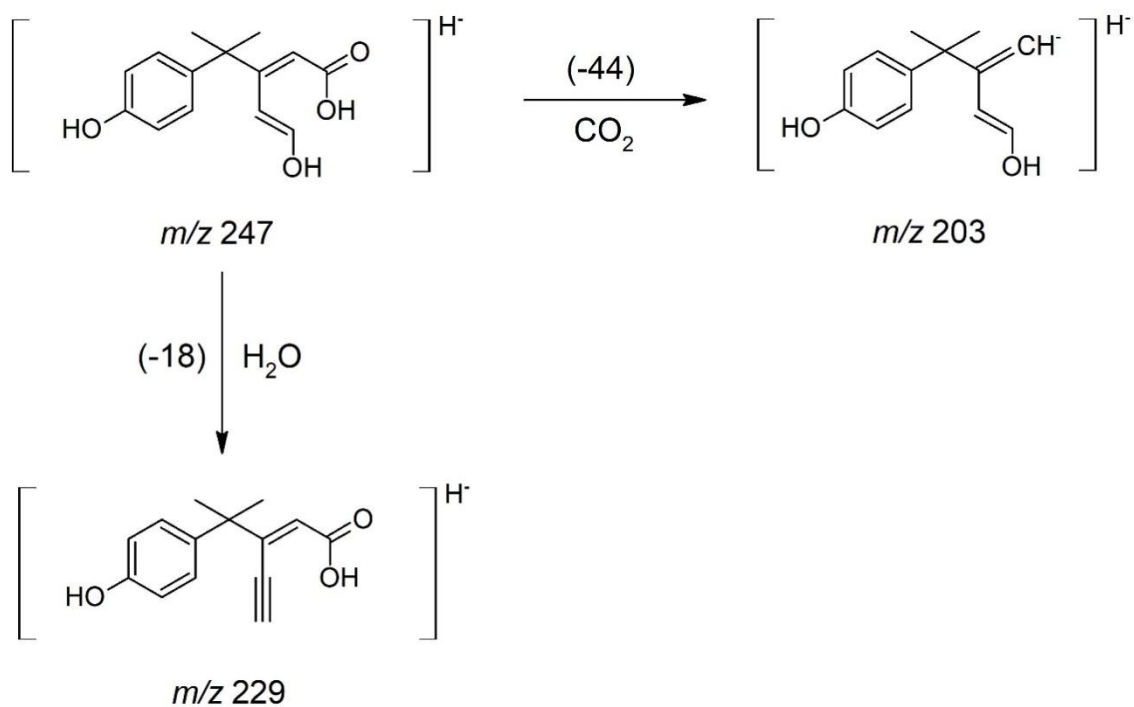
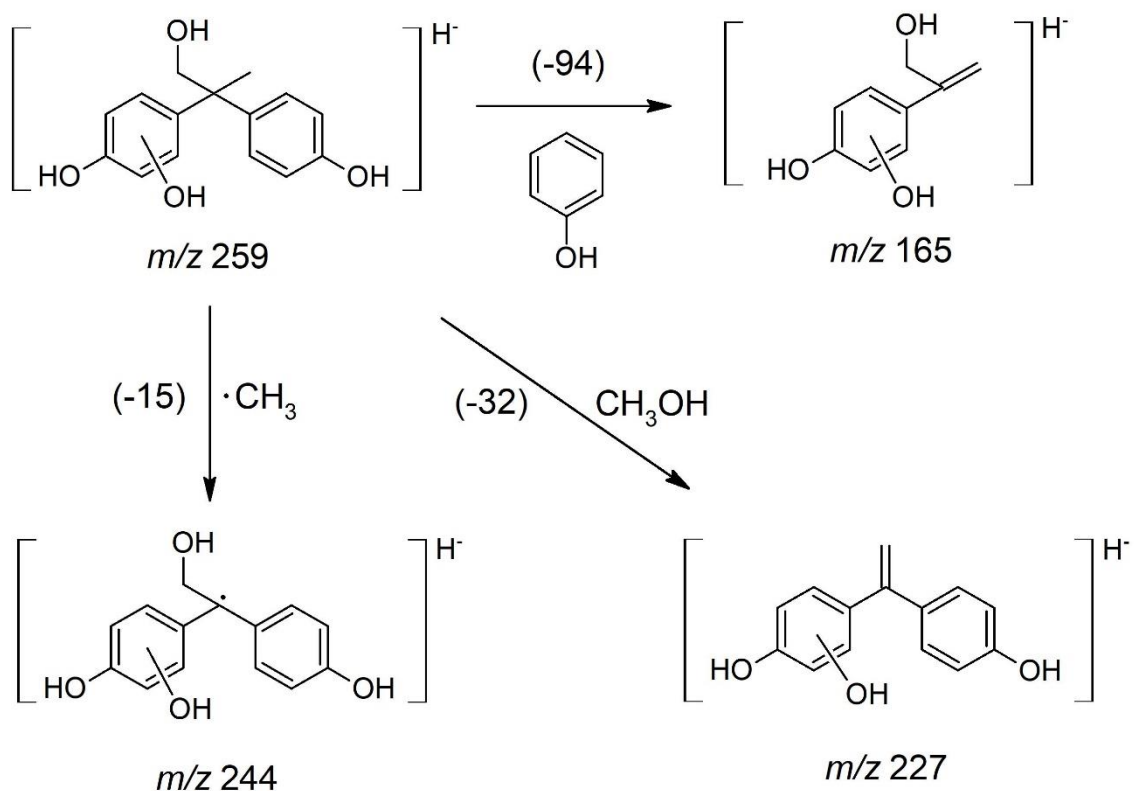
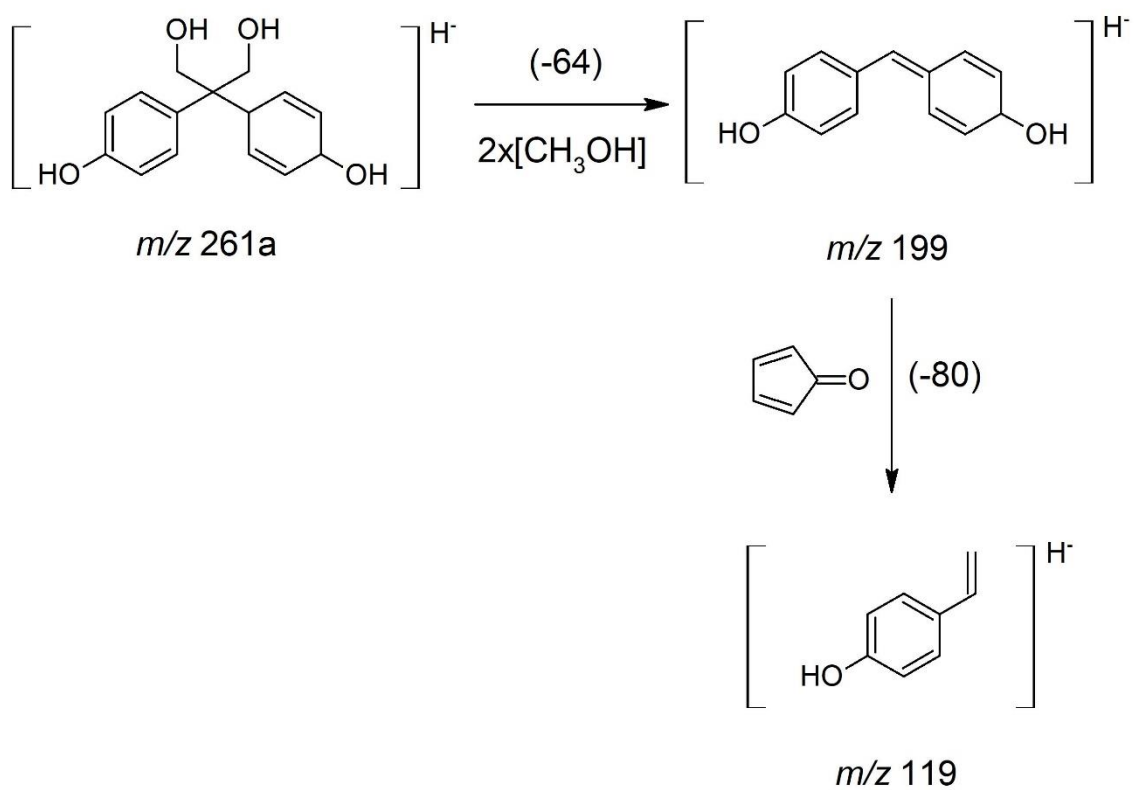
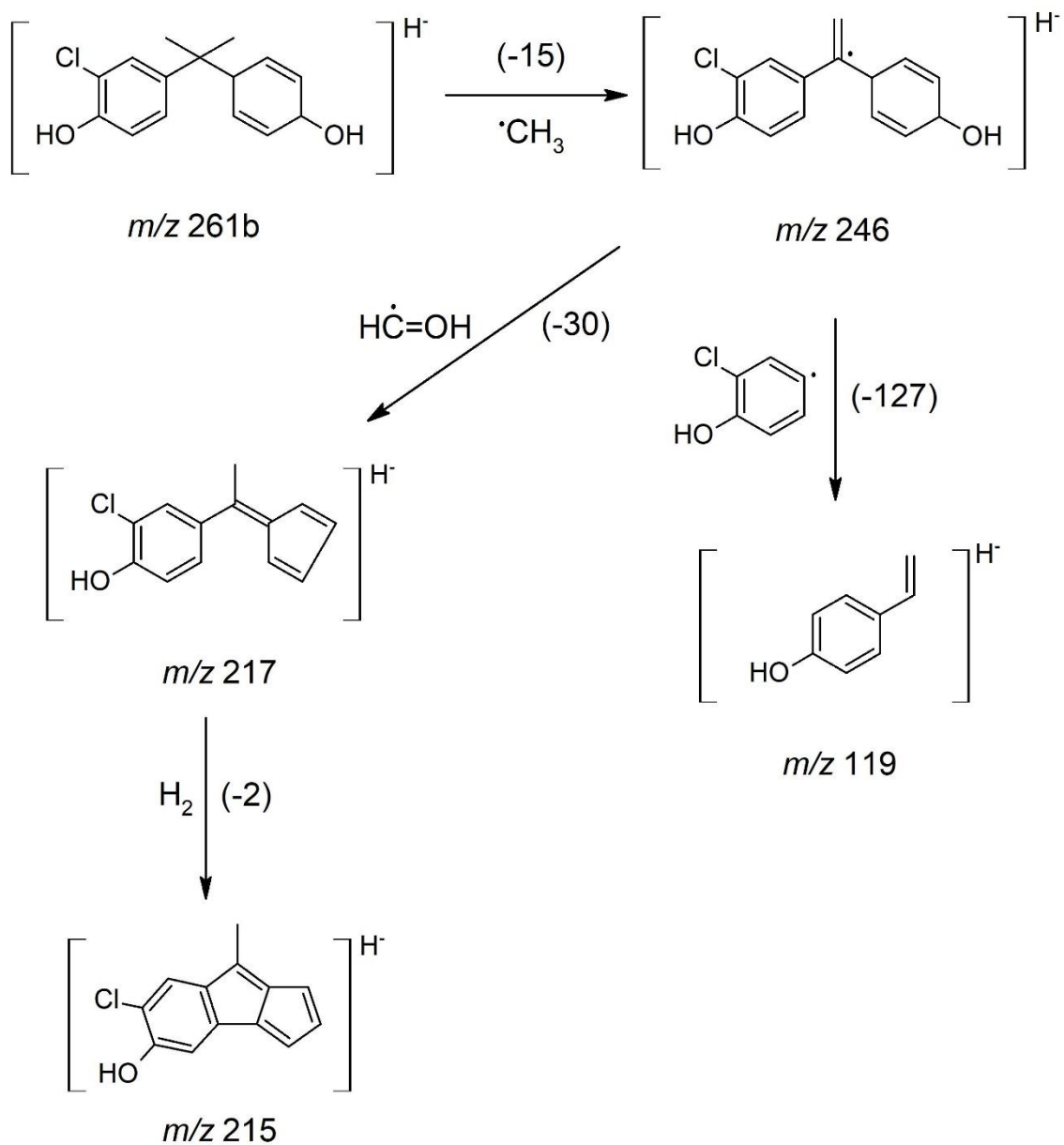


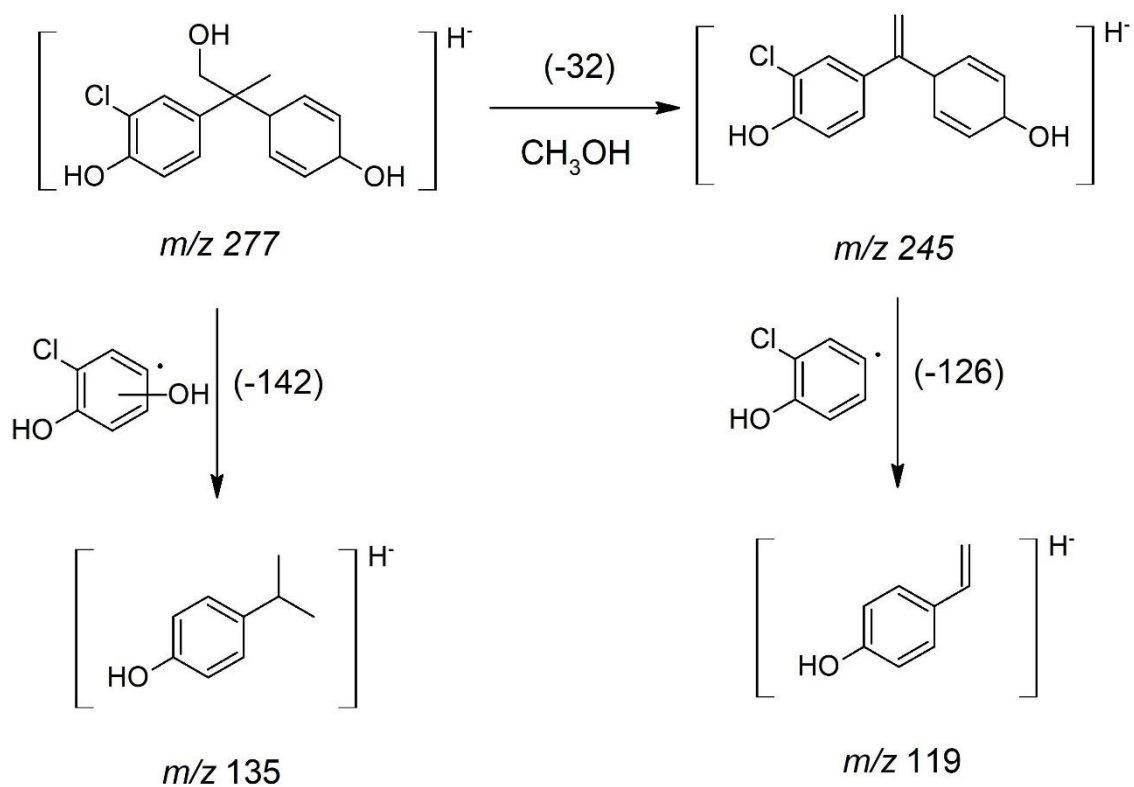
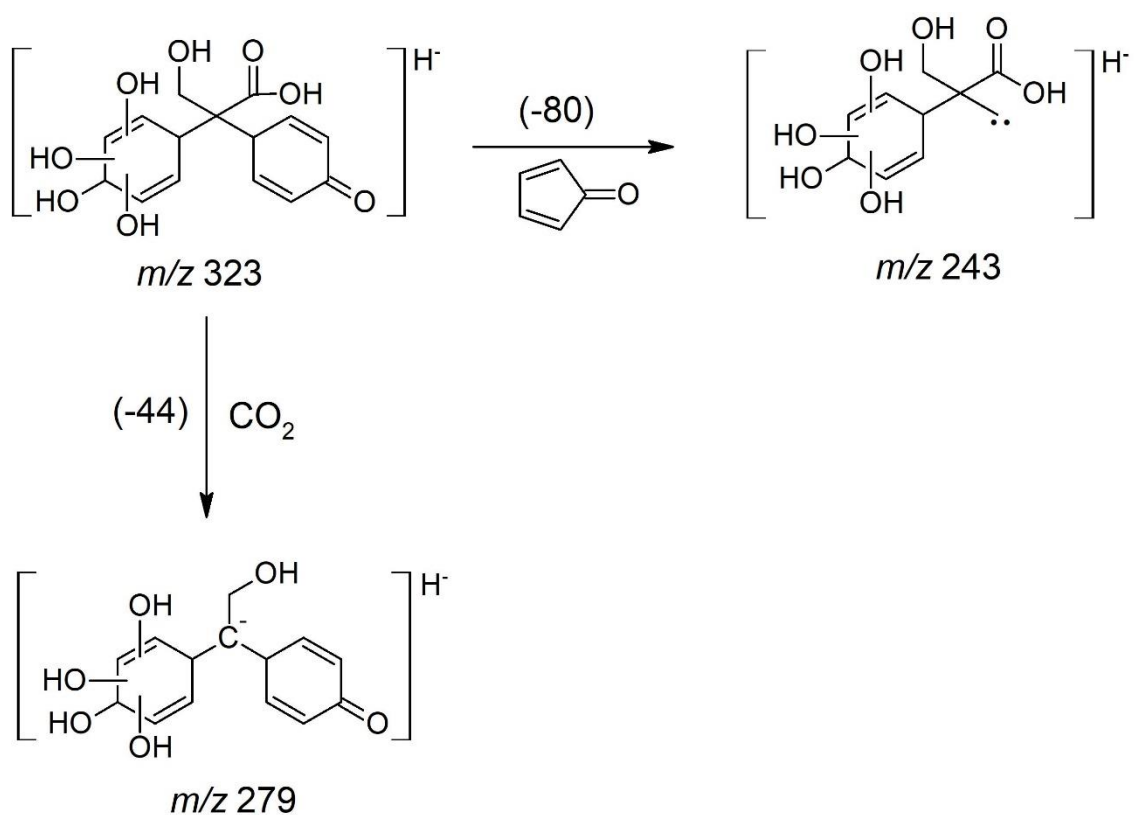
FIGURE A5 – Integrated chromatographic area of m/z 261b (\diamond) and m/z 277 (\square) by-products as a function of the treatment time for the HClO process: Conditions: 0.6 mol L^{-1} of oxidant (flow rate 0.1 mL min^{-1}), pH 3, and $38 \text{ }^\circ\text{C}$.

FIGURE A6 – Proposed fragmentation route of the main detected by-product with m/z 151.FIGURE A7 – Proposed fragmentation route of the main detected by-product with m/z 243.

FIGURE A8 – Proposed fragmentation route of the main detected by-product with m/z 247.FIGURE A9 – Proposed fragmentation route of the main detected by-product with m/z 259.

FIGURE A10 – Proposed fragmentation route of the main detected by-product with m/z 261a.

FIGURE A11 – Proposed fragmentation route of the main detected by-product with m/z 261b.

FIGURE A12 – Proposed fragmentation route of the main detected by-product with m/z 277.FIGURE A13 – Proposed fragmentation route of the main detected by-product with m/z 323.

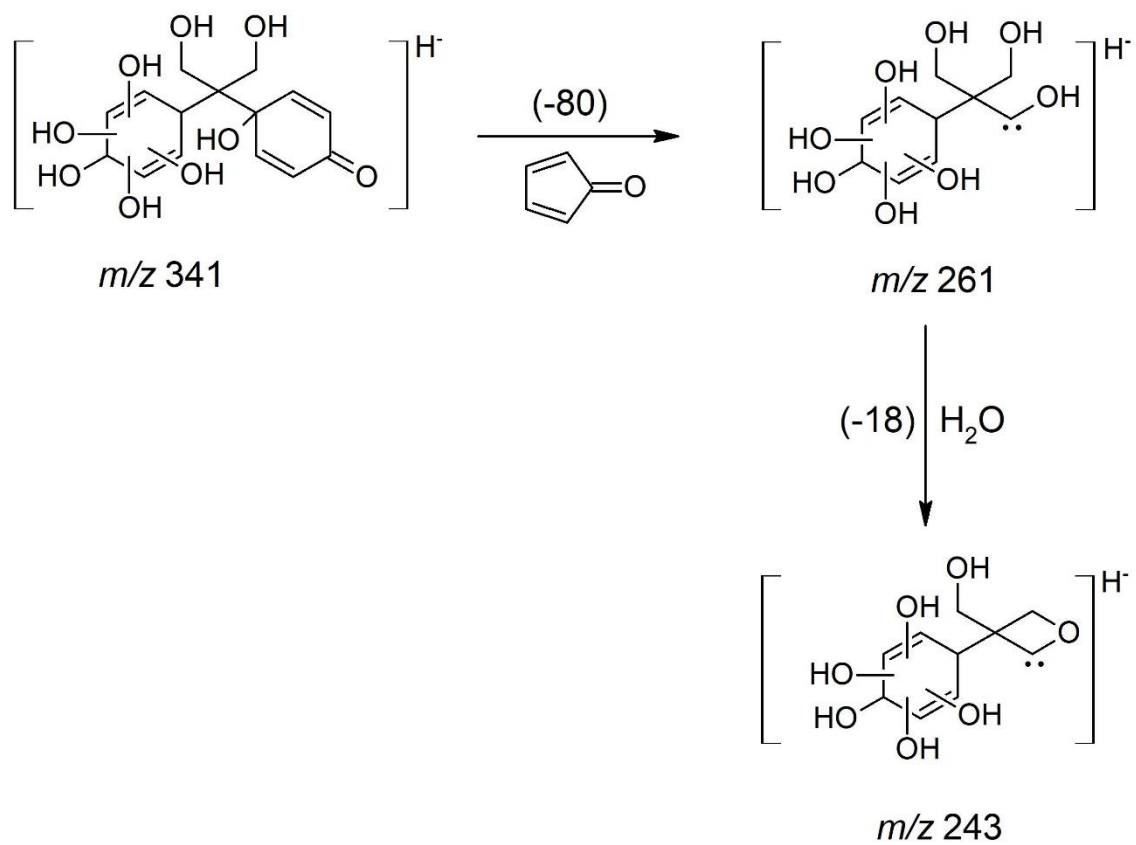
FIGURE A14 – Proposed fragmentation route of the main detected by-product with m/z 341.

TABLE A2 – Toxicity classification for aquatic life according to the Globally Harmonized System of Classification and Labelling of Chemicals (GHS)*.

Toxicity range (mg L⁻¹)	Classification
LC ₅₀ ≤ 1 mg L ⁻¹	Very toxic
LC ₅₀ > 1 mg L ⁻¹ but ≤ 10 mg L ⁻¹	Toxic
LC ₅₀ > 10 mg L ⁻¹ but ≤ 100 mg L ⁻¹	Harmful
LC ₅₀ > 100 mg L ⁻¹	Not harmful

*Available at:

https://www.unece.org/fileadmin/DAM/trans/danger/publi/ghs/ghs_rev07/English/ST_SG_A_C10_30_Rev7e.pdf (Accessed in: 05/23/2019)

APPENDIX B

This appendix includes: 03 TABLES and 05 FIGURES.

TABLE B1 – Chromatographic parameters: retention time, wavelength of maximum absorbance and area of each organic microcontaminant (OMC) at $100 \mu\text{g L}^{-1}$.

OMC	Retention time (min)	λ (nm)	Area - $100 \mu\text{g L}^{-1}$ (a. u.)
Acetaminophen (ACT)	2.48	245	18.2
Caffeine (CAF)	3.60	270	14.0
Carbamazepine (CBZ)	3.94	270	5.5
Trimethoprim (TMP)	5.01	267	20.0
Sulfamethoxazole (SMX)	7.2	2.67	8.7
Diclofenac (DCF)	10.6	2.80	9.7

The detection limit (DL) for all the compounds studied was $5 \mu\text{g L}^{-1}$

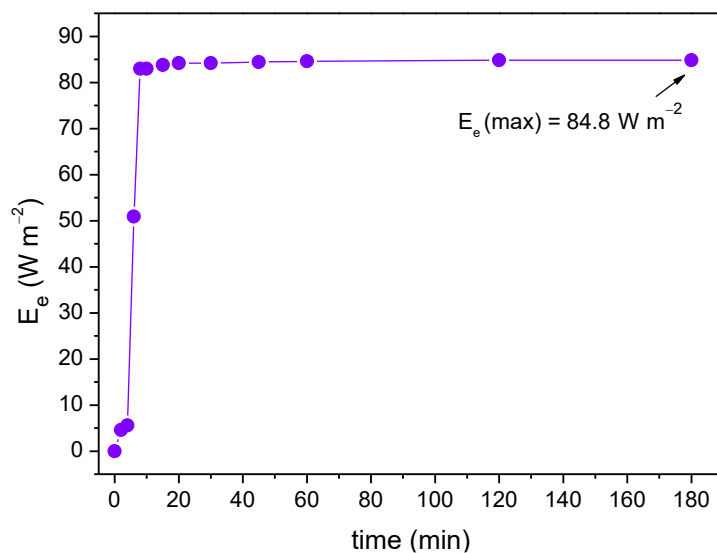


FIGURE B1 – Irradiance profile (E_e ; ●) of the UVC lamp measured during 180 min in distilled water (maximum value 84.8 W m^{-2}).

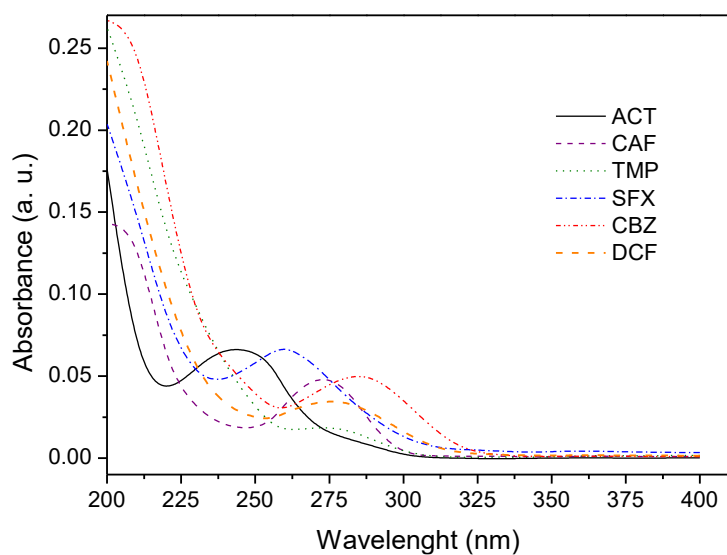


FIGURE B2 – UV absorption spectrum of each OMC. This measurement was carried out using 1 mg L^{-1} of each compound dissolved in distilled water between 200-400 nm.

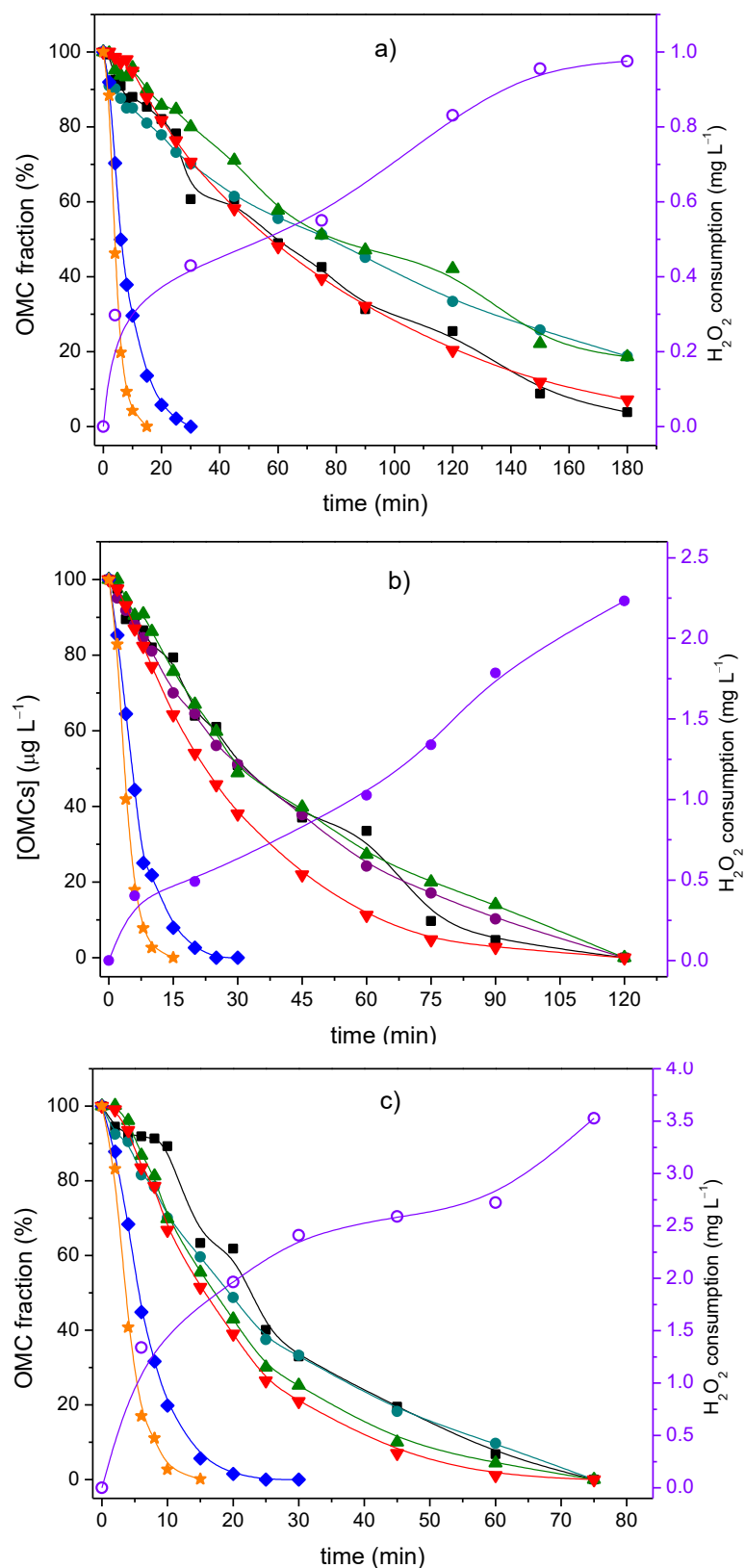
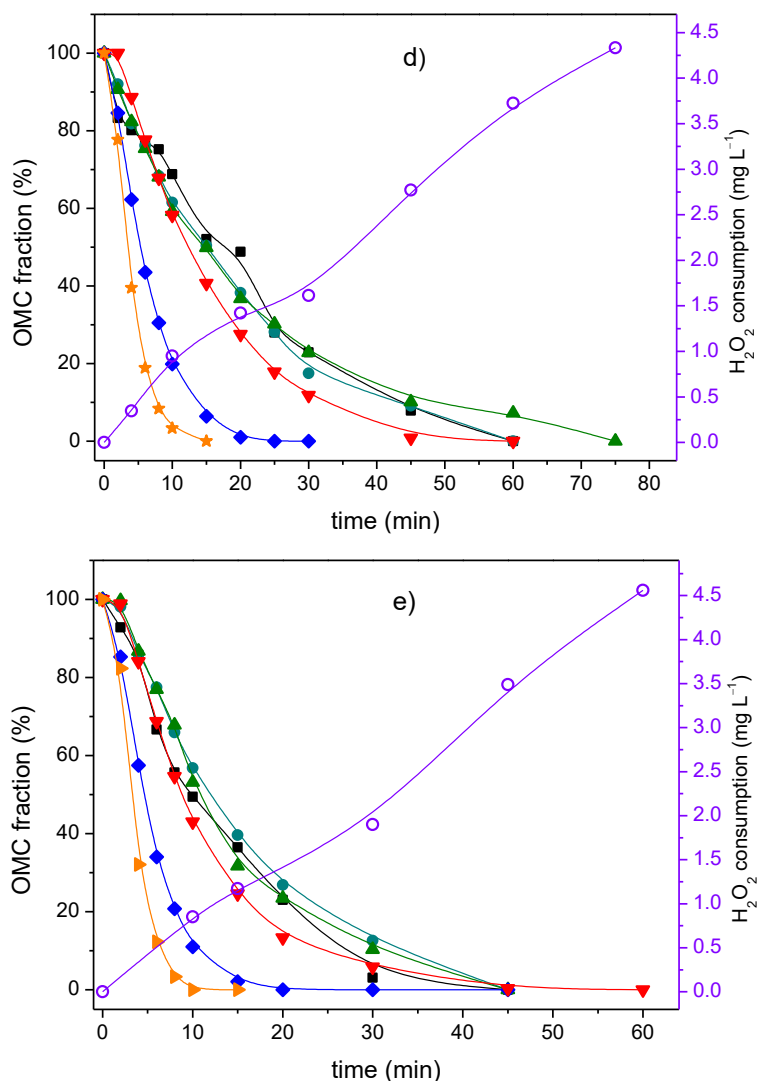


FIGURE B3 – Degradation profile of each OMC (ACT (■), CAF (●), CBZ (▼), DCF (▶), SMX (◆), and TMP (▲)) and H₂O₂ consumption (○) for the UVC/H₂O₂ process at different concentrations: a) 5, b) 15, c) 25, d) 35, and e) 50 mg L⁻¹.



Continuation: FIGURE B3 – Degradation profile of each OMC (ACT (■), CAF (●), CBZ (▼), DCF (▶), SMX (◆), and TMP (▲)) and H₂O₂ consumption (○) for the UVC/H₂O₂ process at different concentrations: a) 5, b) 15, c) 25, d) 35, and e) 50 mg L⁻¹.

TABLE B2 – Pseudo-first order kinetic constants (k) for the UVC/H₂O₂ process at different concentrations during degradation of OMCs. The values in parentheses correspond to the coefficient of determination (R^2).

UV-C/H ₂ O ₂ (mg L ⁻¹)	k (10 ⁻² min ⁻¹)					
	ACT	CAF	TMP	SFX	CBZ	DCF
5	1.7 (0.97)	0.9 (0.99)	1.0 (0.99)	15.5 (0.99)	1.45 (0.97)	32.1 (0.94)
15	3.3 (0.97)	2.4 (0.99)	2.2 (0.99)	18.5 (0.99)	4.0 (0.99)	37.2 (0.97)
25	4.4 (0.97)	4.0 (0.99)	5.4 (0.99)	21.5 (0.98)	7.1 (0.97)	44.4 (0.96)
35	5.5 (0.98)	5.4 (0.99)	4.6 (0.99)	22.5 (0.97)	9.9 (0.94)	35.0 (0.98)
50	11 (0.93)	7.1 (0.99)	8.0 (0.99)	26.4 (0.97)	12.3 (0.98)	43.4 (0.95)

TABLE B3 – Pseudo-first order kinetic constants (k) for the UVC/S₂O₈²⁻ process at different concentrations during degradation of OMCs. The values in parentheses correspond to the coefficient of determination (R^2).

UV-C/S ₂ O ₈ ²⁻ (mg L ⁻¹)	k (10 ⁻² min ⁻¹)					
	ACT	CAF	TMP	SFX	CBZ	DCF
20	2.5 (0.96)	2.1 (0.99)	0.9 (0.98)	16.5 (0.97)	3.1 (0.96)	33.1 (0.96)
40	3.4 (0.97)	3.8 (0.91)	3.6 (0.94)	14.6 (0.95)	4.9 (0.98)	38.1 (0.96)
100	6.0 (0.85)	9.6 (0.91)	8.1 (0.81)	19.5 (0.98)	10.3 (0.95)	48.4 (0.98)

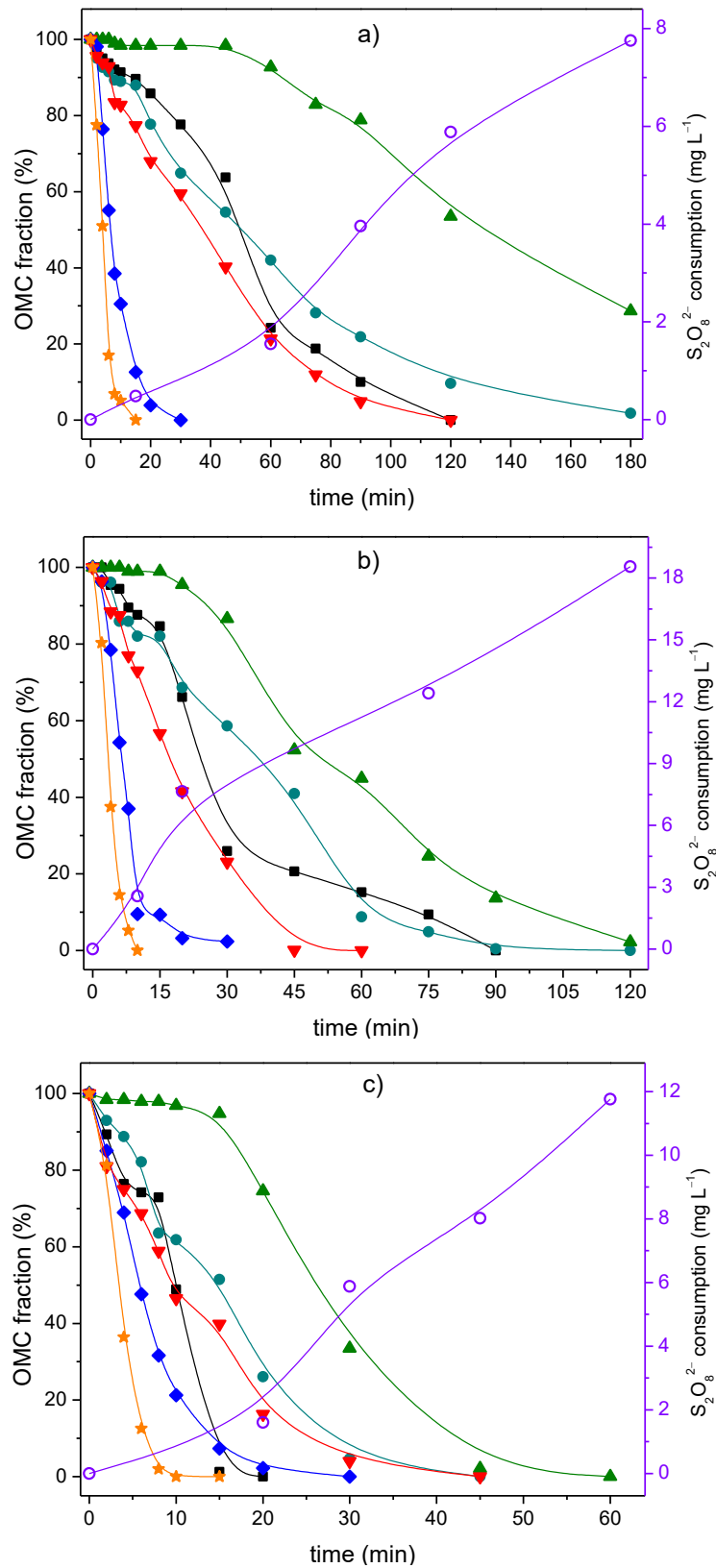


FIGURE B4 – Degradation profile of each OMC (ACT (■), CAF (●), CBZ (▼), DCF (▲), SMX (◆), and TMP (▲)) and $S_2O_8^{2-}$ consumption (○) for the UVC/ $S_2O_8^{2-}$ process at different concentrations: a) 20, b) 40, and c) 100 $mg L^{-1}$.

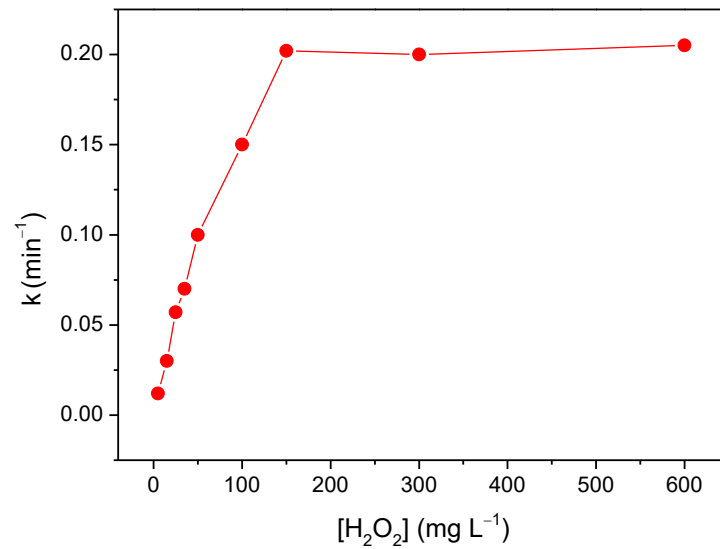


FIGURE B5 – Pseudo first order kinetic constant (k ; ●) as a function of H_2O_2 concentration ($[\text{H}_2\text{O}_2]$) for UVC/ H_2O_2 process.

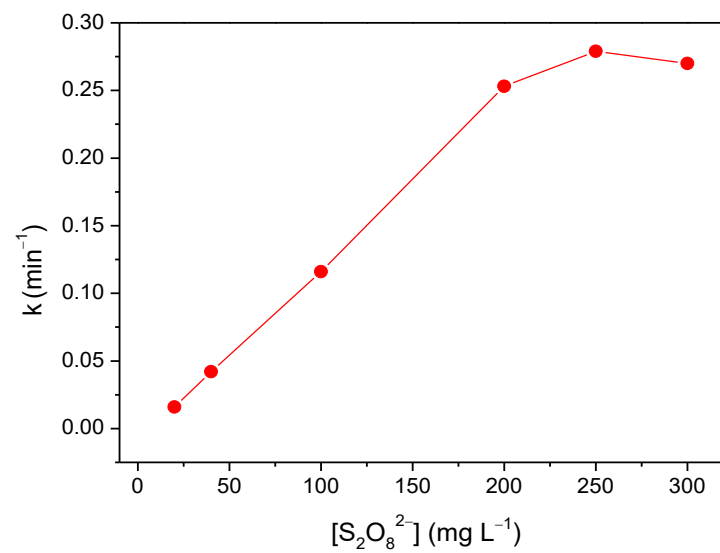


FIGURE B6 – Pseudo first order kinetic constant (k ; ●) as a function of $\text{S}_2\text{O}_8^{2-}$ concentration ($[\text{S}_2\text{O}_8^{2-}]$) for UVC/ $\text{S}_2\text{O}_8^{2-}$ process